

Spring 2000

Soil hydraulic controls over nitrogen oxide emissions and nitrogen cycling in tropical agriculture

Antje M. Weitz

University of New Hampshire, Durham

Follow this and additional works at: <https://scholars.unh.edu/dissertation>

Recommended Citation

Weitz, Antje M., "Soil hydraulic controls over nitrogen oxide emissions and nitrogen cycling in tropical agriculture" (2000). *Doctoral Dissertations*. 2135.

<https://scholars.unh.edu/dissertation/2135>

This Dissertation is brought to you for free and open access by the Student Scholarship at University of New Hampshire Scholars' Repository. It has been accepted for inclusion in Doctoral Dissertations by an authorized administrator of University of New Hampshire Scholars' Repository. For more information, please contact nicole.hentz@unh.edu.

INFORMATION TO USERS

This manuscript has been reproduced from the microfilm master. UMI films the text directly from the original or copy submitted. Thus, some thesis and dissertation copies are in typewriter face, while others may be from any type of computer printer.

The quality of this reproduction is dependent upon the quality of the copy submitted. Broken or indistinct print, colored or poor quality illustrations and photographs, print bleedthrough, substandard margins, and improper alignment can adversely affect reproduction.

In the unlikely event that the author did not send UMI a complete manuscript and there are missing pages, these will be noted. Also, if unauthorized copyright material had to be removed, a note will indicate the deletion.

Oversize materials (e.g., maps, drawings, charts) are reproduced by sectioning the original, beginning at the upper left-hand corner and continuing from left to right in equal sections with small overlaps.

Photographs included in the original manuscript have been reproduced xerographically in this copy. Higher quality 6" x 9" black and white photographic prints are available for any photographs or illustrations appearing in this copy for an additional charge. Contact UMI directly to order.

**Bell & Howell Information and Learning
300 North Zeeb Road, Ann Arbor, MI 48106-1346 USA
800-521-0600**

UMI[®]

SOIL HYDRAULIC CONTROLS OVER NITROGEN OXIDE EMISSIONS AND
NITROGEN CYCLING IN TROPICAL AGRICULTURE

BY

ANTJE M. WEITZ

Masters of Science in Geography, Free University of Hamburg, Germany, 1986

DISSERTATION

Submitted to the University of New Hampshire

In Partial Fulfillment of the

Requirements for the Degree of

Doctor of Philosophy

in

Natural Resources

May, 2000

UMI Number: 9969220

UMI[®]


UMI Microform 9969220

Copyright 2000 by Bell & Howell Information and Learning Company.

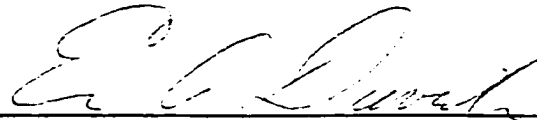
All rights reserved. This microform edition is protected against
unauthorized copying under Title 17, United States Code.

Bell & Howell Information and Learning Company
300 North Zeeb Road
P.O. Box 1346
Ann Arbor, MI 48106-1346

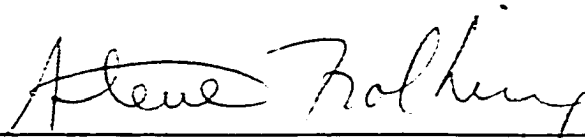
This dissertation has been examined and approved.



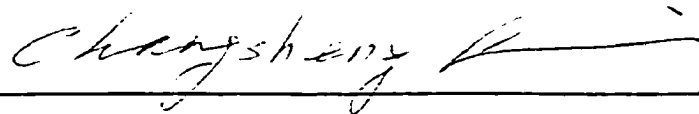
Dissertation Director, Dr. Patrick M. Crill
Research Associate Professor of Earth Sciences and Earth, Oceans, and Space



Dr. Eric A. Davidson
Senior Scientist, The Woods Hole Research Center



Dr. Steven E. Frolking
Research Assistant Professor, Complex Systems Research Center



Dr. Changsheng Li
Research Professor, Complex Systems Research Center



Dr. Ernst Linder
Associate Professor of Mathematics

21 Dec 99

Date

ACKNOWLEDGEMENTS

This study would not have been possible without research support from NASA. The field experiments were conducted within the NASA funded research project 'Nitrous Oxide Emissions From Tropical Agricultural Soils: Intensive Field Experiments and Development of a Process Model' (Principal Investigators Dr. M. Keller, Dr. P. Crill and Dr. C. Li). The first year of my time as a graduate student at the University of New Hampshire was also supported by funds from this project. From August 1997 through March 2000, I received a NASA Earth System Science Fellowship.

My special thanks goes to my advisor Dr. Patrick Crill. First of all for your immediate and 'thoughtless' "Yes" in January 1996, when I asked if I could become your graduate student at UNH. But mainly for your support throughout my time here in New Hampshire, and for the greatest possible freedom I enjoyed for my thesis research. I want to express my honest thanks to Dr. Changsheng Li, Dr. Ernst Linder, Dr. Steve Froking, and Dr. Eric Davidson for offering to be on my PhD committee and for the huge support I received during all these years. Your commitment requested a significant amount of time for committee meetings and reading of my written reports. In addition to this I always found you willing to make time for answering my questions. I had good discussions and I received enormous help with my statistical work, with modeling and writing. I am convinced I have had the best PhD committee imaginable and possible. Thank you very much!

I would like to thank Dr. Michael Keller for hiring me in 1993 to manage the field project at the La Selva Biological Station in Costa Rica, and for your substantial

support of my initiative to continue this work as PhD study at the University of New Hampshire. I would also like to thank Dr. Eric Davidson for supporting my work in Costa Rica from the beginning of the field experiment.

I am very thankful for the friendship and strong support I enjoyed from my new friends here in New Hampshire in and outside of the University community. I especially want to express my strong gratitude to my current and former office- and gym-mates, Cindy and Andy Mosedale, Carolyn Jordan, Ruth Varner, Barry Lefer, Faith Sheridan, Lynn Rosentrater, and Claire McSwiney. I had some rough times in the initial years, but you were always there for me, patient and never fatigued, listened, and helped me to 'get my act together'. With your help I made it through all kinds of crises and really had a great time here. Thanks to you all, and your friends and families, who welcomed me without hesitation. A big thank you to my old friends from the years in Costa Rica, in Holland and in Germany, who stayed in touch with me through all the years. I never felt alone.

A very special thank you to my family for letting me do this work and letting me be here in New Hampshire, far away from you and doing things that are definitely not very important for the life we live together. I am glad to see you 'happy as a clam' that I am going to be 'home' soon. However, I like to be in New England; the climate is very nice, I love being close to the ocean and to the mountains. And people here are very friendly – it was great being here!

TABLE OF CONTENTS

ACKNOWLEDGEMENTS.....	iii
LIST OF TABLES.....	viii
LIST OF FIGURES.....	ix
ABSTRACT.....	xi

CHAPTER	PAGE
CHAPTER 1: NITROUS OXIDE, NITRIC OXIDE, AND METHANE FLUXES FROM SOILS FOLLOWING CLEARING AND BURNING OF TROPICAL SECONDARY FOREST.....	1
Abstract.....	1
Intoduction.....	2
Study Area.....	5
Site Preparation and Management.....	6
Methods.....	7
Results.....	12
Discussion	19
Conclusion.....	28
CHAPTER 2: SPATIAL AND TEMPORAL VARIABILITY OF NITROGEN OXIDE AND METHANE FLUXES FROM A FERTILIZED TREE PLANTATION IN COSTA RICA.....	30
Abstract.....	30
Intoduction.....	31
Study Area.....	33
Experimental Design.....	34
Main Experiment.....	34
Spatial Variability Study.....	35
Spatial-Temporal Variability Study.....	36
Fertilization.....	36
Methods.....	37

Manual Sampling and Analysis.....	37
Automated Measurements.....	39
Statistical Analysis.....	40
Results.....	41
Discussion.....	52
Conclusion.....	59
CHAPTER 3: CALIBRATION OF TIME DOMAIN REFLECTOMETRY TECHNIQUE USING UNDISTURBED SOIL SAMPLES FROM HUMID TROPICAL SOILS OF VOLCANIC ORIGIN.....	
	61
Abstract.....	61
Intoduction.....	61
Materials and Methods.....	65
Sites.....	65
Time Domain Reflectometry (TDR).....	66
Sampling Procedure.....	68
Effect of Sample Size on Calibration.....	70
Effect of Air-Filled Cavities on TDR Measurements.....	72
Calculations.....	72
Results.....	73
Calibration method.....	73
Empirical calibration functions.....	74
Mixing models.....	77
Effects of Air-Filled Holes on TDR Measurements.....	80
Discussion and Conclusion.....	80
CHAPTER 4: EFFECTS OF SOIL MOISTURE DYNAMICS ON N₂O EMISSIONS FROM HUMID TROPICAL AGRICULTURAL SOILS.....	
	87
Abstract.....	87
Intoduction.....	88
Study Area.....	90
Experimental Design.....	90
Methods.....	91

Agricultural Management	96
Results	97
Discussion	104
Conclusion	109
References	122
Appendix	134

LIST OF TABLES

- TABLE 1.1. Soil Characteristics for Soils Under Forest Cover
- TABLE 1.2. Time Schedule of Land Management Categories on Both Soil Types
- TABLE 1.3. Statistics of Measured Variables, Distinguished per Soil Type and Land Management Category
- TABLE 2.1. Sampling Design for the Main Experiment and the Variability Study
- TABLE 3.1. Equations of Mixing Models used in Comparisons of Calibration Models
- TABLE 3.2. Brief Description of Soils Used for Calibration of TDR Technique
- TABLE 3.3. Characterization of Soil Samples Used for Calibration.
- TABLE 4.1. Soil characteristics of the loam and clay measured at 0-0.1 m depth
- TABLE 4.2. Cropping cycles for annual and perennial crop through the experiment
- TABLE 4.3. Fertilization schedule, amount of fertilizer addition, percentage of fertilizer-N lost as N_2O gas for a fertilization event, and soil type studied for each fertilization.
- TABLE 4.4. Mean emissions of N_2O-N , and N-loss from unfertilized and fertilized annual and perennial crop
- TABLE 4.5. Mean soil temperature and water filled pore space ratio at 0.05 m depth.
- TABLE 4.6. Multiple regression models
- TABLE 4.7. Soil characteristics of loam and clay used as input in DNDC.

LIST OF FIGURES

- Figure 1.1: Monthly precipitation and average monthly water filled pore space for Eutropept and Dystropept under forest and during land use change
- Figure 1.2: Time series of extractable soil inorganic NO_3^- and NH_4^+ concentrations for Eutropept and Dystropept
- Figure 1.3: Time series of NO , N_2O and CH_4 fluxes from Dystropept
- Figure 1.4: Boxplot summary of measured data for Eutropept and Dystropept
- Figure 1.5: CH_4 fluxes versus effective diffusivity for the Dystropept
- Figure 2.1: Comparison of trace gas fluxes from and water-filled-pore-space in loam and clay
- Figure 2.2: Time series of trace gas fluxes and water-filled-pore-space from spatial-temporal sampling in June/July, 1996
- Figure 2.3: Semi-variograms for post-fertilization In-NO and $\text{In-N}_2\text{O}$ fluxes
- Figure 2.4: Comparison of NO and N_2O fluxes measured from temporary and permanent sampling locations on clay and loam
- Figure 2.5: Comparison of NO and N_2O fluxes measured from temporary and permanent sampling locations during spatial-temporal sampling in June/July, 1996
- Figure 2.6: Precipitation, soil temperature at 0.05 m depth, and soil N_2O fluxes for the period of June 1 to July 30, 1996
- Figure 2.7: Comparison of NO fluxes from spatial sampling with routine monthly to bi-monthly measurements on unfertilized and fertilized loam
- Figure 3.1: Design of calibration setup
- Figure 3.2: Effect of thickness of soil layer remaining between TDR probe and sample surface
- Figure 3.3: Apparent dielectric number versus soil water content on loam
- Figure 3.4: Apparent dielectric number versus soil water content on clay
- Figure 3.5: Comparison of moisture data from the topsoil of loam to empirical models

Figure 3.6: Comparison of moisture data from the topsoil of loam to mixing models

Figure 3.7: Comparison of measured and modeled soil water content on loam

Figure 3.8: Comparison of measured and modeled soil water content on clay

Figure 3.9: Effect of increasing number of artificial holes in a soil sample on estimated soil water content

Figure 3.10: Comparison of soil water content estimated using two different models

Figure 4.1: Plot design and instrumentation of field sites.

Figure 4.2: Mean bulk density and moisture content at 0-0.07 m depth and contribution of the sub-layers 0-0.02, 0.02-0.04, and 0.04-0.07 m to the mean.

Figure 4.3: Comparison of automatically and manually measured soil moisture content at 0.05 m depth on loam and clay.

Figure 4.4: Daily precipitation, soil temperature and moisture content at 0.05 cm depth and soil-atmosphere N₂O fluxes measured on loam.

Figure 4.5: Post fertilization flux traces on clay and loam.

Figure 4.6: Linear regression between ln-N₂O fluxes and soil moisture content.

Figure 4.7: Daily mean N₂O fluxes from annual and perennial crop simulated using multiple regression modeling compared to measured flux traces.

Figure 4.8a: Daily mean N₂O fluxes from annual crop and daily soil moisture content simulated using the process model DNDC and measured fluxes and moisture dynamics.

Figure 4.8b: Daily mean N₂O fluxes from perennial crop and daily soil moisture content simulated using the process model DNDC and measured fluxes and moisture dynamics.

Figure 4.9: Comparison of simulated and measured fluxes and moisture content for all sub-plots

Figure 4.10: Effect of ants expanding their nest into the soil covered by chamber 3 compared to fluxes from replicated chamber 4.

ABSTRACT

SOIL HYDRAULIC CONTROLS OVER NITROGEN OXIDE EMISSIONS AND NITROGEN CYCLING IN TROPICAL AGRICULTURE

by

Antje M. Weitz

University of New Hampshire, May, 2000

Soils are the major natural source of nitrous oxide (N_2O). Intensive land use increased atmospheric concentrations of this greenhouse gas. Soil microbes produce and consume nitrogen oxides (NO , N_2O) during the processes of nitrification (aerobic) and denitrification (anaerobic). Micro-scale variability of controlling factors cause nitrification and denitrification to occur simultaneously in soils, resulting in high spatial variability of nitrogen oxide emissions. Fertilization increases nutrient availability and thus N_2O fluxes. Forest soils in the humid tropics account for 20-50% of all N_2O sources. Expansion and intensification of tropical agriculture is expected to increase atmospheric N_2O concentrations.

We measured N_2O fluxes from secondary humid tropical forest soils in Costa Rica, followed fluxes during forest conversion and studied emissions from unfertilized and fertilized agricultural soils. We related fluxes to soil moisture dynamics and agricultural practice. Gases were measured using manual and automated chamber techniques. Soil moisture content was measured using manual (auger) and automated (Time Domain Reflectometry; TDR) sampling techniques. A 3-phase-mixing model was found suitable to calibrate TDR technique for the studied soils. The field experiment

was based on a split-plot design, comparing clay versus loam, each under fertilized and unfertilized annual and perennial crop. Soils feature relatively low bulk density, high hydraulic conductivity and high organic matter content. Mean soil moisture content was above 70 % water-filled-pore-space (WFPS) in both soils and land uses. N₂O was emitted throughout the year.

Fluxes from forest soils showed no seasonality. Forest conversion caused fluxes to increase temporarily. Fertilization was the dominant source for temporal variability under agricultural use, differences in flux dynamics were large between individual post-fertilization phases. N₂O-loss as % of applied fertilizer-N increased with soil moisture. Spatial variability was generally high, especially post-fertilization. Repeated fertilization increased mean and variation of fluxes. Emissions simulated by regression models and by the physically based Denitrification-Decomposition model matched field measured fluxes well. Both modeling techniques confirmed that nutrient availability and soil moisture content were the dominant flux controls. In aggregated soils differences in soil structure between the surface layer and soil at 0.05 m depth may affect moisture content and consequently soil N₂O fluxes.

CHAPTER I

NITROUS OXIDE, NITRIC OXIDE, AND METHANE FLUXES FROM SOILS FOLLOWING CLEARING AND BURNING OF TROPICAL SECONDARY FOREST

Abstract

Conversion of humid tropical forest to agriculture significantly alters trace gas emissions from soils. We report nitrous oxide (N_2O), nitric oxide (NO), and methane (CH_4) fluxes from secondary forest soils prior to and during deforestation, and throughout the first agricultural cropping. Annual average nitrogen oxide emissions from forest soils were $1.5 \text{ ng N cm}^{-2} \text{ h}^{-1}$ for N_2O and $0.9 \text{ ng N cm}^{-2} \text{ h}^{-1}$ for NO. Forest clearing increased the level of extractable nitrate in soils and average nitrogen oxides fluxes ($2.7 \text{ ng N cm}^{-2} \text{ h}^{-1}$ for N_2O , and $8.1 \text{ ng N cm}^{-2} \text{ h}^{-1}$ for NO). Immediately after biomass burning, short-term peaks of N_2O and NO ($123 \text{ ng N cm}^{-2} \text{ h}^{-1}$ for N_2O , and $41 \text{ ng N cm}^{-2} \text{ h}^{-1}$ for NO) were superimposed on generally increased fluxes. Peak emissions declined within 3 days after burning. Postburn fluxes stayed higher than measured on adjacent forest sites for 3 to 4 months (averages for postburn fluxes were $17.5 \text{ ng N cm}^{-2} \text{ h}^{-1}$ for N_2O , and $19.2 \text{ ng N cm}^{-2} \text{ h}^{-1}$ for NO). Increased N_2O and NO emissions after clearing and until cropping were probably due to a combination of increased rates of nitrogen cycling and higher gaseous diffusion in drying soils. Compared to emissions from young pastures in the region, fluxes of nitrogen oxides from unfertilized agricultural areas were low ($3.9 \text{ ng N cm}^{-2} \text{ h}^{-1}$ for N_2O and $3.4 \text{ ng N cm}^{-2} \text{ h}^{-1}$ for NO), probably

due to nitrogen uptake by fast growing corn plants and losses by leaching with draining soil water in the wet season. Variation in CH_4 fluxes was high for all land use periods. Forest soils consumed an average of $1.0 \text{ mg CH}_4 \text{ m}^{-2} \text{ d}^{-1}$, which slightly increased in drier soils after clearing ($1.2 \text{ mg CH}_4 \text{ m}^{-2} \text{ d}^{-1}$). Postburn CH_4 consumption by soils was slightly reduced ($0.8 \text{ mg CH}_4 \text{ m}^{-2} \text{ d}^{-1}$) compared to forest soils. Unfertilized agricultural soils consumed less CH_4 than forest soils.

1. Introduction

Soil-atmosphere fluxes of nitrous oxide (N_2O), nitric oxide (NO), and methane (CH_4) affect processes relevant to global warming and environmental pollution (Ramanathan et al., 1987; Intergovernmental Panel on Climate Change (IPCC), 1996). N_2O is an important greenhouse gas because of the spectral properties of the molecule and its relatively long lifetime. N_2O also is involved in stratospheric ozone chemistry (Cicerone, 1987). NO is highly reactive; hence it is important for local and regional atmospheric photochemistry (Williams et al., 1992). In the troposphere, NO is involved in chemical production processes of different environmental pollutants, such as ozone and nitric acid. CH_4 , currently increasing in the atmosphere, is an important greenhouse gas (Ramanathan et al., 1987; Graedel and Crutzen, 1993). Soils are significant sources and sinks of N_2O , NO , and CH_4 . The biological, chemical, and physical conditions in soils determine soil-atmosphere trace gas exchange.

Nitrogen oxides are produced in soils by biotic and abiotic processes, but soil microbial activity is the most important source and sink for NO and N_2O . Several reviews (e.g. Firestone and Davidson, 1989; Galbally, 1989; Robertson, 1989; Williams

et al., 1992; Davidson et al., 1993) discuss soil microbial production and consumption of nitrogen oxides and the controlling factors for soil-atmosphere nitrogen oxide exchange. Briefly, decomposition of soil organic nitrogen compounds releases ammonium (NH_4^+); nitrogen mineralization rates determine the further nitrogen flow in soils. Aerobic microbial metabolism converts NH_4^+ into nitrite (NO_2^-) and nitrate (NO_3^-) (nitrification). Both oxides are reduced to gaseous forms during anaerobic microbial oxidation of organic matter (denitrification). Both microbial processes are sources for NO and N_2O . On the microscale aerobic and anaerobic sites can occur in close proximity (van Cleemput and Samater, 1996); therefore nitrification and denitrification may occur simultaneously in soils. Ultimately, net NO and N_2O soil-atmosphere exchange depends on the balance between gas production and consumption and the rate of nitrogen cycling in the ecosystem (Galbally, 1989).

Soils are important sources and sinks of CH_4 . Soil water content strongly affects CH_4 dynamics. Microbial consumption of CH_4 occurs in most well-aerated soils. Anaerobic soil conditions support microbial CH_4 production. Commonly unsaturated soils are net CH_4 sinks (Steudler et al., 1989; Crill, 1991). Uptake of CH_4 decreases with increasing soil water content and with addition of nitrogen as ammonium-N in fertilizers or from atmospheric deposition (Steudler et al., 1989; Mosier et al., 1991). In moist soils, anaerobic and aerobic microsites can exist in close proximity; thus CH_4 consumption and production can be measured in adjacent areas. Born et al. (1990) suggested that soil CH_4 uptake rates are constrained primarily by gas transport processes and only secondarily by microbial activity.

Humid tropical ecosystems are characterized by high rates of nitrogen mineralization and decomposition of organic matter. On the global scale, tropical forest soils are the largest natural nitrous oxide source, emitting about 3 Tg N_2O -N annually (1 Tg = 10^{12} g), which accounts for 21% of the total annual N_2O production (Matson and Vitousek, 1990). NO fluxes from humid tropical forest soils are of similar range as N_2O emission (Williams et al., 1992; Davidson and Kinglerlee, 1997).

Each year 20 to 60 million hectares of tropical land, mainly forest and savanna, are cleared and burned in preparation for shifting cultivation or permanent agricultural use (Crutzen and Andreae, 1990). Forest conversion affects soil biogeochemical and physical properties. Biomass burning instantaneously increases NO and N_2O emissions through volatilization. On longer timescales, nitrogen mineralization, nitrification, and soil inorganic nitrogen content increase (Ewel et al., 1981; Matson et al., 1987; Anderson et al., 1988). Correspondingly elevated nitrogen gas emissions are measured for periods of several months (Anderson et al., 1988; Neff et al., 1995) up to years after forest conversion (Luizao et al., 1989; Keller et al., 1993). Levine et al. (1996) found that both burning and wetting increase NO fluxes from savanna soils, while N_2O fluxes from those dry soils were below detection limit. Nitrification was the dominant source for NO emissions during the conversion of tropical lowland forest in Costa Rica (Neff et al., 1995). Tropical forest soils commonly are net CH_4 sinks, but under agriculture and pastures, soils may become net CH_4 sources where compaction reduces gaseous diffusion rates favoring anaerobic CH_4 production (Keller et al., 1990, 1993).

We report on trace gas fluxes (NO, N_2O , and CH_4) from two soil types (clay and

loam) measured under secondary forest, during forest conversion, and from the first crop cycle after forest clearing and burning. We include NO emission data for the clearing period originally presented by Neff et al. (1995). Simultaneously with trace gas emissions we measured physical and chemical soil properties.

2. Study Area

The study was performed at the La Selva Biological Station (10°26' N x 84°0' W) in the Atlantic lowlands of the province of Heredia, Costa Rica. The climate is humid tropical, with an average temperature of 25.8 °C and annual precipitation of 3962 mm (Sanford et al., 1994). Precipitation is distributed throughout the year with a maximum monthly mean of 481 mm in July. A weak dry season occurs between January and April with a minimum monthly mean precipitation of 152 mm in March.

In 1993 we selected four 1-ha sites of secondary forest at the La Selva Biological Station. Sites were located on two soil types, both developed on alluvial deposits of andesitic volcanic material (Sollins et al., 1994). Two sites were on a fertile, loamy soil developed on low river terraces (*fluventic Eutropept*), and two were on less fertile clay soils developed on high river terraces (*andic Dystropept*). Physical and chemical soil characteristics are given in Table 1.1. Large parts of the original forest in the areas were cleared for agriculture about 1953. Both Eutropept sites were used for cacao plantations (*Theobroma cacao*) with shade trees of various species, including *Cordia alliodora* (laurel) and *Bactris gasipaes* (peach palm, or pejobaye). Most shade trees were remnants of the partially cleared forest. One Dystropept site was used for a peach palm plantation, and the other was used for pasture. The plantations were abandoned about 1968, and the pastures were abandoned 10 years later. Secondary forest developed on all sites. This

forest is different from primary forest in species composition (Hartshorn and Hammel, 1994); also, secondary forest shows a well-developed understory vegetation.

Table 1.1. Soil Characteristics for Soils Under Forest Cover

Depth, m	Bulk Density		C _{org} , %	N _t , %	pH (H ₂ O)
	Average	s.d.			
Dystropept Forest (Clay)					
0.05	0.77	0.06	7.3	0.4	4.7
0.15	0.88	0.11	4.5	0.3	4.7
0.30	0.88	0.13	2.9	0.2	4.8
0.50	0.83	0.08	1.6	0.1	4.9
0.70	0.82	0.06	1.3	0.1	4.9
0.90	0.83	0.05	1.3	0.1	4.9
Eutropept Forest (Loam)					
0.05	0.66	0.05	7.6	0.4	6.0
0.15	0.74	0.09	4.0	0.3	5.9
0.30	0.69	0.04	3.1	0.2	5.9
0.50	0.71	0.05	1.5	0.1	6.0
0.70	0.76	0.04	0.9	0.1	5.9
0.90	0.93	0.02	1.0	0.0	6.2

3. Site Preparation and Management

In January 1994 (Dystropept) and March 1994 (Eutropept), secondary forest was cleared by manual labor using chain saws and machetes. After removal of the understory, trees were felled and some timber was removed. The remaining slash was chopped and cut into about 1-m-long pieces and allowed to dry on site. Clearing took about 2 weeks for each site. In March 1994 (Dystropept) and April 1994 (Eutropept), dry biomass was burned. For several days after the initial fire, unburned wood was piled by hand and reburned. With start of the wet season in the second half of May 1994, corn (*Zea mays*) was planted by use of planting sticks, the traditional seeding technique applied by local

farmers. Plots were weeded by machete and thinned about 6 weeks after planting. In order to follow traditional low-input farming techniques of the region, we did not fertilize, till the soil, or apply pesticides. Corn was harvested about 4 months after seeding.

The sequence of forest, clearing operations and agriculture provided useful land management periods for the analysis of our experiment: (1) forest, covering all measurements from secondary forests prior to clearing and from adjacent forest sites following clearing; (2) cleared, starting with the day of the cutting and covering the time of full canopy clearance until the biomass was burned; (3) postburn, including the few days of reburning slash until planting; and (4) agriculture, signifying the first cropping cycle established after forest conversion and including the fallow phase after corn harvest (September 20-22, 1994) until planting of the second corn crop (November 15-17, 1994). The time covered by each land management period is given in Table 1.2.

Table 1.2. Time Schedule of Land Management Categories on Both Soil Types

Land Use	Dystropept (Clay)		Eutropept (Loam)	
	Forest	Jul. 1, 1993	to Jan. 10, 1994	Jul 1, 1993
Cleared	Jan. 11, 1994	to Mar. 13, 1994	Feb. 25, 1994	to Apr. 5, 1994
Postburn	Mar. 14, 1994	to May 19, 1994	Apr. 6, 1994	to May 24, 1994
Agriculture	May 20, 1994	to Nov. 15, 1994	May 25, 1994	to Nov. 17, 1994

4. Methods

In July 1993 we started measurements of NO, N₂O, and CH₄ fluxes from secondary forest soils. For gas collection each site was equipped with eight chamber bases (polyvinylchloride (PVC) rings of 0.25 m diameter and 0.12 m height, inserted about 0.02 m into the soil surface). Sampling spots were selected randomly following the

procedure described by Keller and Reiners (1994); chamber bases were maintained throughout the forest and cleared periods. We removed chamber bases immediately before burning of slash, and reinstalled them for permanent use on randomly selected points the day after the fire. Concurrent with clearing, we installed chamber bases at randomly selected points in adjacent forest areas to complete a full year of flux measurements under secondary forest. Forest sites were sampled monthly. During the cleared and postburn periods we sampled more frequently. Under agricultural use, gas fluxes were sampled monthly. During agriculture we started sampling N_2O fluxes in high time resolution (4.6-hour interval) using an automated chamber sampling and measurement system (P.M. Crill, unpublished data, 1998).

Techniques used to measure N_2O , CH_4 and NO fluxes are presented in detail by Keller and Reiners (1994); a slight revision for N_2O was done in October 1993 (Veldkamp and Keller, 1997). Briefly, gas for the analysis of N_2O and CH_4 was sampled from static, vented field chambers (headspace, 0.01 m^3) at 1, 7, 14, 21, and 28 min after a chamber was closed with a removable acrylonitrile-butadiene-styrene top, which exactly fits the PVC chamber base. Chamber tops had two ports to allow gas sampling using nylon syringes while maintaining equilibrium with atmospheric pressure. Gas samples were analyzed within 36 hours after collection. N_2O was measured with an electron capture detector (ECD) (Shimadzu GC-8A equipped with a ^{63}Ni detector) and CH_4 with a flame ionization detector (FID) (Shimadzu GC-mini FID) gas chromatography. Sample concentrations were determined by comparison to commercially prepared standard gases which had been calibrated against NOAA Climate Monitoring and Diagnostics Laboratory (CMDL) and National Institute of Standards and Technology (NIST)

standards. Gas fluxes were calculated from linear regressions of concentration versus time.

NO was determined indirectly after conversion to NO₂. Air was sampled in a continuous air flow from dynamic chambers that also precisely fit the permanent PVC chamber bases. Chamber headspace (0.01-m³ headspace volume) was sampled at a flow rate of 300 mL min⁻¹ and mixed with purified air (1200 mL min⁻¹) prior to analysis; ozone was not scrubbed from air entering the chamber. NO was converted to NO₂ on a CrO₃ catalyst; then NO₂ was quantified by luminol chemiluminescence detection (Scintrex LMA-3). A standard addition of approximately 3 mL min⁻¹ of 1-ppm NO in oxygen-free nitrogen maintained the signal in the instrument's linear range. Between chamber measurements we used larger standard additions to calibrate the instrument response. NO fluxes were calculated from the linear increase in concentration with time after chamber closure.

Measurements were performed between 0730 and 1430 LT. During that period, average changes in air temperature are about 7.5 °C. From previous studies we expected only minor influence of diurnal temperature variation on soil gas fluxes (M. Keller, unpublished data, 1993). Simultaneously with gas sampling we measured shaded air temperature near the soil surface and soil temperature at 0.02-, 0.05-, and 0.1-m depth. Air temperature data were used in gas flux calculations. We report trace gas fluxes from the soil to the atmosphere as positive values; negative fluxes indicate gas consumption by soils.

On each measurement day we collected soil samples (0- to 0.1 m depth) from eight randomly selected locations, gathering soil from four spots into one bulk sample.

The resulting two soil samples (each about 400 g fresh weight) were used to determine soil moisture content and extractable inorganic nitrogen (Keller and Reiners, 1994). The gravimetric soil water content θ_g (g g^{-1}) was derived after oven drying of soil to constant weight within 48 hours at 105 °C and was converted to proportion of water-filled pore space (% wfps) using the formula given by Linn and Doran (1984)

$$\% \text{ wfps} = (\theta_g \times \text{bd} \times 100\%) / (1 - (\text{bd} / 2.65))$$

with bulk density (bd (Mg m^{-3})) data measured from forest soils (Table 1.1), and particle density estimated as 2.65 Mg m^{-3} .

For the determination of soil extractable inorganic nitrogen (nitrate (NO_3^-) and ammonium (NH_4^+)) we prepared 2 M KCl extractions (Keeney and Nelson, 1982) (mixing ratio, 7.5 KCl :1 field moist soil). Soil extracts were refrigerated until samples were analyzed using standard colorimetric methods with an ALPKEM Analyzer (ALPKEM Corporation, 1990). All chemical analyses were done at the laboratory of the U.S. Forest Service, Río Piedras, Puerto Rico.

For soil carbon and total nitrogen analyses bulk soil samples were taken from one soil pit per site at 0.05-, 0.15-, 0.3-, 0.5-, 0.7-, and 0.9 m depth, air dried, passed through a 2 mm sieve, and shipped to the laboratory. Soil organic carbon was determined using the modified Walkley-Black procedure (Nelson and Sommers, 1982), and converted to soil organic matter using the factor 2.16. Soil total nitrogen was determined using the modified Kjeldahl method (Bremner and Mulvaney, 1982). Undisturbed soil samples of $3 \times 10^{-4} \text{ m}^3$ volume were taken at the same profile depths to determine bulk density and soil water retention properties using a hanging water column device (Klute, 1986). Field

capacity was estimated from water retention curves as the soil water content at 6 kPa suction.

We analyzed the variation between soil types and land management periods using analysis of variation (ANOVA) techniques with a split-plot design. Geographically the sites were located in two blocks, spatially separated by about 1.3 km. Each block had two main plots, one on a Eutropept and one on a Dystropept. Each soil type was subdivided into four subplot treatments (forest, cleared, postburn, and agriculture). We choose a conservative test to evaluate a potential effect of the physical location of the plots next to an effect of the soil types and treatments. The analyzed statistical model is

$$y = \mu + \text{block} + \text{soil} + (\text{block} * \text{soil}) + \text{treatment} + (\text{soil} * \text{treatment}) + \varepsilon$$

where y is the considered response variable; μ is the overall mean for the variable; block, soil (main plots), and treatment (subplots) are effects in the model; (block*soil) is the main plot error term; and (soil*treatment) is an interaction term in the ANOVA model; and ε is the subplot error. The F value for the block and the soil effect is calculated using the mean of the sum of squares for the interaction term (block x soil) as the 'main plot', while the mean of the sum of squares for ε is used with the treatment effect and the (soil x treatment) interaction term. For each measured variable we converted daily averages into average responses for each treatment, resulting in a balanced design comparing 16 treatment means. For statistical analysis, NO and N₂O fluxes were log transformed. We analyzed data using the JMP IN software, developed by SAS Institute (Sall and Lehman, 1996). The Tukey criterion was used in multiple comparison tests to distinguish significant differences ($p=0.05$) for treatments and soil-treatment interaction terms. These calculations were done off-line from JMP IN. This analytical design represents the best

approximation of the experiment, ignoring inconsistencies in the temporal and spatial layout which result from the applied slash-and-burn practice and of restrictions in the number of measurements feasible. For analysis of CH₄ dynamics we compared a linear regression model derived for forest to CH₄ flux data measured during subsequent land management periods, and described statistics of the residuals using SigmaPlot version 2.0 for Windows.

5. Results

Bulk densities were low in both soil types (Table 1.1), with higher densities measured in the Dystropept (clay) profile compared to the Eutropept (loam). In both soils the topsoil structure is dominated by well developed, loosely packed crumb aggregates. Generally, throughout the experiment, soils remain highly porous and show high values for total porosity.

Statistical analysis showed no block effect. There was no significant effect due to soil type, but each variable treatment had a significant effect, and CH₄ also had a significant (soil x treatment) interaction. We discuss results for each variable in the following paragraphs. For details on differences between mean values, see Table 1.3.

Monthly rainfall between July 1993 and November 1994 always exceeded 50 mm (Figure 1.1). The period from mid-January to mid-May 1994 was moderately dry (subsequently referred to as 'dry season'). For both soil types, soil moisture data were above field capacity most of the wet season and dropped below field capacity during the dry period (Figure 1.1). Forest soils became drier than cleared soils. Average soil water content under forest (78% wfps Dystropept, and 75% wfps Eutropept) differed significantly between soil types.

Table 1.3. Statistics of Measured Variables, Distinguished per Soil Type and Land Management Category

Period		NH ₄ ⁺ -N, g gds ⁻¹	NO ₃ ⁻ -N, g gds ⁻¹	NO, ng-N cm ⁻² h ⁻¹	N ₂ O, ng-N cm ⁻² h ⁻¹	CH ₄ , mg m ⁻² d ⁻¹	Water- Filled Pore space, %
Dystropept Soil							
Forest	avg.	7.09 ^a	5.66 ^a	0.86 ^a	1.62 ^a	-0.94 ^a	76.79 ^a
	s.d.	3.72	4.08	0.80	1.38	0.78	12.01
	n	(19)	(19)	(20)	(20)	(20)	(20)
Cleared	avg.	7.04 ^a	23.78 ^a	4.50 ^b	2.81 ^a	-1.04 ^a	74.44 ^b
	s.d.	2.35	16.65	5.39	3.94	0.46	6.65
	n	(16)	(16)	(16)	(16)	(16)	(16)
Postburn	avg.	17.57 ^b	69.87 ^b	16.53 ^c	9.30 ^b	-0.58 ^{bc}	72.32 ^{ab}
	s.d.	6.15	25.21	12.55	10.10	0.51	8.82
	n	(17)	(17)	(16)	(17)	(17)	(17)
Agriculture	avg.	8.16 ^a	15.43 ^a	5.50 ^a	5.76 ^a	-0.49 ^b	76.70 ^{ab}
	s.d.	12.75	14.24	13.41	6.18	0.54	8.10
	n	(21)	(21)	(21)	(21)	(21)	(21)
Eutropept Soil							
Forest	avg.	7.45 ^a	7.93 ^a	0.94 ^a	1.46 ^a	-0.98 ^{ac}	73.62 ^a
	s.d.	4.27	7.36	1.06	1.21	0.53	10.20
	n	(22)	(22)	(22)	(22)	(22)	(24)
Cleared	avg.	5.59 ^a	15.94 ^a	12.92 ^b	2.64 ^a	-1.45 ^d	63.08 ^b
	s.d.	2.15	11.78	10.21	2.80	0.48	6.31
	n	(12)	(12)	(12)	(12)	(12)	(12)
Postburn	avg.	18.13 ^b	38.00 ^b	22.76 ^c	28.04 ^b	-0.99 ^a	65.90 ^{ab}
	s.d.	14.76	13.13	17.01	35.63	0.55	3.11
	n	(17)	(17)	(17)	(18)	(18)	(18)
Agriculture	avg.	5.15 ^a	7.43 ^a	1.33 ^a	2.11 ^a	-0.36 ^b	69.18 ^{ab}
	s.d.	3.05	3.71	1.07	1.38	0.67	6.04
	n	(21)	(21)	(21)	(21)	(21)	(21)

Different letter superscripts per variable and category indicate significantly different means; s.d. is standard deviation, and n is number of daily averaged measurements.

For both soil types we show changes in soil inorganic nitrogen (KCl-extractable NO₃⁻ and NH₄⁺) content from forest to agricultural land management in Figure 1.2. Average values for each variable, soil and land management period are listed in Table 1.3. In forest soils, inorganic nitrogen content was comparable for both soil types ($6.9 \pm 6.2 \mu\text{g NO}_3^- \text{N gds}^{-1}$ (mean \pm standard deviation; $n=41$), $7.3 \pm 3.8 \mu\text{g NH}_4^+ \text{N gds}^{-1}$ ($n=41$))

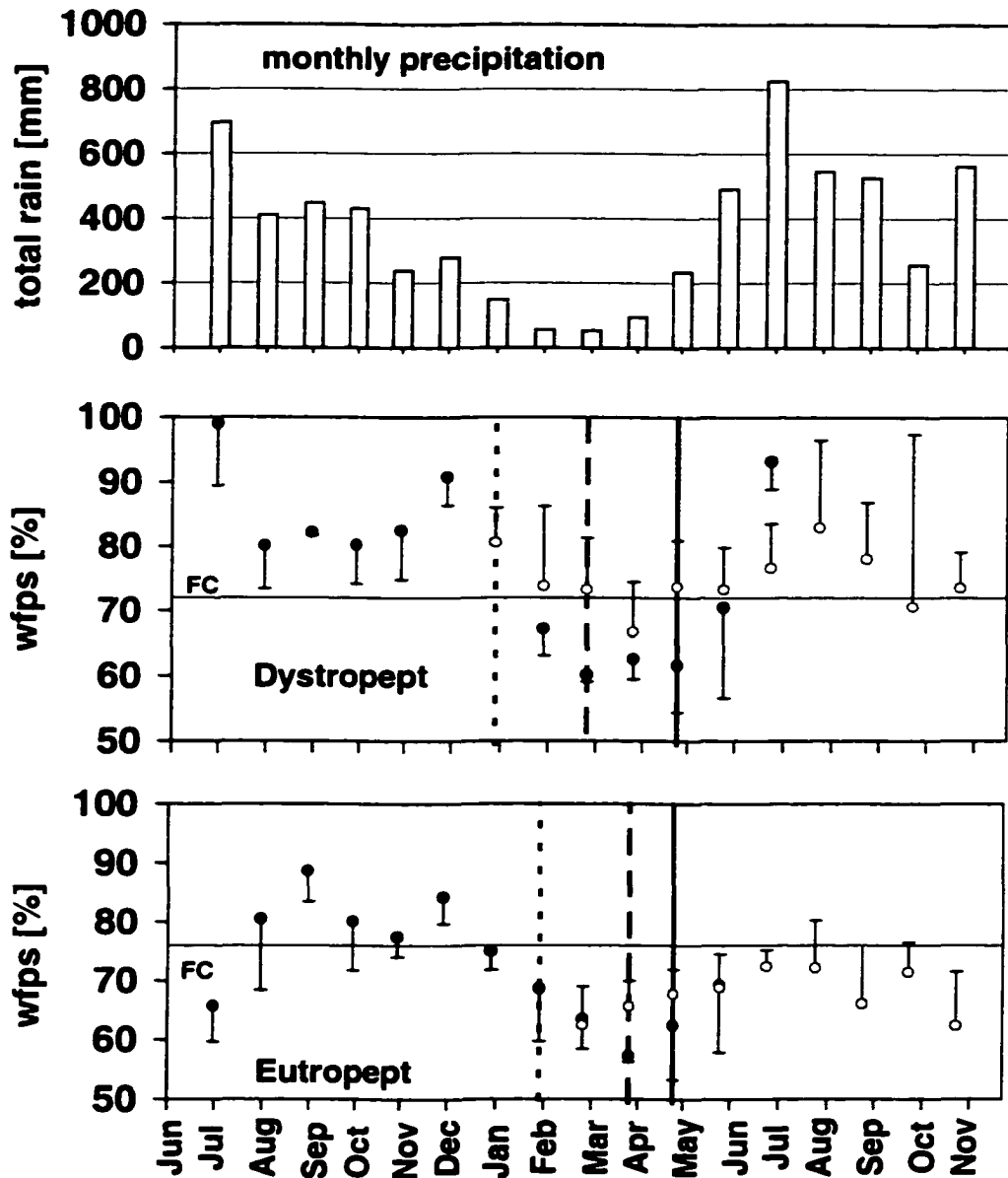


Figure 1.1: Monthly precipitation derived from rainfall data, automatically recorded at the La Selva Biological Station. Water filled pore space (wfps) data are monthly averages; error bars are standard deviations. Solid dots indicate forest soils; open circles indicate agricultural soils. Horizontal lines are field capacity (FC) values estimated from laboratory water retention measurements (71% wfps ($0.52 \text{ cm}^3 \text{ cm}^{-3}$) for the Dystropept, and 76% wfps ($0.58 \text{ cm}^3 \text{ cm}^{-3}$) for the Eutropept). Vertical lines indicate transitions between land use periods: the dotted lines shows the start of cleared (C), the dashed line shows the start of the postburn (B), and the solid line the start of the agriculture (A) period.

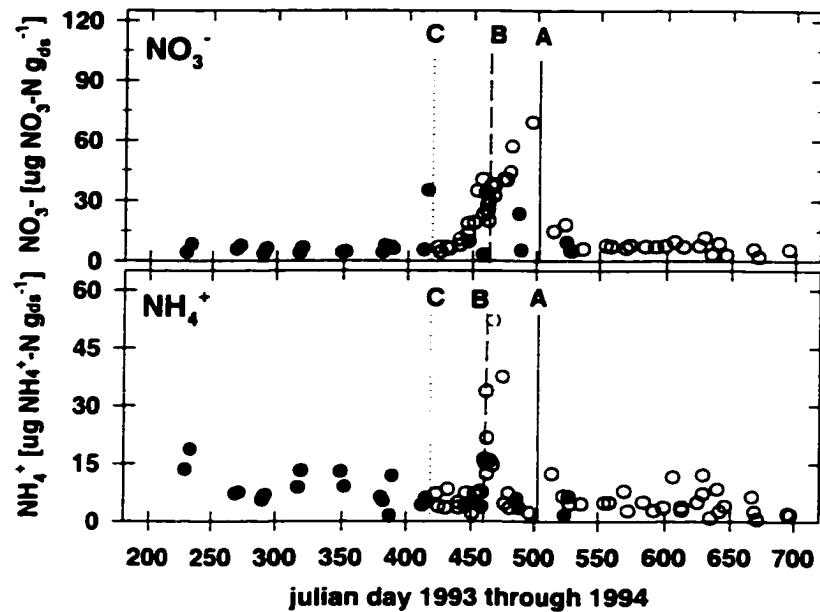
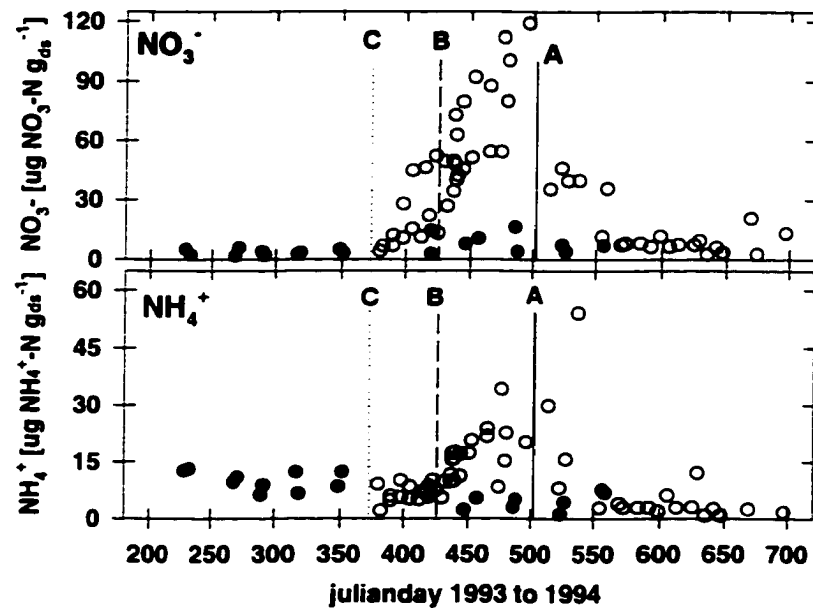
Eutropept**Dystropept**

Figure 1.2: Time series of extractable soil inorganic NO_3^- and NH_4^+ concentrations for both Eutropept and Dystropept soil types. Concentrations are given on microgram nitrogen per gram dry soil basis ($\mu\text{g N g}_{\text{ds}}^{-1}$). Solid circles are daily average concentrations in forest soils, open circles are for cleared soils. Vertical lines indicate transitions between land use periods as in Figure 1.

with little variation throughout the year ($4.9 \pm 2.0 \mu\text{g NO}_3^- \text{-N g}_{\text{ds}}^{-1}$ ($n= 25$) wet season, and $10.9 \pm 5.9 \mu\text{g NO}_3^- \text{-N g}_{\text{ds}}^{-1}$ ($n= 15$) dry season; $8.9 \pm 3.6 \mu\text{g NH}_4^+ \text{-N g}_{\text{ds}}^{-1}$ ($n= 25$) wet season, $5.2 \pm 2.7 \mu\text{g NH}_4^+ \text{-N g}_{\text{ds}}^{-1}$ ($n= 15$) dry season). After forest clearing soil extractable inorganic NO_3^- increased rapidly (Table 1.3, Figure 1.2) until cropping, which coincided with the beginning of the wet season. Postburn NO_3^- concentrations were significantly different from all other land management periods. Clearing had little effect on soil extractable NH_4^+ concentrations. Biomass burning increased NH_4^+ level in both soils. Postburn NH_4^+ concentrations differed significantly from all other land use periods (Table 1.3). During the agriculture period, amounts of extractable soil inorganic nitrogen decreased rapidly (Figure 1.2).

NO , N_2O , and CH_4 fluxes measured between July 1993 and November 1994 for subsequent land management periods are shown for the example of the Dystropept (Figure 1.3). Average nitric oxide fluxes from forest soils were comparable for both soil types (Figure 1.4, Table 1.3); annual emissions average $0.9 \pm 1.2 \text{ ng N cm}^{-2} \text{ h}^{-1}$ ($n= 41$). Fluxes were slightly higher during the dry season ($2.0 \pm 1.7 \text{ ng N cm}^{-2} \text{ h}^{-1}$; $n= 13$). The maximum daily average NO flux measured from forest soils was $4.0 \text{ ng N cm}^{-2} \text{ h}^{-1}$. Clearing increased NO emissions significantly. Fluxes from the relatively dry Eutropept were about 3 times as high as those from the much wetter Dystropept (Figure 1.4, Table 1.3). Variation among individual measurement days was high. On both soil types a peak of NO fluxes (maximum daily average of $38 \text{ ng N cm}^{-2} \text{ h}^{-1}$ on the Eutropept and $41 \text{ ng N cm}^{-2} \text{ h}^{-1}$ on the Dystropept) was associated with biomass burning. Peaks lasted 2-3 days

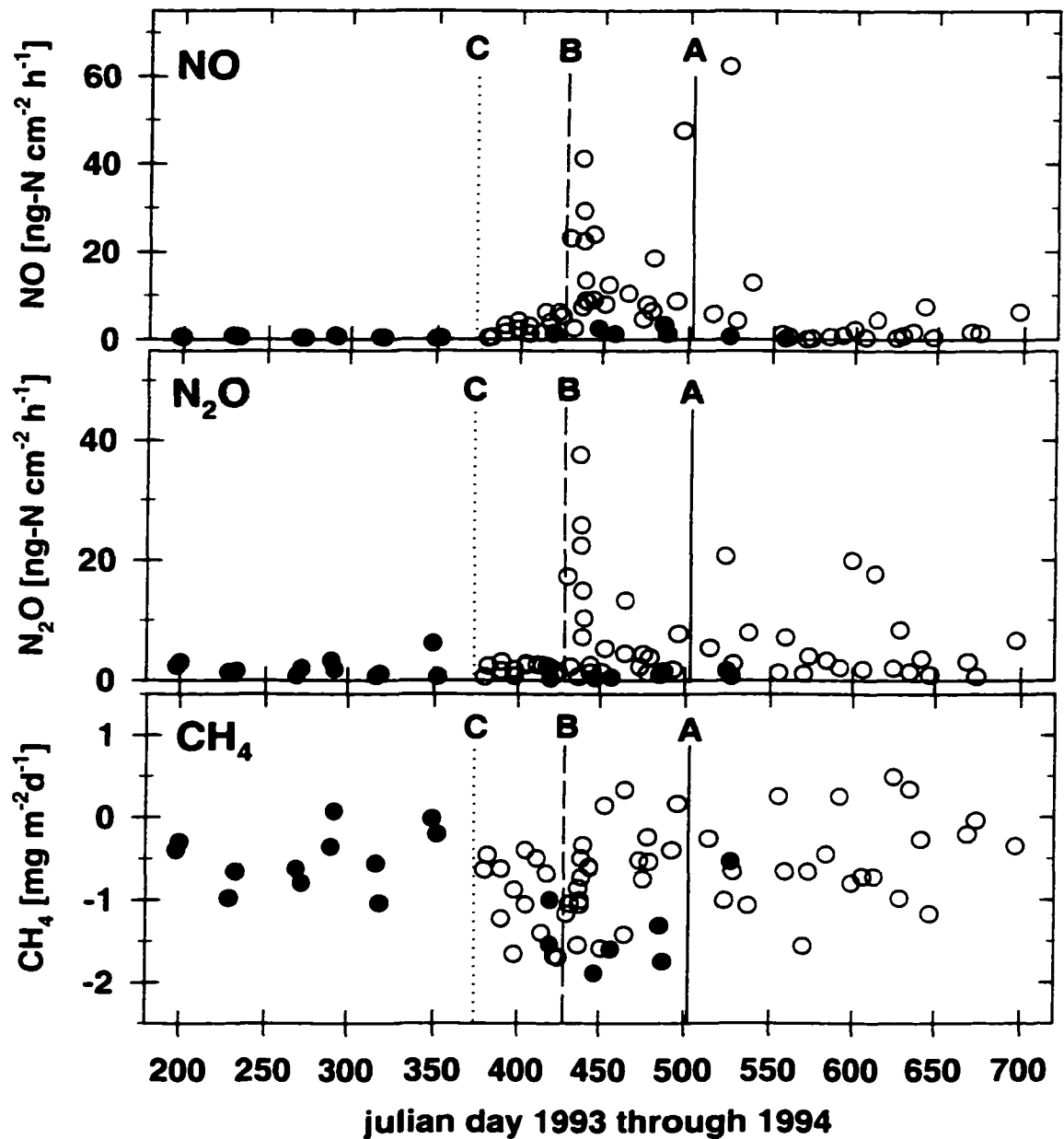


Figure 1.3: Time series of NO, N_2O and CH_4 fluxes from Dystropept soils under forest and during forest conversion. Solid circles are daily average fluxes measured on forest soils; open circles are fluxes after clearing. Vertical lines indicate transitions between land use categories as in Figure 1.

and were superimposed on generally elevated fluxes. For both soil types the high postburn NO fluxes were significantly different from all other land management periods.

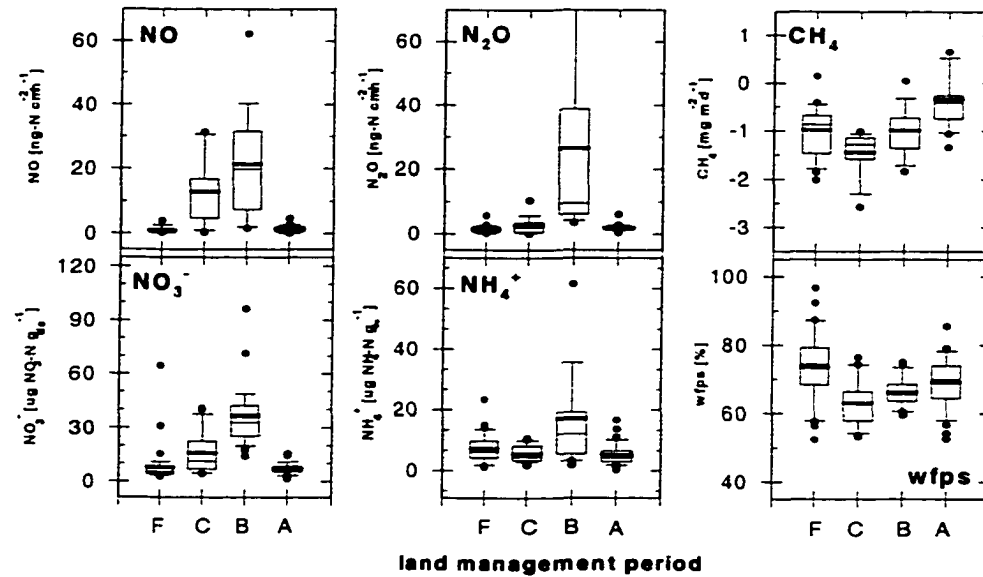
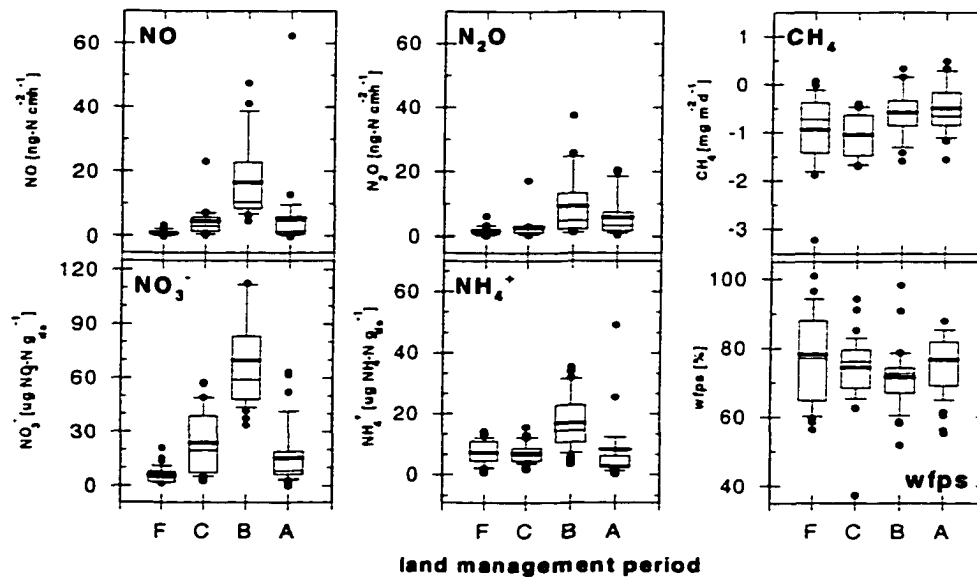
Eutropept**Dystropept**

Figure 1.4: Boxplot summary of the measurements for both Eutropept and Dystropept soil types for all four land management periods (F, forest; C, cleared; B, postburn, A, agriculture). The thick horizontal line in boxes indicates sample mean, the thin line is the sample median, box edges are 25th and 75th percentiles, bars are 5th and 95th percentiles, and dots are extreme values below or above the 5th and 95th percentile. For the Eutropept we did not show extreme values for N₂O postburn (127 and 72 ng-N cm⁻²h⁻¹) and NH₄⁺ postburn (91 μg NH₄⁺-N g_{ds}⁻¹), and for the Dystropept we did not show extreme values for NO₃⁻ postburn (128 and 142 μg NO₃⁻-N g_{ds}⁻¹), and NH₄⁺ agriculture (97 μg NH₄⁺-N g_{ds}⁻¹).

NO emissions declined rapidly on cropped soils. NO fluxes from agricultural soils were not significantly different from forest soil fluxes (Table 1.3).

Annual average N₂O emissions for all forest sites were 1.5 ± 1.3 ng N cm⁻² h⁻¹ ($n= 40$) with higher fluxes during the wet season (1.9 ± 1.4 ng N cm⁻² h⁻¹; $n= 28$) compared to the dry season (0.8 ± 0.6 ng N cm⁻² h⁻¹; $n= 12$). Clearing increased N₂O fluxes only slightly. Brief peaks of N₂O emissions associated with biomass burning were higher on the Eutrocept (123 ng N cm⁻²h⁻¹) than on the Dystrocept (38 ng N cm⁻²h⁻¹). Postburn N₂O emissions remained elevated; variation among daily averages was high on both soil types. Postburn fluxes differed significantly from the other land management periods (Table 1.3).

Forest soils consumed CH₄ (1.0 ± 0.7 mg CH₄ m² d⁻¹; $n= 40$). Average CH₄ consumption was less during the wet season (0.7 ± 0.6 mg CH₄ m² d⁻¹; $n= 27$) and greater in the dry season (1.5 ± 0.4 mg CH₄ m² d⁻¹; $n= 13$). Variation between measurement days was high. CH₄ emissions were measured occasionally from burned sites. Postburn CH₄ fluxes differed significantly from fluxes measured during the cleared period (Table 1.3).

6. Discussion

For both soil types the range of bulk densities (Table 1.1) compares to data for forest soils from the same region (Reiners et al., 1994). No heavy machinery was used for forest clearing; traditional clearing techniques caused very little surface disturbance.

Biomass burning may have stimulated mineralization resulting in significantly increased postburn NH₄⁺ concentrations on both soil types (Table 1.3). Forest was

cleared and slash was burned earlier in the dry season on the Dystropept than on the Eutropept (Table 1.2). We observed different traces of NH_4^+ accumulation in soil types with time after biomass burning (Figure 1.2) primarily because of precipitation. During the postburn period the Dystropept received little rain (4.3 mm the first two weeks, and 27 mm the third week); soil NH_4^+ concentrations increased gradually. In contrast, on the Eutropept, NH_4^+ concentrations increased steeply during the week after biomass burning (Figure 1.2), suggesting that on these sites there was a potential for considerable NH_4^+ accumulation in case dry conditions had continued. Rain (21.3 mm the first week, and 40.1 mm the second week postburn) probably leached NH_4^+ quickly from the upper 0.1 m of the soil, concentrations approached levels similar to forest soils within 2 weeks.

Addition of easily decomposable slash increased net nitrification and the concentration of soil extractable NO_3^- . We estimated the net rate of nitrification from NO_3^- buildup in soils during the cleared period, neglecting leaching losses for that dry time. Net nitrification was similar in the top 0.1 m of both soil types ($0.9 \mu\text{g NO}_3^- \text{-N gds}^{-1}$, about $32 \text{ kg NO}_3^- \text{-N ha}^{-1} \text{yr}^{-1}$). Net nitrification rate did not change after biomass burning (Figure 1.2), suggesting that any potential toxic effects of NO_2^- in ash on nitrifiers (Williams et al., 1992) was negligible on our sites. During the agriculture period, NO_3^- concentrations in soils dropped to levels measured under forest; they were significantly different from postburn levels (Table 1.3).

Clearing of secondary premontane forest in Costa Rica enhanced nitrification rates for about 6 months after which precut levels were approached again (Matson et al.,

1987). Clearing of secondary forest on an oxic Dystropept at La Selva Biological Station resulted in high nitrification rates and elevated NO_3^- pools in soils that were kept free from vegetation for a year (Robertson and Sollins, 1987). On our sites initially high inorganic nitrogen pools declined during agriculture, as growing corn took up available nitrogen, and leaching probably occurred with intense rain events. Leaching losses were reported by Radulovich et al. (1992) for soils at La Selva Biological Station. High denitrification rates were found immediately after clearing of secondary forest in Costa Rica (Matson et al., 1987; Robertson and Tiedje, 1988). For our sites increasing soil nitrate pools after clearing suggest smaller denitrification rates than gross nitrification rates.

NO and N_2O gas emissions from forest soils were similar for both soil types. Soil moisture is a major control of microbial nitrogen gas production and gas transport in soils. On our sites generally wet conditions may contribute to negligibly small seasonal variation in nitrogen oxides fluxes from forest soils. We measured NO fluxes that were about twice the annual mean measured from secondary forest, but comparable to emissions reported from old growth forest in the same area (Keller and Reiners, 1994) and to tropical forest sites in other regions (Williams et al., 1992). We report N_2O fluxes from secondary forest soils that were less than fluxes from forest soils in the same area ($4.3 \text{ ng N cm}^{-2}\text{h}^{-1}$ in secondary forest; $6.7 \text{ ng N cm}^{-2}\text{h}^{-1}$ in old growth forest (Keller and Reiners, 1994)), and only slightly lower than fluxes from tropical upland forest in Brazil ($2.3 \text{ ng N cm}^{-2}\text{h}^{-1}$ (Keller et al., 1988)), but slightly higher than fluxes from upland forest in Brazil ($1.3 \text{ ng N cm}^{-2}\text{h}^{-1}$ (Livingston et al., 1988)).

NO and N_2O fluxes are positively correlated with soil extractable NO_3^-

concentrations for both soil types during the *cleared* period suggesting that substrate availability is the primary determinant for gas fluxes with soil moisture as modifying factor. On the basis of inhibitor experiments by Neff et al. (1995), we assume that enhanced NO fluxes after forest clearing mainly resulted from microbial nitrification and less from microbial denitrification. We observed much lower NO fluxes from the cleared Dystropept than from the cleared Eutropept (Figure 1.4). Wet conditions in the clay soil probably hampered diffusive NO exchange between soil and atmosphere.

Biomass burning increased both the magnitude and variability of nitrogen gas fluxes (Figures 1.3 and 1.4). On both soils, NO and N₂O fluxes peaked after biomass burning. (Neff et al., 1995) measured high NO₂⁻ concentrations in ash (the average for both soil types is 22.4 μg NO₂⁻ g dry ash⁻¹). From laboratory experiments they conclude that the brief NO peak after biomass burning may have been caused by chemodenitrification of NO₂⁻. Nonenzymatic decomposition of NO₂⁻ (van Cleemput and Samater, 1996) could also have contributed to the brief peak in N₂O fluxes measured on all our sites shortly after biomass burning. Peaks were much higher on the Eutropept contributing to three times higher postburn N₂O fluxes compared to the Dystropept. During the postburn period, sufficient substrate was available for microbial activity (Figure 1.4). N₂O fluxes were enhanced at relatively high soil water contents (60-80% wfps), suggesting that denitrification may be important. In seasonally dry Mexican forest soils the major source for N₂O emissions during wet season was denitrification (Davidson et al., 1993). N₂O fluxes measured by Anderson et al. (1988) from wetted soil several days after burning of chaparral were of about the same magnitude as N₂O peaks

we found immediately after biomass burning. About 6 months after biomass burning, N_2O fluxes had decreased to levels comparable to fluxes measured 5 months after burning of tropical lowland forest (Luizao et al., 1989). We report postburn NO fluxes comparable to fluxes Anderson et al. (1988) measured after burning of a temperate chaparral.

Nitrogen oxides emissions dropped during the agriculture period, corresponding with significantly decreased soil inorganic nitrogen concentrations. For both gases (NO and N_2O) on both soil types, fluxes were significantly different from postburn, but were similar to fluxes from forest soils (Table 1.3). High variability in NO fluxes at the start of cropping (Figure 1.3) is caused by extremely high fluxes measured from two chambers. NO fluxes reported for young, unfertilized pastures in the Atlantic lowlands of Costa Rica (Keller et al., 1993) were 2-4 times higher than NO fluxes from unfertilized corn fields. N_2O emissions from those pastures were 10-15 times higher than fluxes from corn fields. In contrast to pasture soils, conversion of forest soils to agricultural soils did not increase bulk density in the upper layers, which may have contributed to lower N_2O losses. Results of our study suggest that recently cleared tropical soils under low-input agricultural use (no tillage, no fertilizer, no pesticide use) emit less nitrogen oxides than young pastures from the same region.

Under forest cover the soil NO_3^- concentration averages $4.4 \text{ kg NO}_3^- \text{-N ha}^{-1}$ on the Dystropept and $5.2 \text{ kg NO}_3^- \text{-N ha}^{-1}$ on the Eutropept. Net nitrification after forest clearing and until cropping increased the soil NO_3^- pool on the Dystropept by $81.0 \text{ kg NO}_3^- \text{-N ha}^{-1}$ estimated from the linear increase in soil NO_3^- concentration over the time

length for both periods. During the 2-month cleared period, 0.7 kg NO-N ha⁻¹ and 0.4 kg N₂O-N ha⁻¹ were lost in gaseous form as calculated from linear interpolation between subsequent flux measurements. During the postburn period the Dystropept lost 1.9 kg NO-N ha⁻¹ and 0.8 kg N₂O-N ha⁻¹. On the Eutropept, net nitrification increased the soil NO₃⁻ pool after clearing and until cropping by 43.1 kg NO₃⁻-N ha⁻¹. During the cleared period (1.5 months), 1.1 kg NO-N ha⁻¹ and 0.2 kg N₂O-N ha⁻¹ were lost in gaseous form. Postburn 1.8 kg NO-N ha⁻¹ and 1.3 kg N₂O-N ha⁻¹ was lost on the Eutropept. Different lengths of the cleared and postburn periods between soils caused differences in the estimated total amount of NO₃⁻ produced. On the Dystropept, 4.7% of the soil inorganic N gained by net nitrification during forest conversion was lost in gaseous form, while the loss was 10.2% on the Eutropept. Soil moisture conditions during the cleared and postburn periods caused differences between soil types.

Forest soils predominantly consumed CH₄ (Table 1.3). Mean annual CH₄ fluxes were -1.0 mg CH₄ m⁻²d⁻¹. Consumption was less during the wet season; we occasionally measured CH₄ production (positive fluxes in Figure 1.3). From forest soils in the same area, Keller and Reiners (1994) measured similar CH₄ consumption during the wet season, while dry season consumption was slightly larger than measured on our sites. *Born et al.* (1990) estimated that temperate zone forest soils consumed less than half the amount of CH₄ we measured for humid tropical forest soils. In contrast, Crill (1991) measured average CH₄ consumption of 1.9 to 2.3 mg CH₄ m⁻²d⁻¹ during 9 frost-free months from an Inceptisol under temperate zone hardwood forest in New

Hampshire, about twice as high as we measured from secondary tropical forest soils. Koschorreck and Conrad (1993) measured soil-atmosphere CH_4 exchange on a Luvisol (Alfisol in UDSA classification) under forest in Germany; they report 1.5 times higher CH_4 consumption during 9 frost-free months than we measured from humid tropical forest soils.

CH_4 fluxes showed high temporal and spatial variability during all land management periods (Figure 1.4). In aerobic soils methane oxidizing bacteria in the surface layers of soils consume CH_4 (negative fluxes). Results of several studies suggest that diffusion into the soil is the major limiting factor for soil CH_4 uptake rates (e.g. Crill, 1991; Striegl, 1993). Air-filled macropore porosity in soils is the physical determinant of gaseous CH_4 transport between soil and atmosphere (Born et al., 1990; Crill, 1991). To evaluate the diffusive control of CH_4 fluxes on our soils, we applied Millington and Shearer's (1971) model of gaseous diffusion in aggregated soils (for details, see appendix). Briefly, the Millington and Shearer model uses soil physical parameters (bulk density, total porosity ϵ , intra-aggregate porosity ϵ_{ra} , and interaggregate porosity ϵ_{er}) and measured soil water content θ_m to estimate effective gas diffusivity D_{eff} . We follow the approach presented by Davidson and Trumbore (1995) using field capacity θ_{fc} as key parameter to subdivide total porosity ϵ into ϵ_{ra} (macropore) and ϵ_{er} (mesopore and micropore porosity). Assuming macropores contain water only above field capacity, while below all soil water is located in the mesopore and micropore volume, this approach allows us to estimate the air-filled porosity for both pore classes from measured soil water content data. Diffusivity in soils (D_s) is calculated as a function of the air

volume in each of the two major pore classes and related to the molecular diffusion coefficient of CH₄ in air (D_0) to derive D_{eff} (see appendix).

We used soil moisture data measured for the forest period in the model to estimate D_{eff} . For each measurement day we correlated estimated D_{eff} values and measured CH₄ fluxes, as shown in Figure 1.5 for the Dystropept. Results suggest that during the forest and cleared periods, soil CH₄ consumption is diffusion controlled, while most of the postburn and agriculture fluxes appear to be dominated by other controls (Figure 1.5). In our modeling approach the estimation of soil field capacity is crucial because it is the key control in the simulation of D_{eff} . We estimated field capacity at 0.48 cm³cm⁻³ using soil moisture data measured in 1995 by time domain reflectometry techniques during our major field experiment (P.M. Crill, unpublished data, 1998). Using this lower value in simulations, emphasizes the previous suggestion that biomass burning decoupled CH₄ fluxes from the diffusion control.

We found no clear effect of increased NO₃⁻ concentrations in cleared soils on CH₄ fluxes, suggesting that during the cleared period, CH₄ fluxes are mainly diffusion controlled. Reduced soil CH₄ consumption after biomass burning may be a combined result of different factors. The heat of the fire may have decreased the size of the CH₄-oxidizing bacteria populations in the surface soils. On our sites, biomass burning increased NH₄⁺ concentrations in the upper 0.1 m of the soils, probably released salts, and added NO₂⁻ with ash. Results of previous studies suggest that the observed postburn inhibition of CH₄ oxidation could be attributed to increased amounts of NH₄⁺, salt

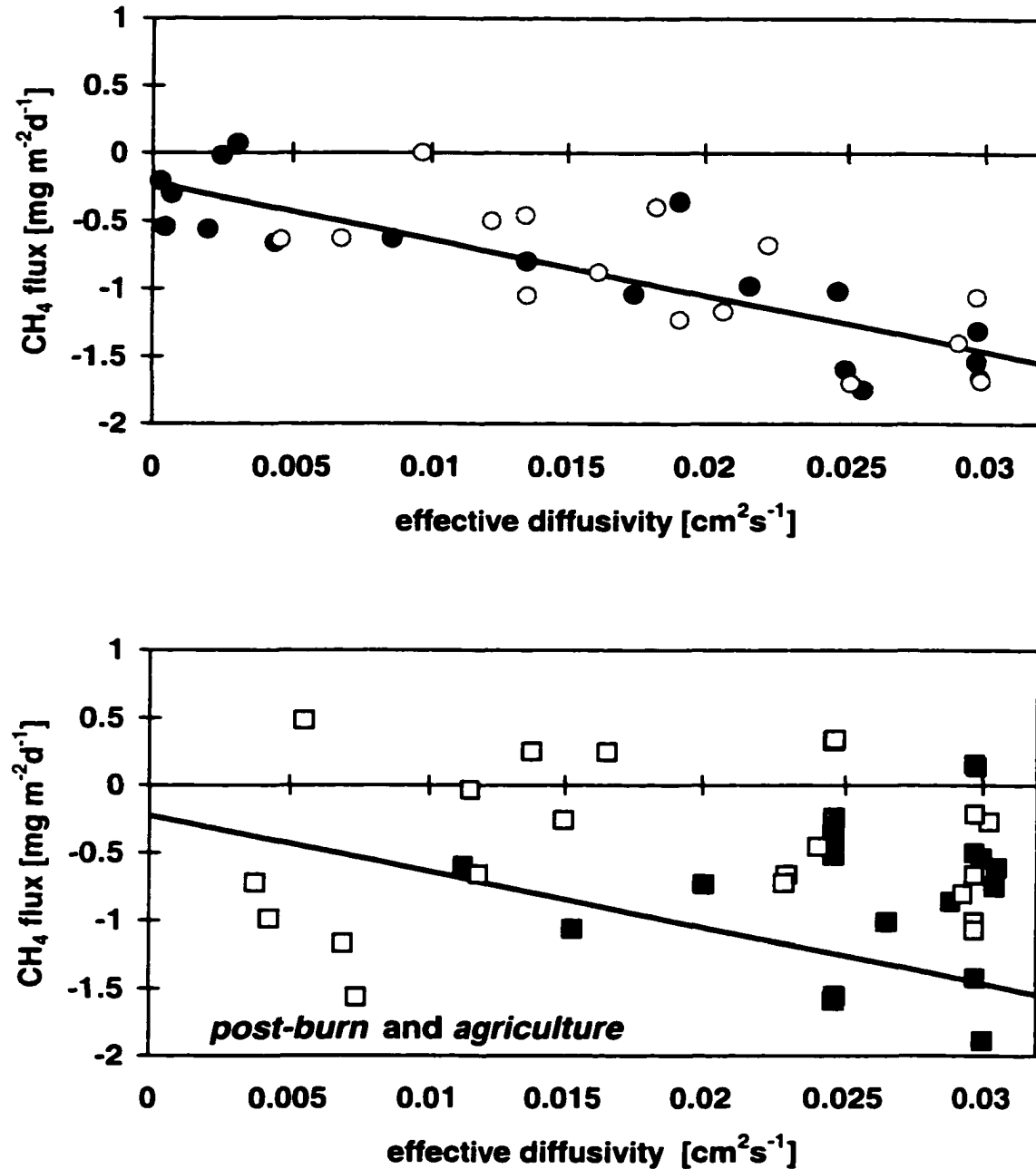


Figure 1.5: CH₄ fluxes versus effective diffusivity estimated from field measured water content data for the Dystropept using the Millington and Shearer [1971] model. The field capacity value used in simulations was 0.52 cm³cm⁻³. The solid line is the regression between CH₄ fluxes and D_{eff} on forest soils ($r^2 = 0.72$). Solid dots are CH₄ fluxes measured from forest, open circles are fluxes measured during cleared (top graph), solid squares are fluxes measured during postburn, and open squares are fluxes measured during agriculture (bottom graph).

effects, and the presence of NO_2^- in the microbiologically active zone of soils. Decreased CH_4 consumption has been measured after soils received extra nitrogen from fertilization (Stuedler et al., 1989; Mosier et al., 1991). Laboratory studies suggest that increased NH_4^+ concentrations in soils may inhibit CH_4 oxidation by methanotrophs as well as by the nitrifying bacteria. Both, salts from fertilizers (Mosier et al., 1991) and NO_2^- inhibits soil CH_4 consumption (Crill et al., 1994; King and Schnell, 1994). Even though the variation encountered in postburn data is high, inhibited CH_4 oxidation suggest that during postburn these factors may have had an effect on CH_4 dynamics.

7. Conclusion

Conversion of secondary tropical rainforest into low-input, traditional agriculture changes soil trace gas fluxes and biogeochemical conditions. Clearing increased the amount of extractable NO_3^- in soils, but did not affect NH_4^+ concentrations. Nitrification was the dominant factor for significantly increased NO_3^- concentrations and NO fluxes. Biomass burning increased soil inorganic NH_4^+ concentrations but had no additional effect on soil NO_3^- . Immediately after burning, short-term peaks of NO and N_2O fluxes were superimposed on previously enhanced emissions, probably both peaks were affected by decomposition of NO_2^- in ashes. Corn growth and probably leaching decreased soil nitrogen pools and gas fluxes from agricultural soils to forest levels.

Under forest and during clearing soils mainly consumed CH_4 . Diffusion and hence soil moisture content was the dominant control of CH_4 fluxes. Biomass burning decoupled CH_4 fluxes and diffusion control. Reduced postburn CH_4 consumption

probably was caused by a combination of reduced bacterial populations after soil heating, NH_4^+ accumulation, salts released by biomass burning, and NO_2^- in ash.

Timing of forest clearing in the progressing dry season affects soil moisture conditions during forest conversion and dynamics of soil inorganic nitrogen content and NO , N_2O , and CH_4 gas fluxes. Our results suggest that in the humid tropical lowland of Costa Rica under low-input management (no tillage, no fertilization, no pesticides), young agricultural areas emit less nitrogen oxides than young pastures and are mainly CH_4 sinks, while pastures may be sources.

CHAPTER 2

SPATIAL AND TEMPORAL VARIABILITY OF NITROGEN OXIDE AND METHANE FLUXES FROM A FERTILIZED TREE PLANTATION IN COSTA RICA

Abstract

Nitric oxide (NO), nitrous oxide (N₂O), and methane (CH₄) are naturally produced and consumed by soil biogeochemical processes. Naturally high variation between trace gas fluxes may temporarily increase due to agricultural management. We studied spatial and temporal variability of fluxes in the context of a 3-year field experiment established to identify and quantify N₂O fluxes and controlling factors using automated field measurements. We measured trace gas fluxes, soil temperature, and moisture from fertilized and unfertilized balsa (*Ochroma lagopus*) plantations. Combining spatial and temporal sampling we evaluate if automatically measured time series of N₂O emissions are representative of overall mean fluxes from fertilized loam under balsa. Soil trace gas fluxes were measured manually at 36 randomly distributed sampling locations per plot. Mean plot emissions were evaluated against fluxes measured by seven chambers commonly used for routine bimonthly manual measurements and against N₂O emissions measured by two automated chambers at 4.6 hour sampling intervals. Trace gas fluxes were highly variable over 40 x 40 m plots. Nitrogen oxide fluxes were mainly spatially independent. Fertilization increased nitrogen oxide emissions but did not introduce spatial dependency of flux data. Within about 6 weeks fluxes approached pre-fertilization level again. Given high spatial variation of nitrogen

oxide fluxes we find that automatically measured N₂O fluxes represent the nature of the flux response well and are in the range of fluxes indicated by spatial sampling. When soils were relatively dry fertilization inhibited CH₄ uptake.

1. Introduction

NO, N₂O, and CH₄ in the atmosphere influence the atmospheric radiation budget and ozone chemistry (Schimel et al., 1996; Williams et al., 1992). Microbial processes in soils are the major natural sources and sinks of these gases (Galbally, 1989). Soil available nitrogen, carbon, and oxygen in combination with soil moisture are the dominant environmental controls of microbial gas production and consumption. High natural spatial and temporal variability of flux controlling factors contributes to uncertainties in the estimation of nitrogen budgets and the prediction of fluxes. Agricultural management modifies natural flux patterns (Matson et al., 1998; Crill et al., 1999). Nitrogen fertilization commonly increases nitrogen oxide fluxes from temperate zone (Eichner, 1990) and tropical soils (e.g., Matson et al., 1996; Mosier and Delgado, 1997). CH₄ consumption decreased after fertilization of dominantly aerobic agricultural soils in the temperate zone (e.g., Steudler et al., 1989; Mosier et al., 1991; Flessa et al., 1996) and in the tropics (Mosier et al., 1998).

Chamber techniques (Mosier, 1989) are an appropriate and economical tool to study trace gas fluxes. Commonly employed chambers cover soil on a small scale (< 0.5 m²). Most studies report high spatial variation of trace gas fluxes on field scale (e.g., Mosier and Hutchinson, 1981; Matson et al., 1990). Some studies attempt to address spatial variability of trace gas fluxes by maximizing the number of chamber sampling locations (Ambus and Christensen, 1994; Clayton et al., 1994) or manipulation of

chamber size (e.g. Galle et al., 1994). Others attempt to describe spatial variability by geostatistical methods (e.g., Van den Pol-van Dasselaar et al., 1998) or by time series methods adapted to transects (one-dimensional distances) (Folorunso and Rolston, 1984). High labor and time demands of chamber measurements usually restrict the amount of data collected. Tower-based eddy correlation techniques can integrate variation in N₂O emissions over a given flux source region (footprint area) (Williams et al., 1992; Smith et al., 1994). However, these techniques are expensive, logistically complex, and applicable only if soil, management, vegetation, and topographic conditions are suitable.

Temporal variability due to seasonal changes in emissions (Groffman and Tiedje, 1989; Wagner-Riddle and Thurtell, 1998), diurnal variation of fluxes (Crill et al., 1988), or short-term increase of gas fluxes after fertilization (e.g., Matson et al., 1996; Crill et al., 1999) increases the uncertainty in gas flux extrapolations. High temporal variability of emissions from a fertilized banana plantation in Costa Rica resulted in an underestimation of mean annual N₂O emissions if monthly sampled flux data are extrapolated compared to extrapolation of fluxes sampled on a fertilization event basis (Veldkamp and Keller, 1997). Temporal variability and short-time responses of fluxes on changes in controlling factors has been demonstrated using automated sampling and analysis systems (Brumme and Beese, 1992; Crill et al., 1999).

Based on results from studies of trace gas fluxes from forest soils and agricultural areas in the humid tropics of Costa Rica (Keller and Reiners, 1994; Weitz et al., 1998), we expected considerable spatial variability of fluxes from balsa tree plantations. Using automated measurement techniques, Crill et al. (1999) documented the temporal increase of fluxes after fertilization of corn and of papaya. Similar fertilization effects were found

on balsa plantations. The present study was designed to (1) identify the overall mean and variability of NO, N₂O, and CH₄ fluxes from humid tropical soils under different agricultural treatments, and changes of spatial-temporal flux pattern after fertilization, (2) to evaluate whether time series of automatically measured N₂O emissions represent spatial mean fluxes from a soil-treatment combination, and (3) to evaluate the impact of infrequent sampling on estimated gaseous nitrogen loss. In February 1996 we sampled trace gas fluxes from 36 randomly distributed locations to evaluate the spatial variability of emissions for two soil types. In June and July 1996 we combined spatial and temporal sampling on one soil type to compare N₂O fluxes measured at high temporal resolution (automated measurements) to fluxes sampled manually at high spatial resolution.

2. Study Area

Our experiments were performed at the La Selva Biological Station (10°26' N x 84°0' W), located in the Atlantic lowlands of Costa Rica. The climate is humid tropical (*Sanford et al.*, 1994), the average annual precipitation is 3962 mm. Rainfall occurs throughout the year (each month receives >100 mm) with a weak dry season between February and April and maximum monthly mean precipitation from June to August and in November (> 400 mm). The annual temperature is 25.8 ± 0.7 °C (average \pm standard deviation) with little seasonal variation. The natural vegetation is tropical wet forest in the Holdridge classification system (Hartshorn, 1983). The soils in our study area are developed on alluvial deposits of andesitic volcanic material (Sollins et al., 1994) and show a high organic matter content (3-7.5% C_{org}). We studied a loamy soil (*fluventic Eutropept*) and a clay soil (*andic Dystropept*). The upper 2-3 cm of the clay consists of distinct aggregates (< 0.5 cm diameter); the loam had only weakly aggregated surface

structure.

3. Experimental Design

Our study of spatial and temporal variability of trace gas fluxes forms part of a 3-year field experiment established to identify controls and to quantify dynamics of N₂O fluxes from humid tropical soils under different agricultural management (Crill et al., 1999). The time schedule for the main experiment and the variability study is given in Table 2.1. The main experiment was started in 1994 after clearing secondary forest (Weitz et al., 1998).

Table 2.1. Sampling Design for the Main Experiment and the Variability Study

Experiment	Time Phase	Measurements
Main experiment	1994 - 1996	- infrequently routine manual NO and N ₂ O measurements (using permanent bases only); - frequent (4.6 hour intervals) automated N ₂ O measurements
Spatial variability	February 1996	- manual NO and N ₂ O measurements (using permanent bases and 29 temporal bases) on unfertilized and fertilized loamy and clay soil (one sampling day per soil treatment)
Spatial-temporal variability	June - July 1996	- manual NO and N ₂ O measurements (using permanent bases and 29 temporary bases) on fertilized loamy soil (8 sampling days on one soil)

3.1. Main Experiment

Using a split-plot design, the main experiment compares two soil types (loamy soil and clay soil), two crop types (annual crops and perennial crops), and two agricultural treatments (unfertilized plots and fertilized plots). Balsa (*Ochroma lagopus*)

was grown as perennial tree crop throughout the variability study presented in this paper. We planted balsa seedlings in November 1995 on 40 x 40 m (0.16 ha) large plots, using a regular planting design with 2 m distance between adjacent plants (distance between rows was 1.86 m).

Throughout the 3-year experiment we measured trace gas fluxes using two different approaches: (1) manual measurements of NO, N₂O, and CH₄ fluxes and (2) automated sampling and measurement of N₂O fluxes. For infrequent routine monthly to bimonthly manual trace gas sampling, each plot was permanently equipped with eight manual chamber bases (*permanent bases*). These chamber bases were manufactured from polyvinylchloride and had a diameter of 0.25 m and a height of 0.12 m. Chamber bases were inserted into the soil surface about 0.02 m. Sampling locations for *permanent bases* were selected randomly in 1994 following the procedure described by Keller and Reiners (1994). *Permanent bases* were repositioned in January 1996. For routine sampling the total flux sampling area of manual chambers per plot is 0.39 m².

We used an automated sampling and gas analysis system (Crill et al., 1999) for semi-continuous, high time frequency (4.6 hour intervals) measurement of N₂O fluxes to identify short-term responses of fluxes to fertilization events. We operated two automatic closed chambers on each plot. The total sampling area of the automated chambers per plot was 0.46 m². Meteorological variables, soil temperature, and moisture at different depths were measured automatically at 0.5 hourly time intervals.

3.2. Spatial Variability Study

In February 1996 we studied the spatial variability of trace gas emissions from balsa plots on two soil types. We collected gas fluxes from unfertilized soils and 2-3 days

post fertilization on fertilized plots. We manually sampled fluxes from a total of 36 locations per soil and agricultural treatment, which equals a total flux area of 1.77 m² per plot. Thirty six flux measurements represented the upper limit of samples we could process per day using the available manual sampling and analysis methods. We chose random sampling over a regular grid design to address small-scale variability given the restricted total sample number.

Seven of the 36 chamber bases were part of the routine measurement efforts (*permanent bases*; total sampling area of 0.34 m² per plot) and 29 bases were temporarily installed for the spatial sampling only (*temporary bases*; total sampling area of 1.42 m² per plot). To assure random installation of *temporary bases* we used random numbers to select one balsa plant in each outmost planting row at opposite sides of the plot. We established a transect between these plants using a metric tape and applied random numbers to select temporary sampling locations while moving along the transect. The minimum distance between neighboring sampling spots along transects was 1 m, the maximum spacing was 9 m. The procedure was repeated until 29 chamber bases were installed.

3.3. Spatial-Temporal Variability Study

In June-July 1996 we studied the spatial and temporal variation of gas fluxes from balsa plots on fertilized loam only. We followed the same sampling design as for the spatial variability study in February 1996. We kept the 36 spatially distributed chambers in place for about 6 weeks and sampled repeatedly, once prior to and at seven dates following a fertilization event (1, 4, 8, 16, 22, 31, and 40 days post fertilization).

4. Fertilization

We fertilized with an ammonium nitrate based granular fertilizer (12-24-12 N-P-K) at approximately 2 month intervals, on February 2, March 28, and June 17, 1996. The applied fertilization rate was 65 kg N ha^{-1} per addition. Fertilizer was broadcast manually. Consequently, spatial variability in trace gas fluxes includes variability due to fertilizer application. However, we added the exact amount of granular fertilizer to the sampling area of each automatic chamber equivalent to the established fertilization rate.

5. Methods

5.1. Manual Sampling and Analysis

We analyzed NO directly in the field following the methods described by Keller and Reiners (1994). Dynamic vented chambers included removable acrylonitrile-butadiene-styrene (ABS) tops that fit the chamber bases. Chamber tops (headspace 0.01 m^3) had two ports to sample a continuous airflow of 300 mL min^{-1} while maintaining equilibrium with atmospheric pressure. The sample flow was mixed with purified air (1200 mL min^{-1}) and a standard gas mixture of 1 ppm NO in oxygen-free nitrogen (approximately 3 mL min^{-1}). NO was analyzed by luminol chemiluminescence detection (Scintrex LMA-3) after conversion to NO_2 on a CrO_3 catalyst. Between chamber measurements we used larger standard additions to calibrate the instrument response. NO fluxes were calculated from the linear increase in concentration versus time as recorded on a paper chart.

We sampled N_2O and CH_4 fluxes using static vented chambers with the same bases. ABS tops were equipped with a sampling port and a vent (Hutchinson and Mosier, 1981). We used nylon syringes to collect gas samples (20 mL) from the headspace at 1, 7,

14, 21, and 28 min after chamber closure. Samples were processed within 24 hours after collection. We analyzed for N₂O by gas chromatography with electron capture detection (Shimadzu GC-8A with a ⁶³Ni detector) and for CH₄ with flame ionization detection (Shimadzu Mini-2). Poropak Q columns were used to separate gas constituents. Commercially prepared standard gases were measured repeatedly alongside the samples. Standard gases were calibrated against NOAA Climate Monitoring and Diagnostics Laboratory and National Institute of Standards and Technology standards. Fluxes were calculated from the linear change in gas concentration with time of chamber closure and related to the chamber sampling area. Net fluxes from the soil to the atmosphere are expressed as positive values; negative fluxes indicate gas consumption by soils. On each measurement day only 18 out of the 36 chamber samples were analyzed for CH₄ due to laboratory constraints.

Simultaneously with gas sampling we measured shaded air temperature near the soil surface for use in gas flux calculations. Soil temperature at 0-0.1 m depth was measured with single probe digital pocket thermometers. Soils moisture content was determined from bulk soil samples (0-0.1 m depth) collected in the vicinity (<0.5 m distance) of each chamber base using a soil auger (0.02 m diameter). About 100 g field moist soil was oven dried to constant weight within 48 hours at 105 °C and gravimetric soil water content θ_g (g g⁻¹) was calculated (Gardener, 1986). Subsequently we converted θ_g to proportion of water-filled pore space (WFPS) using the formula given by *Linn and Doran (1984)*,

$$\text{WFPS} = (\theta_g \times \rho_b) / (1 - (\rho_b / \rho_p))$$

Particle density (ρ_p (Mg m^{-3})) was estimated as 2.65 Mg m^{-3} . Surface soil bulk density (ρ_b (Mg m^{-3})) was determined for each soil type using undisturbed samples (300 cm^3 cores) collected from 0 to 0.07 m depth. In 1996 we sampled from different locations on each plot and calculated an average bulk density of 0.77 ± 0.03 on clay and of 0.69 ± 0.04 on loam (mean \pm standard deviation). After completion of gas sampling for the spatial and temporal variability study in July, we sampled two undisturbed soil cores from 0 to 0.07 m depth inside of each manual chamber base. We calculated bulk density values and estimated WFPS for each sampling location separately.

5.2. Automated Measurements

The automated chamber system is described in detail by Crill et al. (1999). Briefly, two bases for pneumatically actuated box-shaped aluminum chambers were permanently installed on each soil-crop-treatment combination. Nylon tubing connected chamber headspaces (about 0.03 m^3) via a stream-select valve to a gas chromatograph (GC) located inside of an air-conditioned field laboratory. The maximum distance between GC and chambers was 30 m. A pump maintained a continuous closed gas flow between a sampled chamber and the GC. We used a GC with electron capture detection (Shimadzu Mini-2, equipped with a ^{63}Ni detector) to analyze for N_2O . Chamber headspace was sampled 4 times during 26.5 min of chamber closure and transferred immediately to the GC. We alternated flow of sample air and standard gas to the GC, using two different standards of N_2O in air. Fluxes were calculated from the linear increase of N_2O concentration during chamber closure. A desk-top computer controlled the automated sampling procedure, data acquisition, and storage of raw data. The

sampling interval for a single chamber was 4.6 hours. Throughout the spatial variability study the automated system was located on the loam soil.

Precipitation was measured using a tipping bucket gauge (*Qualimetrics Inc.*, Sacramento, California) located adjacent to the field laboratory. Data were stored as half hourly sums. Soil temperature was measured in 2-min intervals at two sampling locations on each plot using type-T thermocouple wire sensors. Data were stored as half hourly averages. At two locations per plot we measured soil moisture content in half hourly intervals using time domain reflectometry technique. Automatically measured soil temperature and moisture refer to 0.05 m depth. Data collection and storage was controlled by CR10 data loggers (*Campbell Scientific*, Logan, Utah) housed inside the air-conditioned field laboratory.

5.3. Statistical Analysis

We used the software package JMP-IN (Sall and Lehman, 1996). February data were analyzed using a two-way analysis of variance test (ANOVA) distinguishing soils (clay or loam) and agricultural treatment (unfertilized or fertilized). For the analysis of the June-July data we used one-way ANOVA to evaluate means of variables for subsequent measurement days, and we used the Tukey-Kramer Honestly Significant Difference (HSD) criterion to evaluate least significant differences between means. Wilcoxon rank scores tests were used to test for differences between *permanent* (n=7) and *temporary* (n=29) chamber groups.

Spatial analysis of nitrogen oxide fluxes was performed using a regression technique and spatial statistics (geostatistical package GEO-EAS 1.2.1 (Englund and Sparks, 1991)). We recognize the limitation for geostatistical analysis due to our

relatively small sample number ($n=36$). We used semi-variograms of NO, N₂O, and soil moisture to analyze spatial auto-correlation between points as a function of their distance. Variograms describe the mean variance of paired measurement points separated by the same distance (Isaaks and Srivastava, 1989). We evaluated semi-variograms up to lag 20, which is half of the length of the sampled plots (40 m). Geostatistical analysis was not useful for the limited amount of CH₄ flux data. Prior to spatial analysis we transformed NO and N₂O fluxes to natural logarithm.

We developed and tested statistical regression models that included an average temporal response of fluxes to fertilization as fixed effects, basically spatial mean fluxes for each sampling day, and spatial variation as independent random effects at each location as well as covariates WFPS (water fill pore space) and DTR (distance to nearest planting row). We report results from fitting the following three models (M1 to M3):

$$\text{M1: } y_{st} = m_t + b_1 * \text{WFPS}_{st} + e_{st}$$

$$\text{M2: } y_{st} = m_t + b_1 * \text{WFPS}_{st} + b_2 * \text{DTR}_s + e_{st}$$

$$\text{M3: } y_{st} = m_t + b_1 * \text{WFPS}_{st} + d_s + e_{st}$$

where y_{st} denotes the $\ln(\text{flux})$ at location s ($s=1, \dots, 36$) and day t ($t=1, \dots, 7$), m_t is an average response at day t , d_s is a random effect at location s , e_{st} are independent Gaussian error terms, and b_1, b_2 are regression slopes.

6. Results

Sampling 36 chambers on each soil-treatment combination in February 1996, we measured similar mean NO emissions from unfertilized clay and loam (2.2 ± 1.4 NO-N $\text{cm}^{-2} \text{h}^{-1}$, 3.7 ± 5.3 NO-N $\text{cm}^{-2} \text{h}^{-1}$, respectively; mean \pm standard deviation). The

magnitude and variation of N₂O fluxes from unfertilized clay were smaller than from unfertilized loam (5.1 ± 6.9 ng N₂O-N cm⁻² h⁻¹ versus 11.5 ± 22.4 ng N₂O-N cm⁻² h⁻¹). On loam the frequency distribution of both gases were highly positively skewed as indicated by large standard deviations. Balsa plantations were fertilized on February 2, 1996. We measured trace gas fluxes, soil temperature, and moisture on the third and fourth day post fertilization from loam and clay, respectively. Fertilization increased the magnitude and variation of NO fluxes on both soils. Post fertilization in February we measured larger NO emissions from clay compared to loam (16.1 ± 18.9 ng NO-N cm⁻² h⁻¹ versus 6.9 ± 7.2 ng NO-N cm⁻² h⁻¹) but smaller N₂O emissions from clay compared to loam (51.1 ± 52.0 ng N₂O-N cm⁻² h⁻¹ versus 121.8 ± 136.6 ng N₂O-N cm⁻² h⁻¹ loam). See Figure 2.1 for comparisons at the natural logarithm scale. NO fluxes were significantly different for soil ($p=0.01$) and treatment ($p<0.01$), N₂O fluxes were significantly different for treatment ($p<0.01$; two-way ANOVA using natural logarithm transformed flux data).

The last fertilization of the balsa prior to the experiment in June-July occurred on March 28, 1996, a total of 91 days before the June 10 'pre-fertilization' measurements. At the beginning of the spatial-temporal sampling campaign there was no remnant effect from the previous fertilization; nitrogen oxide fluxes were lower and had smaller variation (0.5 ± 0.3 ng NO-N cm⁻² h⁻¹ and 4.4 ± 2.8 ng N₂O-N cm⁻² h⁻¹) compared to fluxes from unfertilized loam in February (Figure 2.2a). Magnitude and variation of NO and N₂O emissions increased significantly within 1 day after fertilization on June 17, 1996; fluxes kept rising through the first week. On the third day post fertilization NO

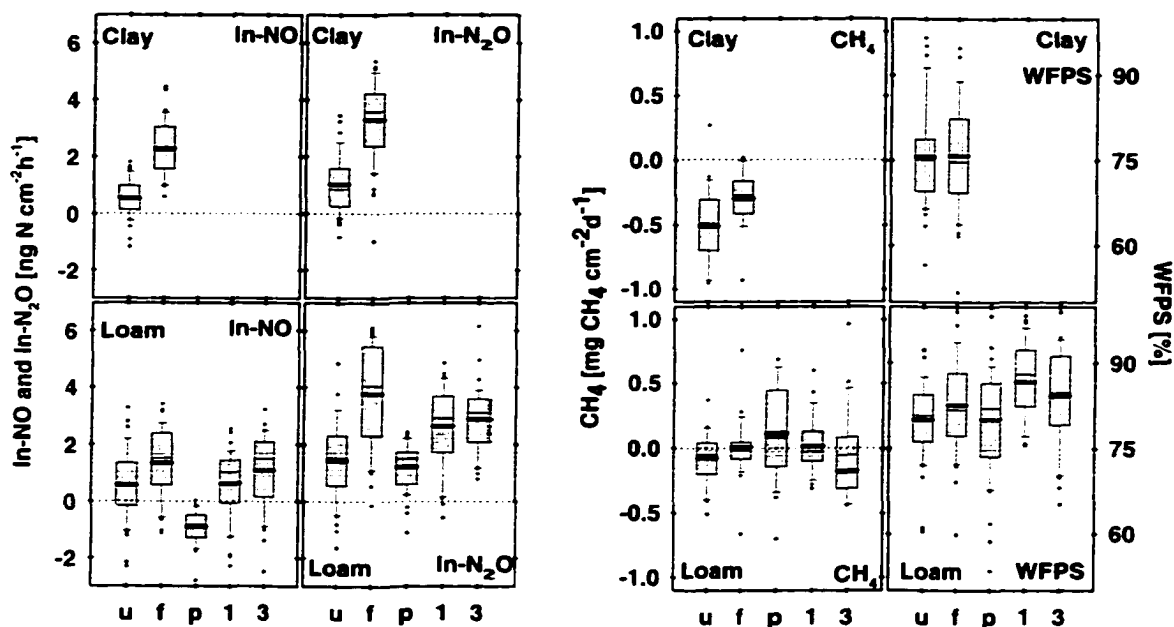


Figure 2.1: Box-plot comparison of NO, N₂O, and CH₄ fluxes and WFPS from spatially distributed manual chambers for both soil types on sampling dates in February and June. Thick horizontal lines in boxes indicates sample mean, thin lines are sample median, box edges at the bottom and top are 25th and 75th percentile respectively, bars are 10th and 90th percentile, dots are values below or above the 10th and 90th percentile. On the horizontal axis read 'u' for unfertilized and 'f' for fertilized treatment during the February sampling, 'p' indicates pre-fertilization sampling, '1' sampling on the first day and '3' on the third day post fertilization in June. (Note: we did not sample from clay in June.)

fluxes were similar in magnitude and variability to February data, while N₂O emissions were slightly lower and less variable. Fertilization enhanced nitrogen oxide fluxes throughout 4 weeks. Highest NO emissions (13.2 ± 16.2 ng NO-N cm⁻² h⁻¹) were measured 1 week and highest N₂O fluxes (59.0 ± 53.9 ng N₂O-N cm⁻² h⁻¹) about 2 weeks post fertilization. With declining level of mean fluxes, variability decreased also. NO emissions were significantly different between 7 and 15 days post fertilization ($p=0.01$). Within 5 weeks both gases approached pre-fertilization flux rates (0.3 ± 0.2 ng

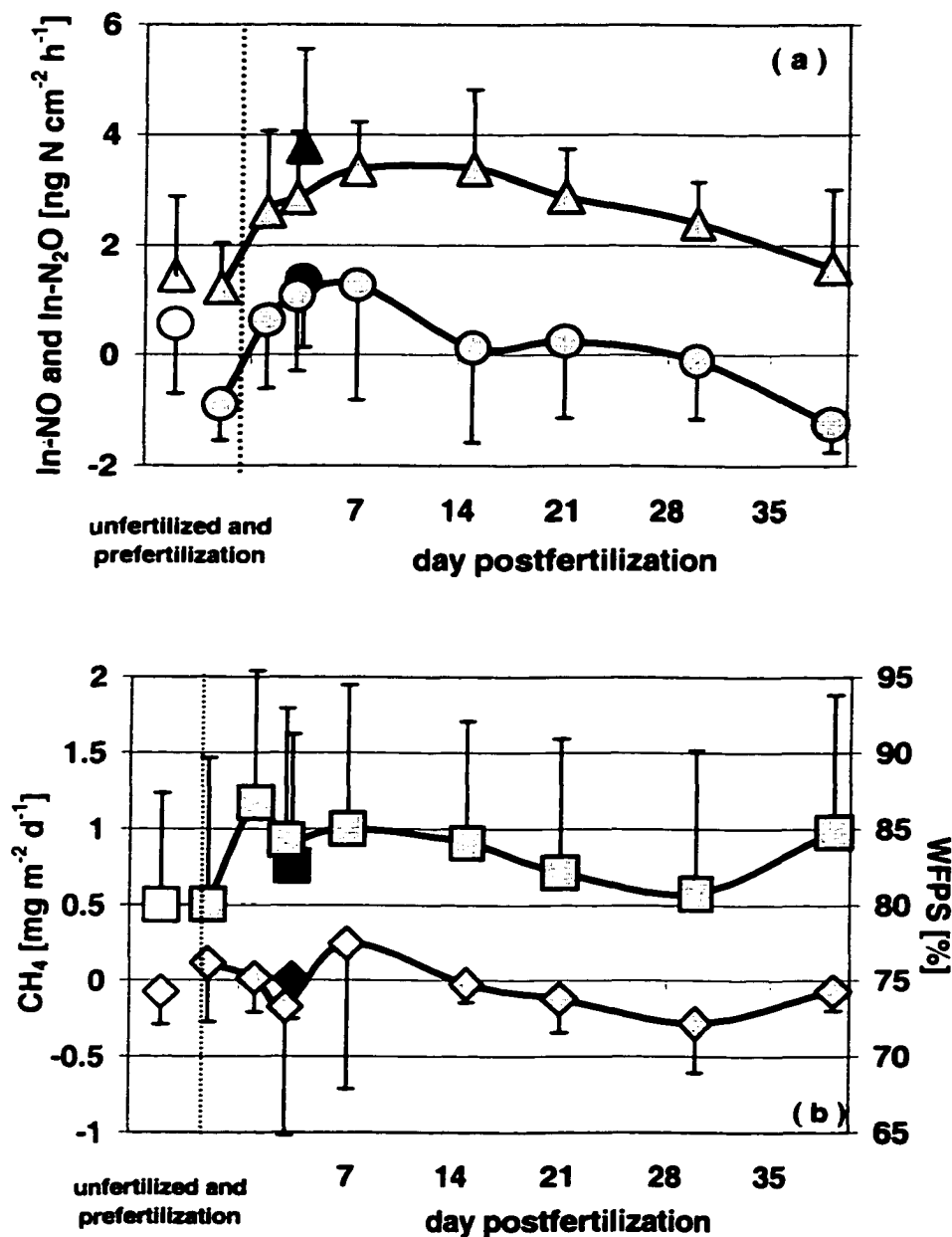


Figure 2. 2: Time series, mean and variance of (a) NO and N₂O emissions and (b) CH₄ fluxes and soil water-filled-pore-space (WFPS) from repeated sampling during the spatial-temporal study in June/July, 1996. Triangles are In-N₂O, dots are In-NO, and diamonds are CH₄ fluxes, squares indicate soil WFPS. Grey symbols are measured during the June/July study from loam under fertilized balsa, open symbols are measured from unfertilized plots in February, filled symbols post-fertilization in February. Error bars are standard deviation. The dotted vertical line indicates the day of fertilization.

$\text{NO-N cm}^{-2} \text{ h}^{-1}$, and $12.1 \pm 18.3 \text{ ng N}_2\text{O-N cm}^{-2} \text{ h}^{-1}$; Figure 2.2a).

For each sampling day we calculated semi-variograms for natural logarithm NO ($\ln\text{-NO}$) and natural logarithm N_2O ($\ln\text{-N}_2\text{O}$) data. Most of the semi-variograms did not show clear spatial autocorrelation of fluxes on either soil type-treatment combination or during the spatial-temporal study (Figure 2.3). On several days in June-July, fluxes appeared spatially independent while on others semi-variograms do suggest a weak spatial dependency up to about 10 m sampling distance. However, there was no relation between the time since fertilization and the spatial dependence.

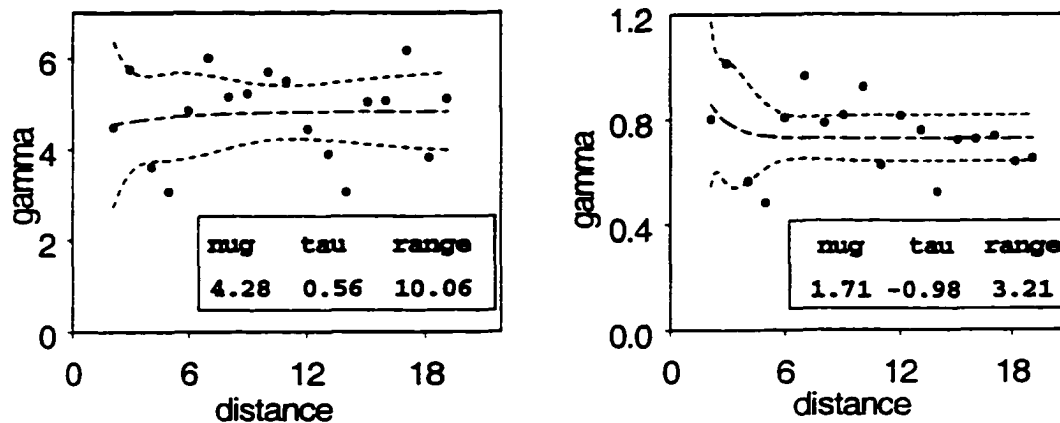


Figure 2.3: Semi-variograms for $\ln\text{-NO}$ and $\ln\text{-N}_2\text{O}$ fluxes measured on day 7 post-fertilization during the spatial-temporal study. An exponential variogram fit (dashed lines) and 95% confidence bands (dotted lines) are given; 'nug' indicates the variogram nugget, 'tau' the sill parameter, and range the range of spatial influence. The sum of nugget and sill parameter gives the variance for the data set analyzed.

Analyzing our three regression models we found that WFPS had no significant effect in all models. From the model 1 (M1) fit we found that the daily spatial means explained 24% of the total variation of $\ln\text{-NO}$ fluxes (19% for $\ln\text{-N}_2\text{O}$). Adding the covariate DTR in model 2 (M2) explains an additional 7% of the variation of $\ln\text{-NO}$ fluxes (5% for $\ln\text{-N}_2\text{O}$). DTR is negatively correlated with fluxes. Adding the random

effect terms of M3 that model the variability due to location explained the largest portion of the variation in fluxes, namely, 47% for ln-NO and 57% for ln-N₂O. This is in addition to the portion that was explained by the model 1 fit. Note that the covariate DTR's effect on the response is included in the random effect and can not be estimated separately in model M3.

We extensively examined the residuals of the above models as well as the random effects d_s of model M3 for spatial patterns and spatial autocorrelations. We estimated variograms of the residuals and we attempted to fit a local spatial regression using a nonparametric smoothing technique (*loess* fit) (Cleveland and Devlin, 1988) in addition to the parameters included in model M3. The latter did not improve the overall fit, and hence model M3 was the best fitting model that we could find. Model diagnostics indicate that the substantial spatial variation in the data is due to factors at a micro scale below the minimum separation of our spatial sampling design. Thus for the given data, the assumptions of independent error terms and independent random effects in our models are justified. Model M3 states that while the responses to fertilization at different locations are similar in nature, the actual amounts of fluxes can differ considerably.

Overall means and variability of nitrogen oxide fluxes are based on measurements from 36 sampling locations. To evaluate if routine bimonthly measurements are representative of the larger plot area, we separate the 36 locations into two groups: seven *permanent* and 29 *temporary* chambers that were installed for the spatial study only. We compared the two unequally sized chamber groups using the Mann-Whitney U nonparametric rank score test. In February 1996 we found no significant difference of NO fluxes between *permanent* and *temporary* chambers on either soil-treatment

combination (Figure 2.4). N_2O fluxes between groups were similar on unfertilized clay, while on the three other plots, *temporary* chambers had significantly larger N_2O fluxes than permanent locations. In June only NO fluxes differed significantly between chamber

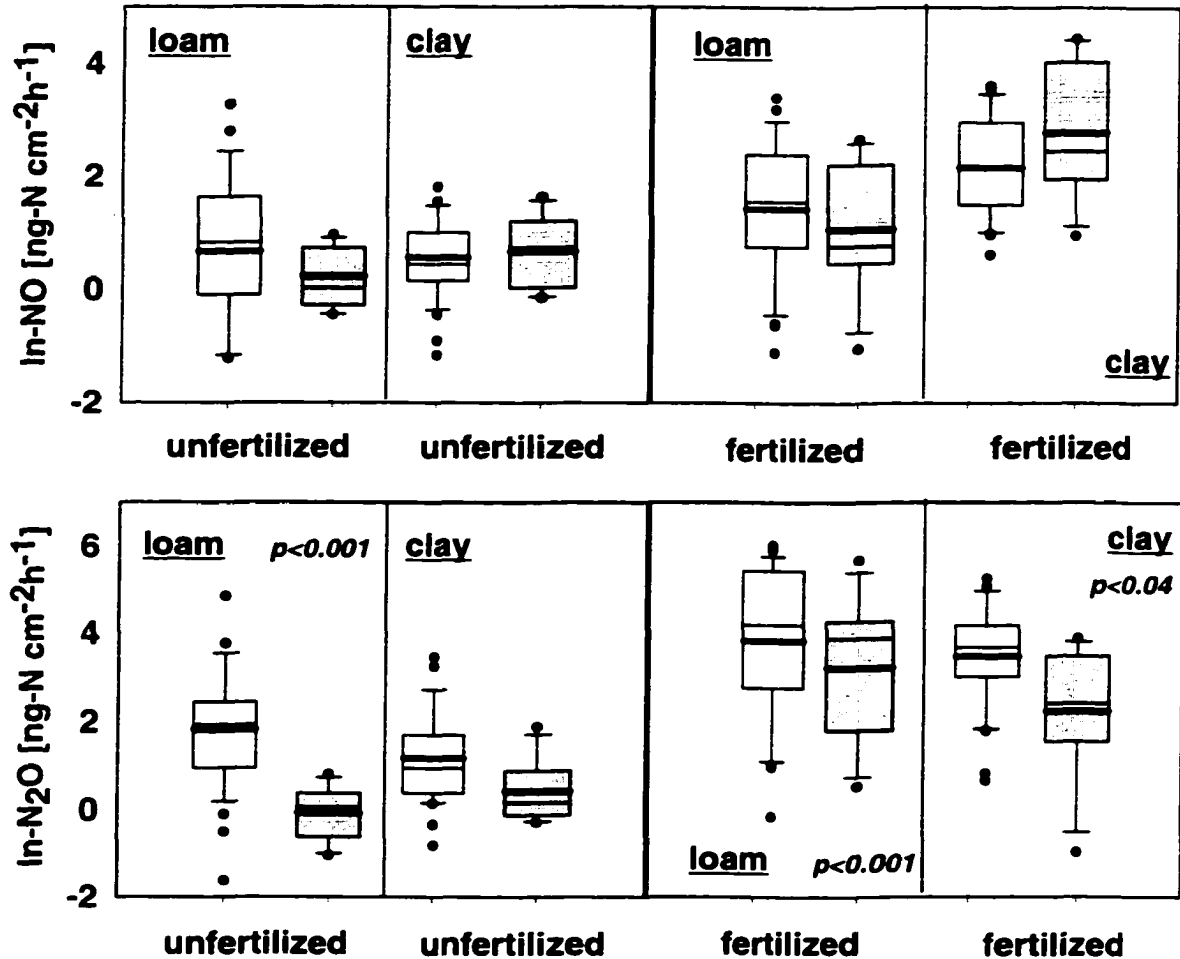


Figure 2.4: Comparison of NO and N_2O fluxes measured from 29 temporary (open box) and 7 permanent sampling locations (hatched box) from unfertilized and fertilized balsa plots on loam and clay soil. Flux data were \ln -transformed prior to presentation. If given, p -values indicate significant differences between fluxes on a soil-treatment combination as determined using the Mann-Whitney U -test of rank scores on data prior to \ln -transformation.

groups during the first week post fertilization, while there were no differences for N_2O emissions at any sampling day (Figure 2.5). Fluxes from *temporary* chambers always

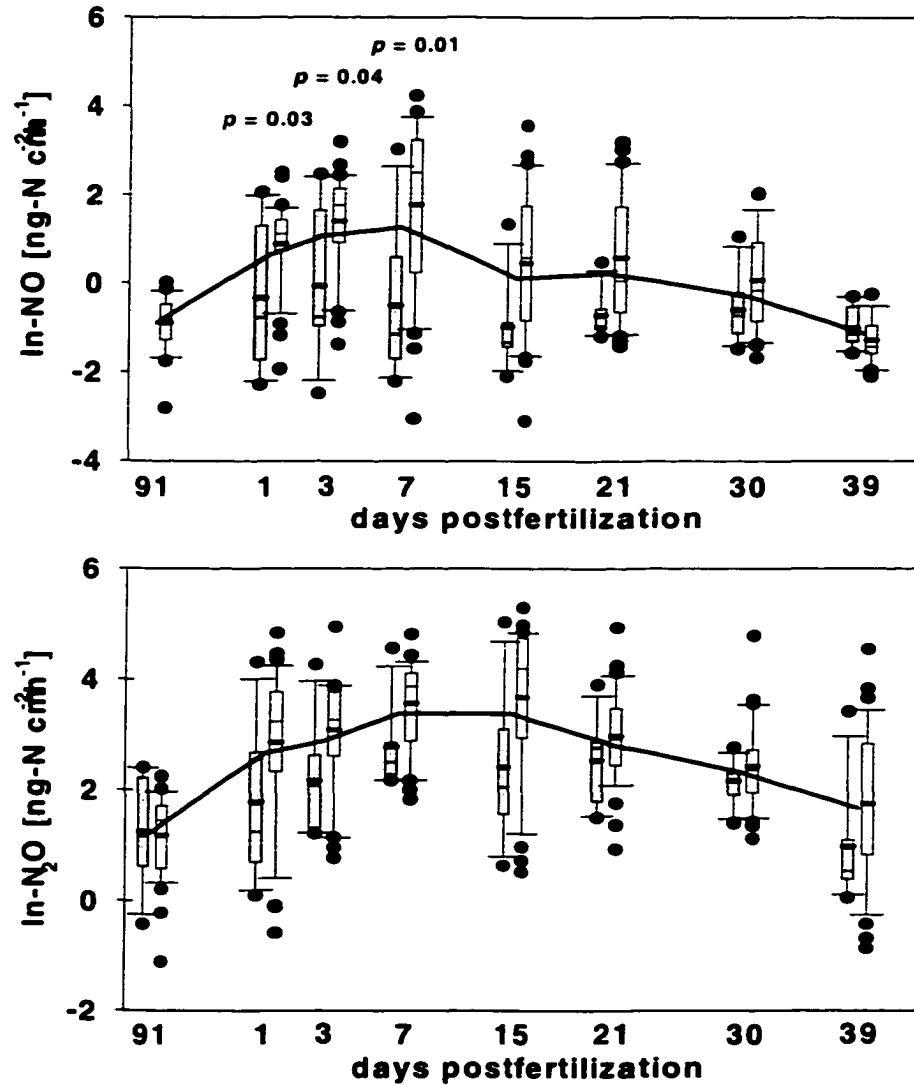


Figure 2.5: Comparison of NO and N_2O fluxes measured from 29 temporary (open box) and 7 permanent sampling locations (hatched box) prior and post fertilization of balsa on loam soil in June, 1996. Flux data were \ln -transformed. If given, p -values indicate significant differences between fluxes on a soil-treatment combination as determined using the Mann-Whitney U -test of rank scores. The thick line combines means of fluxes calculated from 36 sampling locations. We did not measure pre-fertilization NO fluxes in June due to instrument trouble.

covered larger ranges than emissions from *permanent* chambers, except from fertilized clay in February (Figure 2.4) and for NO fluxes during the first week post fertilization in June 1996 (Figure 2.5).

Daily averages of automatically measured N₂O fluxes were inside the range indicated by standard deviations of spatially sampled fluxes (Figure 2.6). Even though chamber flux areas of automated chambers were fertilized by the exact equal amount of granular fertilizer, the fluxes from the two chambers were similar only in the first week post fertilization and diverged considerably during the following 3 weeks. Automatically

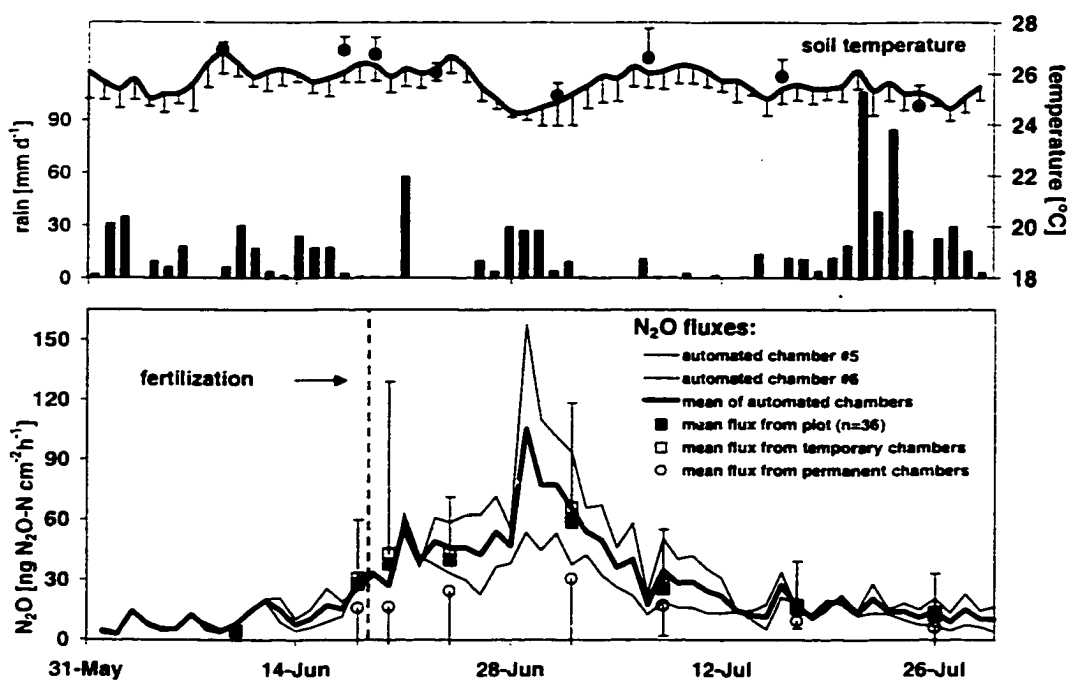


Figure 2.6: Precipitation, soil temperature at 0.05 m depth, and soil N₂O fluxes for the period June 1 to July 30, 1996. Precipitation bars are the daily sum of rainfall in mm, soil temperatures time series are daily averages (°C) (top panel). Dots indicate average soil temperatures measured using the spatial design; error bars are standard deviation. In the bottom panel the thick solid lines indicates automatically measured daily averages of N₂O fluxes, thin lines show mean daily fluxes separately for each of the two pneumatic chambers. Symbols are manually measured daily average N₂O fluxes. Error bars are standard deviation for overall averages (positive bars) or permanent chambers (negative bars). The vertical dashed line indicates the day of fertilization.

measured N₂O emissions and fluxes calculated from 36 sampling locations were significant different on July 8 ($p < 0.03$; Kruskal-Wallis test). Fluxes from 29 *temporary* chambers and automatically measured N₂O fluxes were similar on each sampling day. In contrast, fluxes from seven *permanent* chambers were different from automatically measured N₂O fluxes on each day post fertilization ($p = 0.01$ from June 18 through June 24, $p = 0.03$ on July 2, $p = 0.02$ on July 8, $p = 0.04$ on July 17, and $p = 0.01$ on July 26, Kruskal-Wallis test).

Daily averages of manually and automatically measured soil temperatures were similar (Figure 2.6). Error bars for manual measurements indicate spatial variation in soil temperature, those for automatically measured time series indicate diurnal changes. Spatial variation of soil moisture was high during both experiments. Throughout the spatial-temporal sampling period in June-July, temporal variation between daily means of soil moisture was smaller than spatial variation on single measurement days (Figure 2.2b).

Nitrogen oxide fluxes measured routinely throughout the main experiment clearly show the fertilization effect on emissions from agricultural areas. Mean fluxes from fertilized plots are larger than fluxes from unfertilized plots; fertilization in combination with precipitation increase fluxes. Nitrogen oxide fluxes measured during the spatial and spatial-temporal study are within the range routinely measured from the studied soils (Figure 2.7). Compared to fluxes sampled over the entire experiment (1994 to 1996), the noticed differences between *permanent* and *temporary* chambers are small.

In February, sampling occurred during the drier period of the year. Throughout the week prior to the spatial sampling the study area received 30.5 mm rain and 84 mm

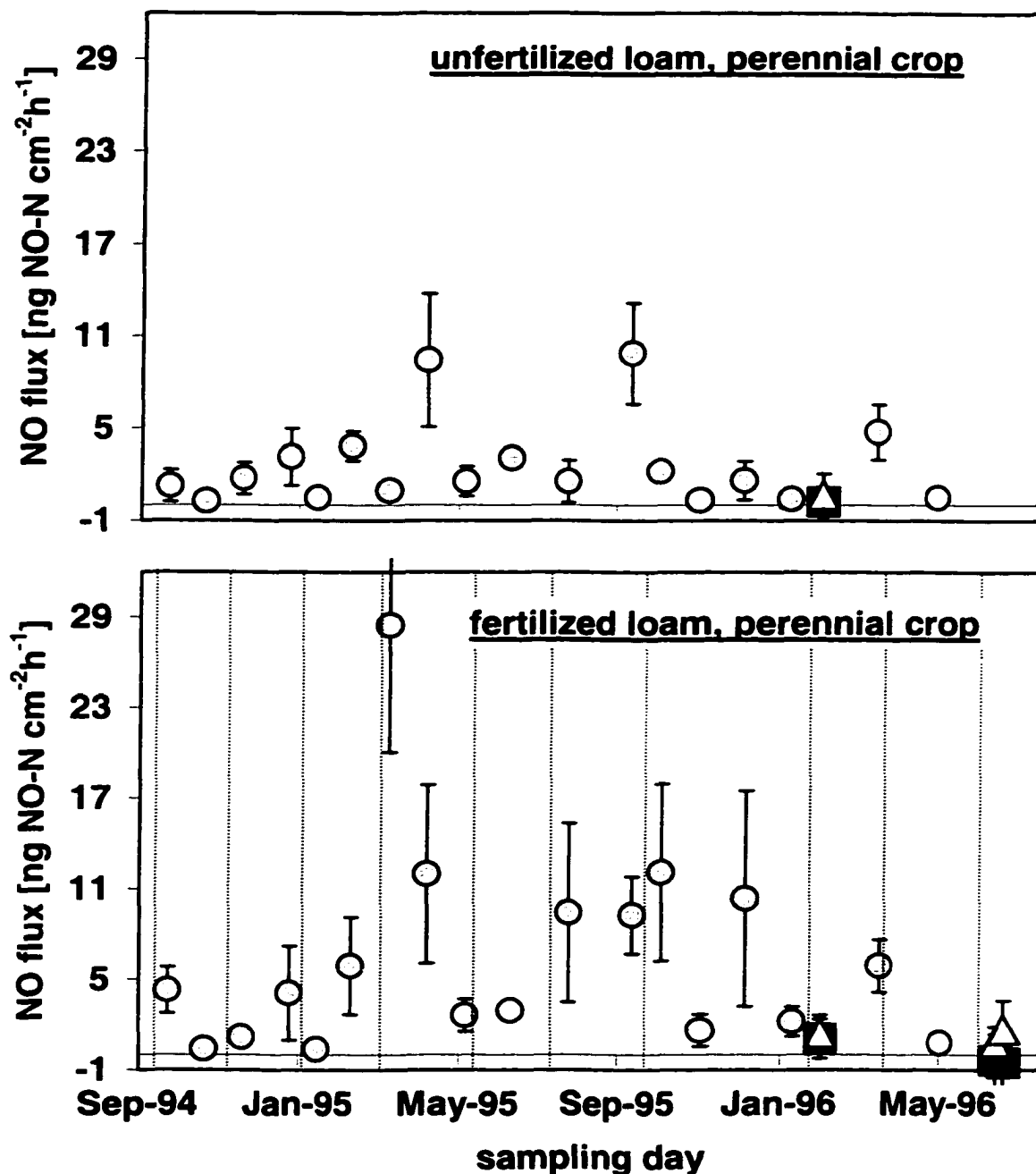


Figure 2.7: Comparison of NO fluxes from spatial sampling with routine monthly to bi-monthly measurements on unfertilized and fertilized loam. Circles are mean fluxes from 8 permanent chambers, squares indicate the mean flux from 7 of these permanent chambers included into the spatial sampling design, open triangles show the mean from 29 temporary chambers. Error bars are standard deviations. Vertical dotted lines indicate days of fertilization (bottom panel).

during the 4 days of sampling. On both soil types, moisture content varied considerably among 36 sampling locations (Figure 2.1). The well aggregated, drier clay was a larger CH₄ sink ($-0.5 \pm 0.3 \text{ mg CH}_4 \text{ m}^{-2} \text{ d}^{-1}$) than the less aggregated, wetter loam ($-0.1 \pm 0.2 \text{ mg CH}_4 \text{ m}^{-2} \text{ d}^{-1}$). In February, fertilization decreased CH₄ consumption on both soils ($-0.3 \pm 0.2 \text{ mg CH}_4 \text{ m}^{-2} \text{ d}^{-1}$ on clay and $0.01 \pm 0.3 \text{ mg CH}_4 \text{ m}^{-2} \text{ d}^{-1}$ on loam). In contrast, fertilization in June increased rather than decreased CH₄ consumption relative to pre-fertilization CH₄ fluxes (Figure 2.1). The first day post fertilization production and consumption were almost equal ($-0.02 \pm 0.2 \text{ mg CH}_4 \text{ m}^{-2} \text{ d}^{-1}$), while on the third day, CH₄ consumption dominated ($-0.2 \pm 0.8 \text{ mg CH}_4 \text{ m}^{-2} \text{ d}^{-1}$). Variation in fluxes and in soil moisture content was large on each day of the spatial-temporal study. The area received 97.3 mm rain in the week prior to fertilization, and 60.8, 94.7, 22.5, 25.6, and 270.7 mm during the first to fifth week post fertilization, respectively. CH₄ and moisture dynamics were correlated in the very moist loam. Concomitant with decreasing soil water-filled pore space (WFPS) we measured an increase in soil CH₄ consumption (Figure 2.2b), while soil CH₄ consumption decreased with increasing WFPS at the end of the measurement period.

7. Discussion

Soil-atmosphere nitrogen oxide fluxes are controlled by substrate availability and environmental factors (e.g., moisture and temperature) which fuel microbial processes (nitrification and denitrification) and restrain microbial activity, respectively (Firestone and Davidson, 1989; Davidson, 1993). We found that mean nitrogen oxide fluxes were closer between unfertilized soil types than between the unfertilized and fertilized

counterparts (Figure 2.1) underlining the importance of substrate availability for trace gas production. On both soil types variation between fluxes was large. Mean and variance of fluxes increased after fertilization, and fluxes were increased for about 4 weeks (Figure 2.2). Other studies report that background level of emissions were reached between 1 and 4 weeks after fertilization (Matson et al., 1996; Veldkamp and Keller, 1997; Crill et al., 1999). For those studies and for this work we consider background (or pre-fertilization) flux level the average magnitude of emissions during periods between fertilization events when fluxes are approaching a constant magnitude. Background fluxes are generally low and respond relatively little to changes in soil moisture content.

We found substantial spatial variability (about 60%) of trace gas fluxes at very small scales below the minimum separation of our spatial field scale experiment. Explanatory geostatistical analysis with variograms and local spatial regression fitting did not reveal consistent spatial patterns at larger than the 1 m scale. Large spatial variability of trace gases was reported from fertilized temperate zone soils (Folorunso and Rolston, 1984; Ambus and Christensen, 1994; Van den Pol-van Dasselaar et al., 1998) as well as tropical soils (Matson et al., 1996; Veldkamp and Keller, 1997). Ambus and Christensen (1994) found substantial variation in N₂O fluxes from a fertilized grassland below the scale of minimum separation (0.11 m) for their experiments. They attributed small-scale variability (< 1 m) of N₂O fluxes to denitrification, which in soils occurs on micro-sites scale. Soil moisture on our sites was in ranges favorable for denitrification, though WFPS and N₂O fluxes showed large small-scale variation on all sampling days.

The relatively uniform fertilizer application technique on balsa plantations did not introduce clear spatial dependency of nitrogen gas emissions with respect to planting

rows. Similarly, broadcasting of fertilizer by plane did not introduce a spatial effect on a sugar cane plantation on Hawaii, while mechanically broadcasting of fertilizer on cane rows caused spatial pattern (Matson et al., 1996). On banana plantations in Costa Rica, the fertilization technique introduced large spatial differences in nitrogen oxide fluxes (Veldkamp and Keller, 1997). Fertilizer is concentrated in the vicinity of a banana plant where the major root activity is expected.

During the 3-4 weeks after fertilization in June 1996 we measured larger nitrogen oxide emissions from recently inserted *temporary* chamber bases compared to fluxes from permanent sampling locations, though only few of the identified differences were significant (Figures 2.4 and 2.5). Matson et al. (1990) suggest that installation of chamber bases may cause an increase of trace gas fluxes. When sampling repeatedly during 12 hours after chamber base installation in an Amazonian forest, they noticed that N₂O emissions increased about 3 ng N₂O-N cm⁻² h⁻¹ compared to fluxes from chambers installed immediately prior to measurements. Experiments in a forest in Costa Rica did not show a similar chamber installation effect (Keller and Reiners, 1994). In contrast, nitrogen oxide emissions measured from different land uses in Puerto Rico confirmed increased emissions from chamber bases installed less than 5 weeks prior to flux measurements (M. Keller, unpublished data, 1999), similar to the observations of our spatial-temporal study. Research in hurricane-disturbed forest and from trench plots in Puerto Rico revealed that easily decaying roots together with the lack of root nutrient uptake after disturbance may increase soil nitrate concentrations (Silver and Vogt, 1993). We recognize the possibility of increased nitrogen oxide fluxes from *temporary* chamber bases due to decay of root material cut in the near-surface soil with chamber base

insertion. *Temporary bases* were installed about 15 hours prior to each sampling in February and about 2 days prior to the first sampling date in June. Chamber bases stayed in place throughout the spatial-temporal study. Differences in average fluxes from *temporary* and *permanent* chambers were probably caused by a combined effect of a relatively short-lived installation artifact, highly skewed frequency distribution of nitrogen gas emissions, the different sample size of the two groups, and the large natural variability of trace gas fluxes together with fertilization. The contribution of any of these factors to the measured fluxes can not be quantified unambiguously.

In February 1996, magnitude and variation of fluxes from both chamber groups (*permanent* and *temporary*) were within the range covered by data from routine sampling between 1994 and 1996 and matched expectations based on flux measurements from January/February 1995 (Figure 2.7). With respect to these long-term observations, the possible effect of an installation artifact and overall spatial variability on the sampling day are small. Considering that the spatial variability encountered by the spatial sampling campaigns is small compared to the overall high range and the temporal dynamics of fluxes throughout the field experiment, we expect that NO and N₂O fluxes measured from *permanent* chambers represent a reasonable estimate of mean plot emissions.

Large temporal variability of nitrogen oxide fluxes is reported by several studies (e.g., Grundmann et al., 1987; Matson et al., 1990; Brumme and Beese, 1992). Parkin (1993) recognizes in his review that for many microbial processes temporal variation may be larger than spatial variation. We compared flux data of high spatial resolution (manual sampling with n=36) to those of high temporal resolution (automated sampling with n=2; Figure 2.6). Considering the differences in sampling area for the used chamber types, we

compare fluxes sampled from 1.77 m² and from 0.34 m² using 36 and 7 spatially distributed chambers, respectively, to fluxes from 0.46 m² (two automatic chambers). Results of the spatial-temporal sampling in June-July suggest that the automatically measured N₂O flux pattern reliably trace overall flux dynamics. We conclude that due to the small-scale variability (<1 m) of N₂O fluxes increasing the size of the sampling area of a chamber improves the estimated N₂O flux compared to fluxes from smaller chambers. Thus a smaller number of large chambers can be considered equivalent to a larger number of smaller chambers.

In February 1996, overall mean N₂O fluxes from the unfertilized (11.5 ± 22.4 ng N₂O-N cm⁻² h⁻¹) and the fertilized balsa plot (121.8 ± 136.6 ng N₂O-N cm⁻² h⁻¹) were significantly different (Mann-Whitney U test) from automatically measured daily fluxes (unfertilized 0.74 ± 0.03 ng N₂O-N cm⁻² h⁻¹; and fertilized 13.57 ± 4.85 ng N₂O-N cm⁻² h⁻¹). Automatically measured N₂O fluxes peaked about 4 days after fertilization (maximum 137.21 ng N₂O-N cm⁻² h⁻¹) when no manual measurements were performed. Considering differences in the temporal variation of the N₂O flux response to fertilization as observed during the June-July study (Figure 2.6), we expect that differences between manual and automated measurements in February mainly represent temporal variation in post fertilization fluxes.

The June-July N₂O flux time series from the fertilized balsa plot showed a relatively long phase (3-4 weeks) of elevated emissions. Most of the N₂O flux pattern measured between 1994 and 1996 from this experimental plot show mainly short-lasting (1-2 weeks) post fertilization peaks (Crill et al., 1999). Automatically measured N₂O flux

time series from a fertilized temperate zone forest show similar temporal flux pattern as our June-July data (Brumme and Beese, 1992). Short post fertilization peaks are reported by studies from various climatic zones and land uses (e.g., Shepherd et al., 1991; Hutchinson et al., 1993; Velthof and Oenema, 1995; Matson et al., 1996; Crill et al., 1999). Most post fertilization peaks last 1 to 7 days; height, shape, and duration are mainly controlled by soil moisture and temperature. The large potential for spatial-temporal variability on our sites is documented by the diverging N_2O fluxes from the two automated chambers about a week post fertilization in June 1996. Chamber sampling areas received exactly the same amount of fertilizer. The distance between the two automated chambers was only about 5 m.

To evaluate the impact of infrequent sampling on estimated gaseous nitrogen loss, we assume that 36 fluxes sampled from spatially distributed chambers deliver an appropriate estimate of the trace gas emissions from the plot. Assuming further that the measured pre-fertilization fluxes were constant to the day of fertilization, then linear interpolation between fluxes measured from 36 chambers through 39 post fertilization days delivers a gaseous nitrogen loss of $0.41 \text{ kg NO-N ha}^{-1}$ and $2.84 \text{ kg N}_2\text{O-N ha}^{-1}$. Integration between automatically measured daily mean N_2O fluxes over the same time period delivers a loss of $3.24 \text{ kg N}_2\text{O-N ha}^{-1}$, which is 5% of the applied fertilizer nitrogen (65 kg N ha^{-1}). Linear integration only between mean daily N_2O fluxes measured automatically on the days on which we performed manual sampling delivers a gaseous nitrogen loss of $3.2 \text{ kg N}_2\text{O-N ha}^{-1}$. Comparing automated measurements to sampling at weekly intervals, Brumme and Beese (1992) concluded that regular weekly

measurements resulted in reasonable flux estimates for their forest site in Germany. In a similar comparison, Crill et al. (1999) found that infrequent sampling from unfertilized plots resulted in less deviation between mean fluxes from weekly and from automatically measured emissions compared to infrequent sampling from fertilized plots. Results of our spatial-temporal study show that the chosen frequency of sampling days with higher intensity during the first week post fertilization characterizes the flux pattern well. Differences in calculated gaseous nitrogen loss are due to spatial variability of N₂O fluxes.

Temperature dynamics are an important constraint on biogeochemical processes in temperate zone soils (Williams et al., 1992). However, they play a comparatively small role in humid tropical soils where seasonal temperature fluctuations are negligibly small. At La Selva Biological station, 7-year records show a mean monthly air temperature of 25.8 °C which changes only little between months (< 3 °C). The diurnal range of air temperature (6-12 °C) is larger than the monthly change (Sanford et al., 1994). Crill et al. (1999) did not measure clear diurnal pattern of N₂O emissions from soils at La Selva Biological station and reason that minimal diurnal variation minimizes temperature effects. During our spatial study we measured variation in soil temperature of only 3-8 °C per sampling day. This includes temporal and spatial variation, because measurements were done over a 6-hour period during which 36 locations were sampled. Temperature changes have negligible effect on gas flux dynamics on our study sites. Automatically measured soil temperatures reflect the overall plot soil temperature very well.

Soil water content and soil structure play important roles in CH₄ dynamics in soils due to their importance for soil redox conditions. When under forest the clay and the

loam soil consumed CH_4 even at high soil moisture contents throughout the rainy season. On well-aggregated forest soils, CH_4 fluxes were well correlated to effective diffusivity (Weitz et al., 1998). Under agricultural use the loam lost most of its well-developed surface aggregation, probably due to rain drop impact and splash effects. We expect that the observed changes in surface layer (top 2-3 cm) structure may have contributed to low CH_4 consumption rates at high soil moisture content by loam under balsa. In contrast, aggregation of the clay surface soil was very stable throughout the agricultural land use. Possibly high temperature caused by burning of slash during site preparation reinforced aggregate stability of the clay surface soil. Higher gas diffusion in aggregated soils together with lower soil moisture content contributed to larger CH_4 consumption by the clay compared to the loam (Figure 2.1).

CH_4 dynamics and soil moisture content are strongly correlated (Born et al., 1990; Keller and Reiners, 1994). High nitrogen turnover in naturally fertile and in artificially fertilized soils may suppress soil CH_4 uptake (Mosier et al., 1991; Steudler et al., 1989). However, increased soil nitrate concentrations after clear-cut during site preparation for our main experiment did not decrease soil CH_4 consumption (Weitz et al., 1998). Fertilization did not show an unambiguous effect on CH_4 production and consumption from balsa plantation (Figure 2.1b). In the drier period (February 1996), data suggest a slight inhibition of soil CH_4 uptake after fertilization. CH_4 fluxes measured during the spatial-temporal study in June-July did not display a fertilization effect, though the variability in fluxes increased during the first week after fertilizer application. Results may be affected by the high water content in the loam in June-July. The distribution of water in the soil pores affects redox conditions and diffusive transport

on small scale, and both variables are essential for CH₄ dynamics.

8. Conclusion

The overall variability of NO, N₂O, and CH₄ fluxes from unfertilized and fertilized balsa plots (0.16 ha) was high. Fertilization enhanced nitrogen oxide emissions and the variability of fluxes. Data did not show a clear fertilization effect on CH₄ dynamics other than increased variability in fluxes. Nitrogen oxide emissions were spatially independent at scales greater than 1 m. Fertilizer application technique (broadcasting) did not introduce a detectable spatial effect. High small-scale and temporal variability of nitrogen oxide fluxes and soil moisture content together with the relatively small sample size available per measurement day limits the applicability of geostatistical techniques. Due to small-scale variability of N₂O fluxes, both a larger chamber sampling area and a larger number of samples in case of small chamber size improve estimates of N₂O fluxes, though commonly practical constraints limit the size of a sampling area and the number of chambers to sample. The spatial-temporal variability study showed that post fertilization time series of automatically measured N₂O emissions reliably reflected the temporal pattern of fluxes. Automatically measured fluxes fill information gaps left by infrequent manual samplings. Our results suggest that we may estimate site representative N₂O emissions from agricultural soils reasonably well from automatically measured fluxes by simple spatial extrapolation.

CHAPTER 3

CALIBRATION OF TIME DOMAIN REFLECTOMETRY TECHNIQUE USING UNDISTURBED SOIL SAMPLES FROM HUMID TROPICAL SOILS OF VOLCANIC ORIGIN

Abstract

Time domain reflectometry (TDR) is used to measure the apparent dielectric number (K_a) in soils. We studied two soil types (*Humitropept* and *Hapludand*) of low bulk density (about 0.7 Mg m^{-3} at 0.05 m to 0.8 Mg m^{-3} at 0.3 m depth) and high organic matter content (about 7 % at 0.05 m to 4 % at 0.3 m depth). Soils are located in a humid tropical environment (average annual soil water content is 0.51 to $0.58 \text{ m}^3 \text{ m}^{-3}$). For calibration, undisturbed soil blocks, with a TDR probe installed in the center, were saturated and then allowed to dry by evaporation. Volumetric water content was calculated from measured K_a values and from gravimetrically measurements. Because we used undisturbed soil samples, our calibration accounts for the natural heterogeneity in soils. We tested the suitability of various calibration functions relating K_a to soil water content for our soils. TDR technique underestimated the actual soil water content by 0.05 to $0.15 \text{ m}^3 \text{ m}^{-3}$, when using the widely applied Topp-calibration function. A three-phase mixing model with a geometry parameter, $\alpha = 0.47$, fit our data best. We consider mixing models to be a robust approach for calibration of TDR technique on various soils.

1. Introduction

Soil water content is a driving variable for every important soil biogeochemical processes. Nitrification and denitrification are bacterial processes that directly affect the

composition and amount of nitrogen trace gas emissions from soils. Linn and Doran (1984) showed that 60 % water filled pore space in soils may be considered a threshold value at which microbial activity switches from being aerobic dominated to being anaerobic dominated with increasing soil water content. We study trace gas emissions from tropical, agricultural soils in relation to soil water dynamics on short-time scales. Accurate measurements of soil water content, and its rapid changes in time are essential in our study to establish and validate a relation between composition and amount of nitrogen trace gas emissions and soil water dynamics.

Time domain reflectometry (TDR) has become a common tool to quantify the soil volumetric water content (θ). The theoretical background for this specific use of TDR is well explained (e.g. Topp et al., 1980; Dobson et al., 1985; Roth et al., 1990; Herkelrath et al., 1991). The apparent dielectric number (K_a) of the soil is derived from the measured velocity of propagation of an electromagnetic pulse which travels along a transmission line (TDR probe) of known length. K_a depends mainly upon the soil water content in the vicinity of the probe. Various calibration functions relate K_a to the volumetric soil water content. The most widely used model is the calibration function of Topp et al. (1980). This is an empirically derived third-order polynomial which fits a range of soils that have an average bulk density of about 1.3 to 1.4 Mg m⁻³ and the water content ranging from 0.1 to 0.5 m³ m⁻³. This calibration function does not include any soil specific parameter, and has become popular in automated TDR applications (Baker and Almares, 1989; Heimovaara and Bouten, 1990). However, Topp's calibration function is not suitable for organic soils (Topp et al., 1980; Herkelrath et al., 1991), clay soils with high bulk density (Dasberg and Hopmans, 1992; Dirksen and Dasberg, 1993; Vielhaber,

1995), or soils of low bulk density (Dirksen and Dasberg, 1993). Consequently, a growing number of authors have presented empirical calibration functions derived for particular soils. The empirical models used are power functions (e.g. Ledieu et al., 1986; Herkelrath et al., 1991), or third-order polynomials (e.g. Dasberg and Hopmans, 1992; Roth et al., 1992). Empirical relations are valid only in the range of soil water contents covered by its source data. Therefore extrapolation outside this range may result in improper water content estimates (Roth et al., 1990).

In contrast, physically based theoretical models (Table 3.1) cover a broad range of soils, by accounting for soil physical properties. Mixing models approach a soil as a mixture of randomly distributed components, each having a specific dielectric number. The apparent dielectric number K_a measured in a soil is assumed to be the result of a volumetric mixing of the dielectric numbers of the distinguished phases. Three-phase mixing models (Dobson et al. 1985; Roth et al. 1990) distinguish dielectric numbers of soil matrix (with $\epsilon_s \cong 3$ for mineral soils and $\epsilon_s \cong 5$ for organic soils), air ($\epsilon_a \cong 1$) and water ($\epsilon_{fw} \cong 81$). For free water the dielectric number is non-linearly anti-correlated to temperature (Roth et al., 1990). In four-phase mixing models (Dobson et al., 1985) the water component is subdivided into bound water and free water, assuming that soil particles are covered by a thin water layer (thickness $\delta = 3 \times 10^{-8}$ cm) of chemically bound

Table 3.1. Equations of Mixing Models used in Comparisons of Calibration Models

Model	Equation
Three-phase α mixing model	$\theta = [K^\alpha - (1-\phi) \epsilon_s^\alpha - \phi \epsilon_a^\alpha] / (\epsilon_w^\alpha - \epsilon_a^\alpha)$
Four-phase α mixing model	$\theta = [K^\alpha - \theta_{bw}(\epsilon_{bw}^\alpha - \epsilon_{fw}^\alpha) - (1-\phi) \epsilon_s^\alpha - \phi \epsilon_a^\alpha] / (\epsilon_{fw}^\alpha - \epsilon_a^\alpha) \quad \theta > \theta_{bw}$
Maxwell-De Looor mixing model	$\theta = \frac{[3(\epsilon_s - K_a) - 2\theta_{bw}(\epsilon_{bw} - \epsilon_{fw}) + 2\phi(\epsilon_a - \epsilon_s) + K_a\theta_{bw}(\epsilon_s\epsilon_{fw}^{-1} - \epsilon_s\epsilon_{bw}^{-1}) - K_a\phi(\epsilon_s\epsilon_a^{-1} - 1)]}{[K_a(\epsilon_s\epsilon_{fw}^{-1} - \epsilon_s\epsilon_a^{-1}) + 2(\epsilon_a - \epsilon_{fw})]} \quad \theta > \theta_{bw}$

water, which has a much lower dielectric number ($\epsilon_{bw} \cong 3.2$) than free water. To estimate the amount of bound water in a soil, δ is multiplied with the specific surface area S of the soil matrix and the soil bulk density. Mixing models use soil porosity for partitioning between soil components (water, air and soil matrix), and apply a soil specific geometry parameter α to estimate θ from a measured K_a value. The parameter α accounts for soil structure, therefore it must be determined empirically for every soil studied. Mathematically α is a geometry factor that defines the shape of the calibration function between very low and very high K_a values. Roth et al. (1990) used undisturbed samples and a wide range of soil water contents for calibration of a volumetric mixing model to their soils. They find the three-phase-mixing model with $\alpha = 0.46$ fit their data best, but on theoretical reasoning consider 0.5 as an acceptable value for α . In contrast with the three-phase- α and four-phase- α mixing models, the Maxwell-De Looor mixing model (Dobson et al., 1985) uses only physical parameters such as soil porosity, soil specific surface area (S), the thickness of bound water layers and the dielectric numbers ϵ_s , ϵ_a , ϵ_{fw} , and ϵ_{bw} to derive soil water content from K_a (Table 3.1). The Maxwell-De Looor mixing model does not contain empirical parameters such as α .

Soil organic matter content, bulk density and small-scale soil heterogeneity as caused by soil structure influence TDR measurements (Ledieu et al., 1986; Jacobsen and Schjønning, 1993; Roth et al., 1993; Herkelrath et al., 1991, Heimovaara et al., 1994). Soils in the present study are low in bulk density and have relatively high organic matter content throughout the depth profile, thereby differing markedly from temperate zone soils. Furthermore, our soils generally show higher water contents throughout the year

than common temperate zone soils. Most calibration experiments take bulk soil samples from the field, dry, sieve, and repack them to a desired bulk density. It is likely that calibrations with homogenized, repacked soil samples bias results to less variation, which may not be reflected in field conditions. Soils of volcanic origin are very sensitive to disturbance of the original soil structure and to compaction; both factors have a major influence on soil hydraulic behavior. After homogenizing and repacking it is unlikely that original soil physical properties can be reconstructed in this soil. Especially repacking at high soil water contents results in samples with a structure incomparable to soil in situ. Therefore we used undisturbed soil samples in a saturation/desaturation procedure to experimentally define a calibration function that is valid for our structured, low bulk density soils.

2. Materials and Methods

2.1. Sites

We studied two soil types at the La Selva Biological Station (10°20 N, 83°50 W) in the Atlantic zone of Costa Rica. Selected soils are representing the two most common soil groups in the lowlands of the Atlantic zone. We selected a young, fertile low terrace soil (*eutric Hapludand*) and an older, less fertile soil located on a higher terrace (*oxic Humitropept*). Both soils are developed on alluvial terraces in a parent material of volcanic origin. They have low bulk densities and high organic matter content (Table 3.2). The *Humitropept* (clay) may be regarded as the weathered remnant of the loamy *Hapludand*. The climate at La Selva is humid tropical, with an average annual precipitation of 3962 mm, an average monthly temperature of 25.8 °C (Sanford et al., 1993), and an estimated annual average evapotranspiration of 1500 mm. There is a drier

period from February to March, however the soils stay close to field capacity throughout the year. Using monthly sampling from 1993 to 1996 and gravimetric methods we measured an average annual water content in the top 0.1 m of the *Humitropept* of $0.51 \text{ m}^3 \text{ m}^{-3}$ (std. 0.07), and $0.58 \text{ m}^3 \text{ m}^{-3}$ (std. 0.08) for the *Hapludand*.

Table 3.2. Brief Description of Soils Used for Calibration of TDR Technique

Depth, m	Texture	Bulk Density Mg/m^3	Organic Matter %	pH (H_2O)
0.00-0.10	loam	0.67	7.59	6.0
0.10-0.35	loam	0.72	3.62	5.9
0.35-0.70	loam	0.77	2.76	6.0
0.70-0.80	sandy loam	0.73	1.07	5.9
0.80-1.00	loamy sand	0.94	0.63	6.0
0.00-0.10	clay	0.77	7.26	4.7
0.10-0.20	clay	0.81	4.44	4.5
0.20-0.50	clay	0.81	3.18	4.8
0.50-1.00	clay	0.77	1.32	4.9

2.2. Time Domain Reflectometry (TDR)

We used a commercially available TDR setup, that combines a cable tester (*Tektronix 1502B*), a *SDM152* interface and a *CR10* data logger (both *Campbell Scientific Inc.*). A 50 ohm coaxial cable connected TDR probes to the cable tester. We used probes of two parallel stainless steel rods with 0.0032 m diameter, 0.3 m rod length, and 0.03 m spacing between rod centers (Spaans and Baker, 1993). Rod ends were fixed in epoxy, in which a 1:1 balun was embedded water proofed at the connection of coaxial cable to the parallel rods. Spaans and Baker (1993) found that 1:1 baluns are preferable to others for measurements in wet soils. We derived K_a values from TDR measurements by collection of raw waveform data and interpretation of traces using a modification of the *TRACE.41* program developed by Spaans and Baker (personal communication).

Heimovaara and Bouten (1990) corrected the measured travel time of an electromagnetic signal to propagate along the probe rods for the time the signal travels in the epoxy head of the probe. The TRACE.41 software we used does not account for this small time delay before the signal enters the soil.

For calibration we prepared undisturbed soil blocks of 0.35x0.13x0.07 m. Sample dimensions were chosen by considering probe design and published information on expected measurement volume, saturation procedure and workability of final sample size. To estimate the appropriate distance between TDR probe and sample surface, we considered the model presented by Knight et al. (1994; in Petersen et al., 1995). Based on this model we calculated that 99 % of the TDR measurement volume would be restricted to a cylinder of 0.042 m diameter surrounding the probes. According to De Clerk (1985; in: Petersen et al. 1995) for probes with rod spacing of 0.025 m 99 % of the TDR measurement volume is restricted to a cylinder with radius 2.4 times the rod spacing, and 94 % is restricted in a cylinder with a radius equal to the rod spacing. For our probes the corresponding measurement volumes are cylinders with radius of 0.07 m and 0.03 m. Laboratory experiments of Baker and Lascano (1989) show that for probes spaced 0.05 m apart, 0.02 m is the minimum distance between probe and soil surface to provide 94 % of the actual soil water content being measured. Taking information of these sources into account, we choose a sample height of 0.07 m for our calibration experiments. A sample height of 0.07 m also corresponds with heights of undisturbed soil samples used in soil water retention experiments. With the probe installed horizontally in the center of the block, the chosen design for our calibration experiment leaves about 0.035 m between TDR rods and top and bottom plane of the soil block, and 0.05 m undisturbed soil

between TDR probe and block walls. Saturated soil blocks weighted 7 to 6.5 kg.

2.3. Sampling Procedure

We inserted TDR probes horizontally from a pit wall at 0.05 m, 0.15 m, 0.3 m and 0.5 m depth. These depths represent installation depths of TDR probes used in an ongoing research project. Undisturbed soil samples were removed from profile pits at 0.02-0.09 m, 0.12-0.19 m, 0.27-0.34 m and 0.47-0.54 m depth. Six replicates were taken from the top 0.09 m of each soil type, three replicates from each deeper sampling depth. Starting from the soil surface, we removed soil material until a horizontal plane was established, leaving a 0.035 m thick layer of undisturbed soil above the probe. The final distance between soil surface and probes was checked by pushing a thin needle through the remaining soil layer down to the rods. Installation was repeated if the distance was found to be less than 0.03 m.

We used stainless steel frames (wall thickness 0.0018 m) of 0.35 m length, 0.13 m width, and 0.07 m height for sampling (Figure 3.1). The frame was placed on the leveled soil surface above the probe. Then we excavated an undisturbed soil block using a knife, while carefully pushing down the frame. A rectangular opening in the front wall of the frame allowed us to push half of the frame's height below installation depth of the TDR probe, until the probe finally was located in the center of the soil block without contacting the metal frame. A thin layer of a cement-sand-water mix (dry sand sieved to 0.5 mm, mixed with 10 % cement; and 10 % water added to that mixture) was applied on the surface of the soil block. The mixture was allowed to harden for a night, forming a very porous crust of high hydraulic conductivity (Booltink et al. 1991). The porous crust was necessary during the start up of saturation, to prevent internal erosion in the soil

block by a rapid water entry into wide macro-pores.

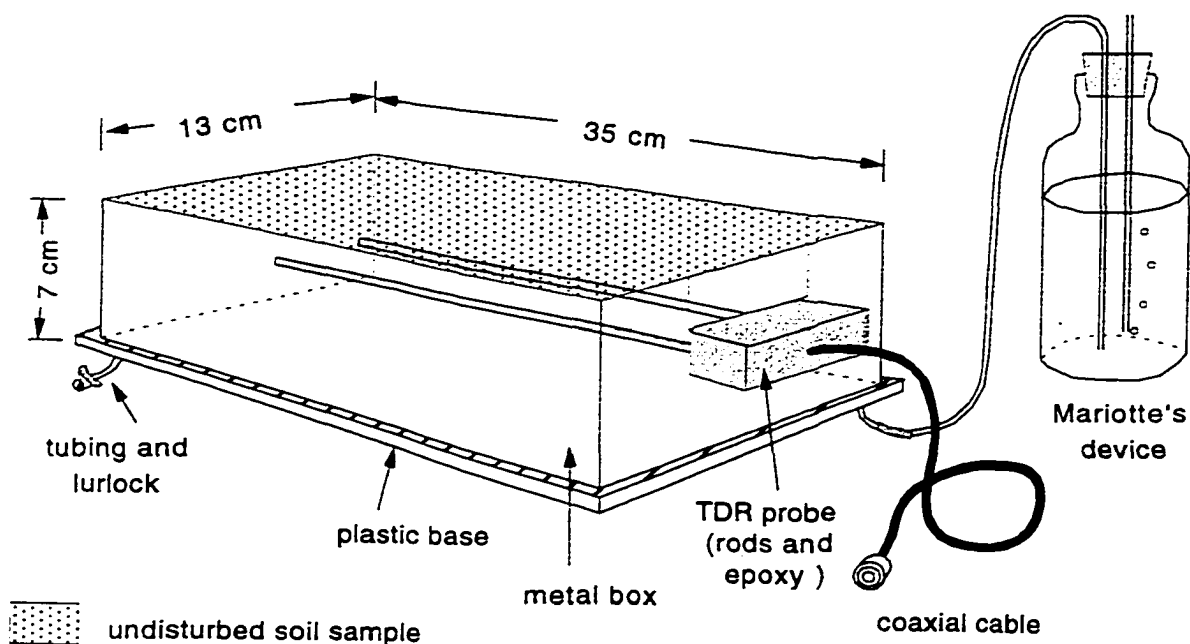


Figure 3.1: Design of calibration setup. An undisturbed soil sample (dotted area) with TDR probe in its center is connected to a Mariotte's device for slow saturation of the soil from the bottom of the sample to its top.

The soil block was cut from its location in the pit using a thin wire. The sample was removed from the pit and placed with the crust side down on a plastic base. Then we created a water tight enclosure around the undisturbed soil sample by sealing spaces between the plastic base and the metal frame using silicone glue. A small piece of plastic was glued to the metal frame, to cover the opening above the epoxy head of the TDR probe. The plastic base had tygon tubing with small stopcocks on opposite edges of its length sides. Water was added at one end while air escaped on the diametrically opposed end of the base. When the bottom of the sample was water filled we closed one stopcock

and connected the other one to a Mariotte's device, allowing continuous slow saturation (Figure 3.1) while avoiding air inclusions in the soil block. During a three week saturation period the block surface was covered with a plastic sheet to prevent evaporation losses. At the end of the saturation period we removed excess water from the plastic base using a syringe, and took the plastic cover off from the sample surface to allow evaporation. Daily, we measured the apparent dielectric constant K_a using TDR and weighted the whole soil block (including probe, metal frame and plastic base) on an electronic balance for gravimetric calculation of soil water content. In our air-conditioned laboratory samples lost about 70 to 100 ml water each day by evaporation. After two to three weeks of evaporation we finished the desaturation phase, determined the final soil water content by drying the soil in the oven for 48 hours at 105 °C. For each daily measurement, we calculated the volumetric water content of the soil sample from its weight, using bulk density values measured from the sampling pit. For bulk density determination we used the core method (Blake and Hartge, 1986) on 5 to 6 undisturbed samples of 0.003 m³ (core diameter 0.07 m).

2.4. Effect of Sample Size on Calibration

In a separate field experiment we tested if the metal frame used to excavate soil blocks, and if the chosen sample dimension affected TDR measurements during calibration. We installed a probe as described above but established an initial soil level such that 0.05 m undisturbed soil remained above the probe. Using that probe we measured K_a by TDR. Then we excavated the soil block as described while installing the metal frame. We repeated the measurement of K_a after the frame was installed. This experiment was replicated nine times.

We tested the influence of the distance between probe and soil surface on TDR measurements using undisturbed soil blocks. A probe was installed as described leaving 0.05 m undisturbed soil above the rods. Assuming that the model of Knight et al. (1994) is valid for our soils, we predict that at this point 99 % of the measurement volume is inside our sample. We measured the K_a value of the soil using TDR and then we subsequently removed soil layers of 0.01 m thickness, until the TDR probe was visible. We repeated K_a measurements after each soil removal, and determined the gravimetric water content for each layer removed. The water content showed little variation between layers. We repeated the experiment 7 times. The effect of the distance to the soil block edges was tested in the same manner. We subsequently removed 0.01 m thick soil layers from both sides of the soil block, until the probe was visible. This experiment was replicated three times.

We choose to use undisturbed soil samples for TDR calibration to avoid problems in repacking, which occur especially with very moist soil material. The soil types studied easily loose their microstructure when manipulated. Establishing different soil moisture conditions in a previously saturated, undisturbed soil sample by evaporation from its surface, implies an non-uniform moisture distribution in the soil sample during desaturation. We found the amount of water lost per day by evaporation was high during the whole desaturation phase, indicating that the sample block lost water through its entire height. However, we did not determine actual moisture distribution inside the sample. Assuming that during evaporation the hydraulic gradient inside the sample varies linear with sample depth, the TDR measurement taken in the center of the sample represents the average moisture condition of the sample core. Under this assumption

gravimetrically determined soil water content can be compared with TDR derived values.

2.5. Effect of Air-Filled Cavities on TDR Measurements

Bulk density varies in our soils as a result of biological activity. Refilled burrows of mammals and invertebrates have lower bulk densities than surrounding soils, by this they will affect the TDR measurement when located inside the measurement volume. We tested the effect of air filled spaces on TDR measurements using undisturbed blocks as described before. We measured the K_a value of the soil sample in its original condition. With a thin metal cylinder of 0.016 m diameter, we cut a vertical soil column of 0.07 m height out of the volume between the two rods of the TDR probe, by this creating an air-filled hole in the center of the TDR measurement volume. After removal of the soil the corresponding K_a value was measured. We repeated this procedure until 5 air filled holes were created in the measured soil block.

2.6. Calculations

We used students-t test in a spreadsheet program (EXCEL for Windows) to test on significant difference between sample means of interest. To evaluate the suitability of different calibration functions on our data, we calculated the root mean square error (*RMSE*) for water content derived from gravimetrically measurements (θ_{grav}) and the corresponding water contents estimated using a particular calibration model (θ_{est}) according to:

$$RMSE = \left(\frac{\sum (\theta_{grav} - \theta_{est})^2}{n} \right)^{0.5}$$

with n is the number of observations (Jacobsen and Schjønning, 1995).

3. Results

3.1. Calibration method

We found no significant difference between apparent dielectric constant measured by TDR on the soil prior to frame installation and following installation. But there was a measurable effect on K_a due to distance between TDR probe and soil surface (Figure 3.2). Measured K_a values are shown as percentage of the initially measured K_a . Variation in data points result from soil small-scale heterogeneity in undisturbed samples and from inaccuracies in thickness of removed layers. Because measurement sensitivity is greatest in the immediate vicinity of the probe the latter can contribute noticeable to the variation encountered close to the TDR probe. Using soil blocks of 0.35x0.13x.007 m size, we detected an average 98.7 % of the K_a value measured prior to frame installation. When

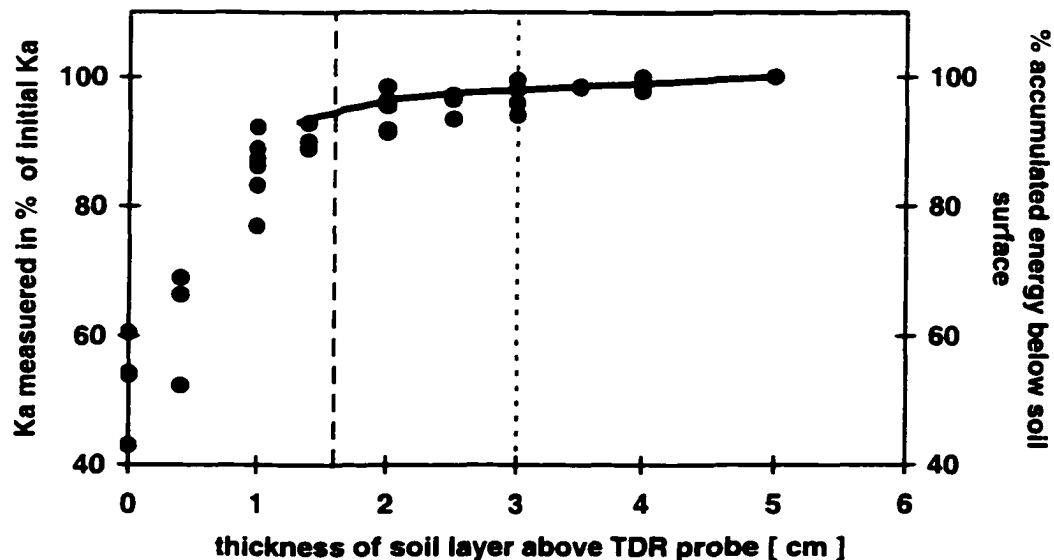


Figure 3.2: Effect of thickness of soil layer remaining between TDR probe (located at zero) and surface of the remaining soil sample on measured K_a values (dots) and estimated energy of TDR signal inside the soil sample (solid line).

the block surface or edges approached to within 0.02 m the measured K_a decreased to 95 % of the value prior to frame installation. The decrease in measured K_a with decreasing thickness of soil layer remaining between probe and sample is consistent with the theoretical model of Knight et al. (1994) (solid line in Figure 3.2). Knight's model predicts 0.016 m (dotted line in Figure 3.2) as the critical distance between probe and soil surface for 95 % of the effective measurement volume. For our probes the model De Clerk et al. (1985, in: Petersen et al., 1995) used predicts 0.03 m as the distance between probe and the soil surface up to which 94 % of the energy of a waveform is restricted in the soil (dashed line in Figure 3.2).

3.2. Empirical Calibration Functions

Comparison of soil water content as derived from measured K_a values using the Topp-calibration function to that calculated from gravimetrically measurements revealed the inadequacy of the Topp-calibration for our soils (Figure 3.3 and 3.4). Each point represents a measurement taken from a soil block at a particular time step during desaturation. On both soils, measurements in topsoils (open circles) compare to those in subsoil (dots). For all K_a values measured in the *Humitropept* (well aggregated clay) showed a wider variation in measured water content than the *Hapludand* (less aggregated loam). The *Hapludand* saturates to higher water contents ($0.8 \text{ m}^3 \text{ m}^{-3}$) than the *Humitropept* ($0.7 \text{ m}^3 \text{ m}^{-3}$). This agrees with field samplings for soil moisture measurements, where the *Hapludand* had higher soil water contents than the *Humitropept* during very wet periods. For both soil types we find that using Topp's calibration function results in an underestimation of the soil water content, and the offset is not linear.

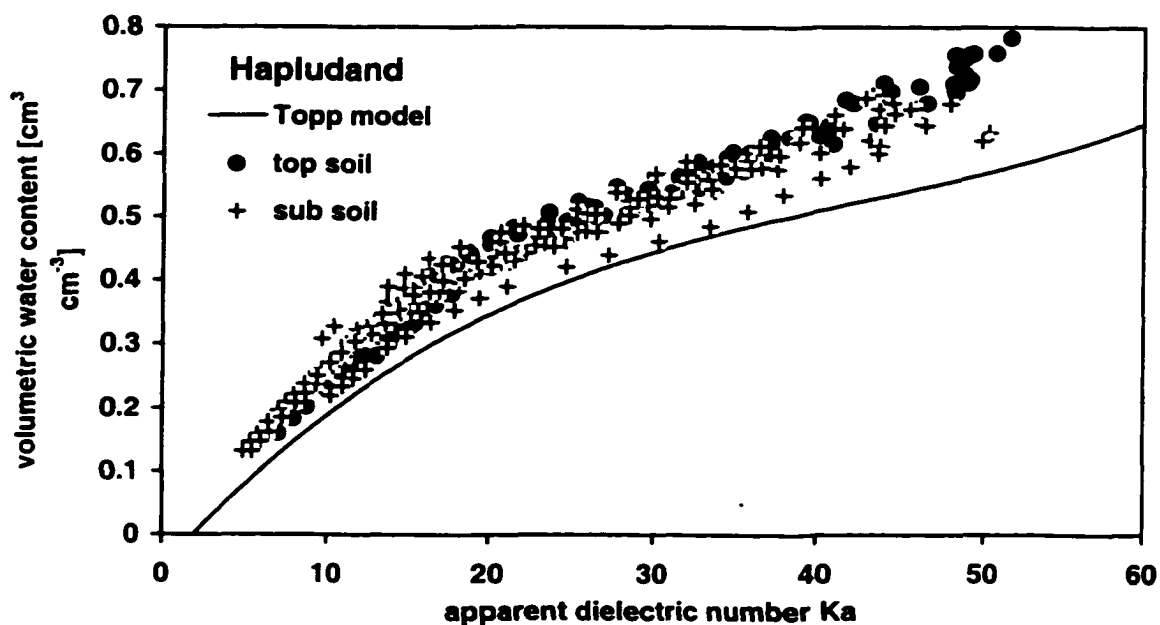


Figure 3.3: Relation between measured apparent dielectric number and gravimetrically determined soil water content for samples from the Hapludand. Calibration results are compared to the Topp calibration function (solid line).

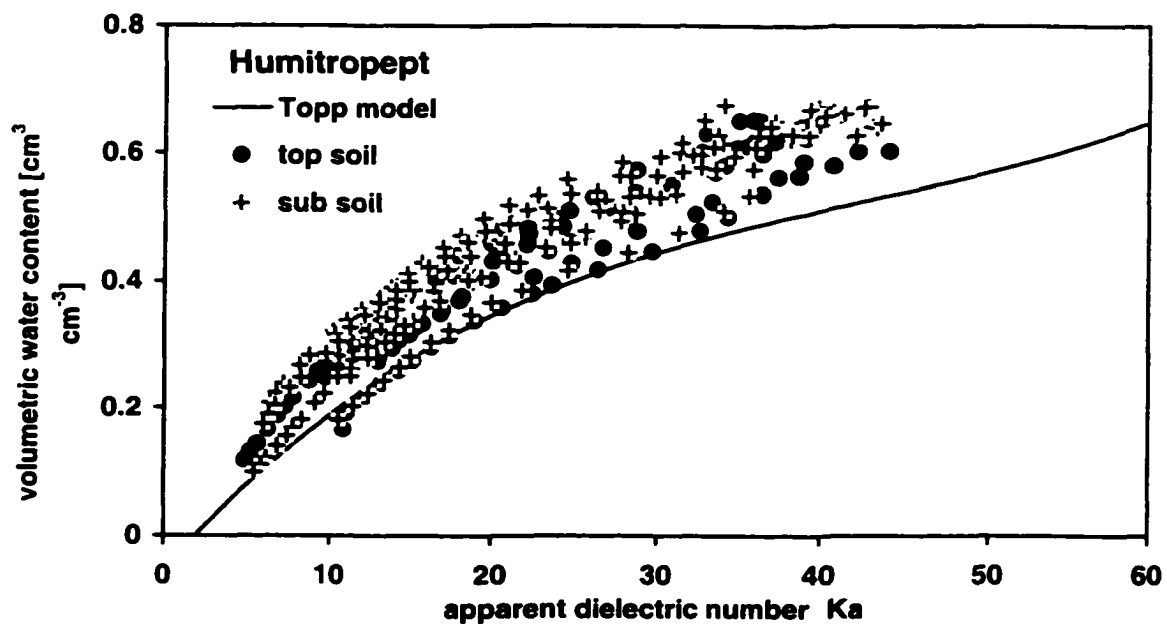


Figure 3.4: Relation between measured apparent dielectric number and gravimetrically determined soil water content for samples from the Humitropept. Calibration results are compared to the Topp calibration function (solid line).

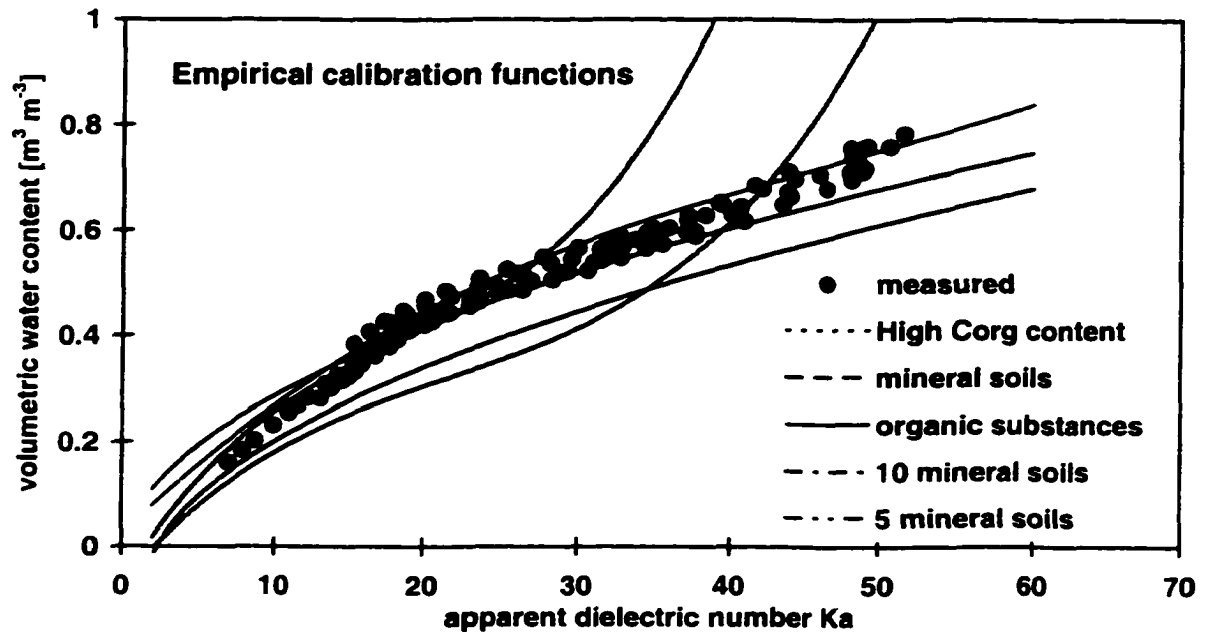


Figure 3.5: Comparison of calibration data measured on the samples from the topsoil of the *Hapludand* to five selected empirical models (dotted line, that of Gray and Spies [1995] for mineral soils with high organic matter content; dashed line, that of Roth et al. [1992] for mineral soils; solid line, that of Roth et al. [1992] for organic substances; dash-dotted line, that of Jacobsen and Schjønning [1994] for 10 mineral soils; dash-dot-dotted line, that of Malicki and Skirucha [1998] for 5 mineral soils).

Jacobsen and Schjønning (1995) present a valuable summary of published calibration functions. We used those functions and the models presented by Gray and Spies (1995) on our data. Here we present a selection of empirical (Figure 3.5) and mixing models (Figure 3.6) in comparison to data we measured on samples from the topsoil of the *Hapludand*. Using empirical power functions (e.g. Gray and Spies, 1995; Herkelrath et al., 1991) and third-order polynomials (e.g. Roth et al., 1992; Dasberg and Hopmans, 1992; Jacobsen and Schjønning, 1993) on our calibration data confirm that empirical models do not necessarily fit other soils (Figure 3.5). Generally, empirical models derived for mineral soils of temperate areas fit our data poorly, because in humid tropical soils of low bulk density the range of water content is different. Extrapolation of

empirical functions to high water contents often render physically unrealistic results. The model for organic substances by Roth et al. (1992) best matched our data, even though our soils are preliminary of mineral composition.

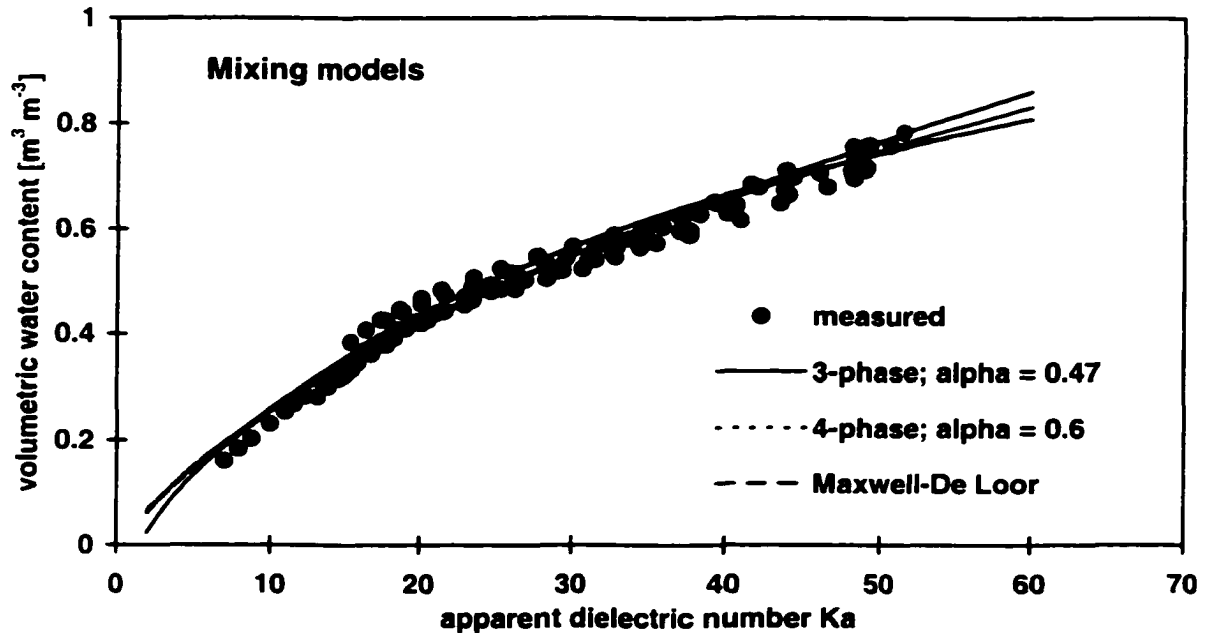


Figure 3.6: Comparison of calibration data measured on the samples from the topsoil of the Hapludand to three mixing models as presented by Dobson et al. [1985] (dotted line: in the four-phase α mixing model we used a specific surface area of $250 \text{ m}^2 \text{ g}^{-1}$ soil; dashed line: for the Maxwell-De Loor mixing model we used a specific surface area of $250 \text{ m}^2 \text{ g}^{-1}$ soil).

3.3. Mixing Models

The three-phase- α and four-phase- α mixing models (Dobson et al. 1985) match our data well (Figure 3.6). We corrected the dielectric number of free water for the average temperature measured in the laboratory during calibration. Based on a sensitivity analysis in which only the dielectric number of soil was manipulated, we choose $\epsilon_s = 4$ for our soils. The three-phase mixing model with $\alpha = 0.47$ fits our data best for both

topsoil and subsoil of the *Hapludand* (Figure 3.7) (RMSE = 0.021 and 0.035; Table 3.3) as well as the topsoil of the *Humitropept* (Figure 3.8) (RMSE = 0.043; Table 3.3). The Maxwell-De Looer mixing model with a specific surface area $S = 250 \text{ m}^2\text{g}^{-1}$ fits the subsoil samples of the *Humitropept* best (RMSE = 0.041; Table 3.3). Assuming different specific surface areas in the range of 50 to $500 \text{ m}^2\text{g}^{-1}$ we found that for low surface area the four-phase- α model does not differ much from the three-phase model, while high values for S moved the calibration function up to volumetric water contents that exceeded the range covered by our calibration data. Because S is included in the model as a linear factor only, the shape of the calibration function stays unchanged with different S . The four-phase- α model matched our data best when using an $\alpha = 0.6$ and a specific surface area of $250 \text{ m}^2\text{g}^{-1}$. Because we have no adequate estimate of S , we also tested the

Table 3.3. Characterization of Soil Samples Used for Calibration, Differentiated by Soil Type and Sampling Depth, and Root Mean Square Error for Selected Empirical and Mixing Models When Applied to Calibration Schemes

	<i>Hapludand</i>		<i>Humitropept</i>	
	Topsoil	Subsoil	Topsoil	Subsoil
Bulk density	0.668	0.753	0.767	0.816
Porosity	0.748	0.716	0.711	0.692
Number of observations, n	107	134	86	141
<i>Empirical Calibration Functions</i>				
Topp calibration function	0.114	0.092	0.095	0.116
<i>Roth et al.</i> , 1992; mineral soils	0.486	0.362	0.191	0.214
<i>Roth et al.</i> , 1992; organic soils	0.030	0.051	0.054	0.040
<i>Jacobsen and Schjønning</i> , 1993; 10 mineral soils	0.133	0.124	0.109	0.127
<i>Gray and Spies</i> , 1995; high organic carbon content	0.038	0.028	0.041	0.047
<i>Malicki and Skierucha</i> , 1989; mineral soils	0.102	0.086	0.091	0.111
<i>Herkelrath et al.</i> , 1991; organic soils	0.104	0.119	0.117	0.093
<i>Ledieu et al.</i> , 1986; loam	0.099	0.088	0.092	0.114
<i>Mixing Models</i>				
<i>Roth et al.</i> , 1990; three phases, $\alpha = 0.47$	0.022	0.042	0.044	0.045
<i>Dobson et al.</i> , 1985; three phases, $\alpha = 0.5$	0.023	0.041	0.044	0.051
<i>Dobson et al.</i> , 1985; four phases, $\alpha = 0.6$, $S = 250 \times 10^4$	0.025	0.047	0.047	0.043
<i>Dobson et al.</i> , 1985; Maxwell-De Looer model	0.023	0.041	0.045	0.050
<i>Jacobsen & Schjønning</i> , 1993; Maxwell-De Looer, three phases	0.024	0.041	0.045	0.056

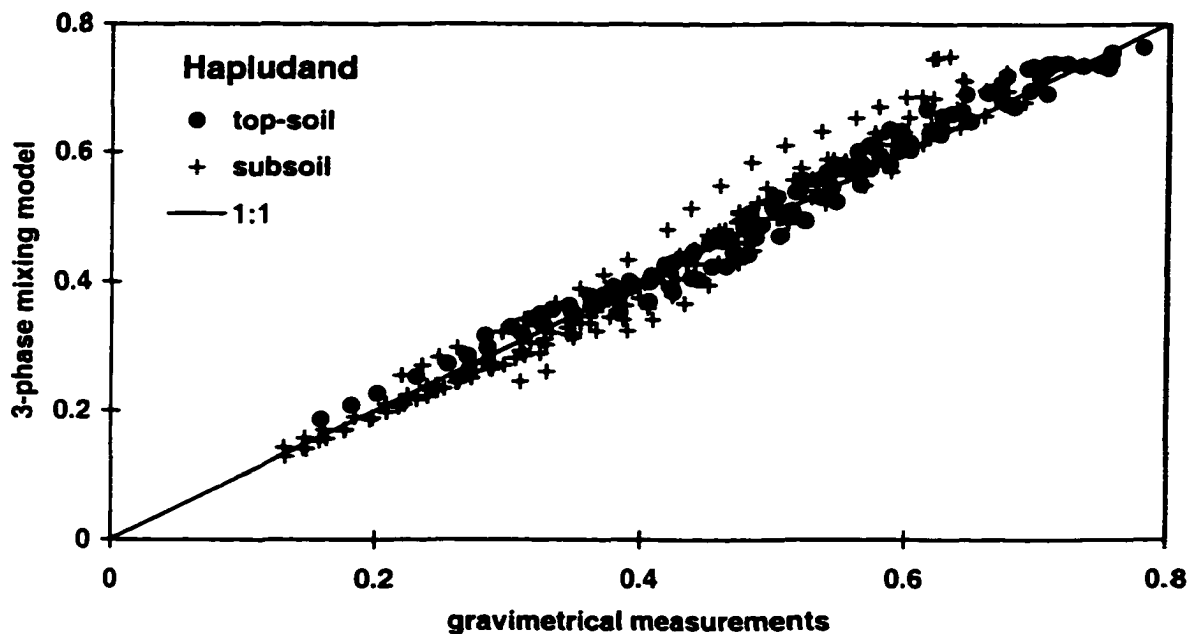


Figure 3.7: Comparison of gravimetrically measured soil water content to that derived using the three-phase α mixing model with $\alpha = 0.47$. Calibration values are measured from samples of the Hapludand.

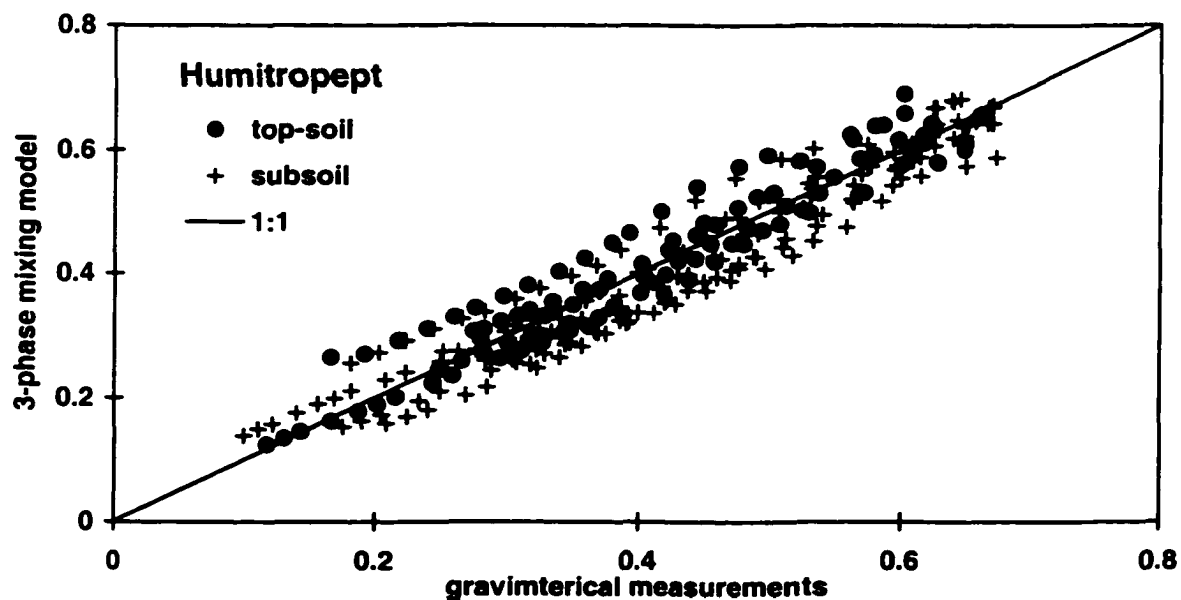


Figure 3.8: Comparison of gravimetrically measured soil water content to that derived using the three-phase α mixing model with $\alpha = 0.47$. Calibration values are measured from samples of the Humitropept.

simplification of the Maxwell-De Looer model as presented by Jacobsen and Schjønning (1995) which excludes bound water from the function. But the simplification of the Maxwell-De Looer model did not improve results received from the three-phase- α mixing model with $\alpha = 0.47$.

3.4. Effects of Air-Filled Holes on TDR Measurements

Calibration results of the well structured *Humitropept* (Figure 3.4) as well as field measurements emphasize the influence of soil heterogeneity on TDR measurements. We studied the effect of spatial variation in soil-air composition by creating air-filled holes in a soil block measured. We determined initial bulk density and soil water content of the sample, and compared it to the initial soil water content estimated using the three-phase- α mixing model using $\alpha = 0.47$ (Figure 3.9). With each soil core taken from the sample block we removed a known amount of soil material and humidity. After each removal we recalculated bulk density and gravimetrically based water content of the sample and estimated the soil water content from measured K_a value, using the recalculated value for bulk density in the model. For both, recalculation and estimation, we distinguished two approaches: (1) we related the removed soil material to the whole sample block, (2) we related the removed core to the TDR measurement volume only.

Subsequent removal of soil cores from the central area of the TDR measurement volume decreased both, the calculated and the estimated water content (Figure 3.9). Because the TDR measurement volume covers only a part of the total sample volume, changes in water content after removal of cores are more pronounced when recalculated for the cylindrical TDR measurement volume only, rather than for the whole sample block. The three-phase- α mixing model with $\alpha = 0.47$ matched the soil water content

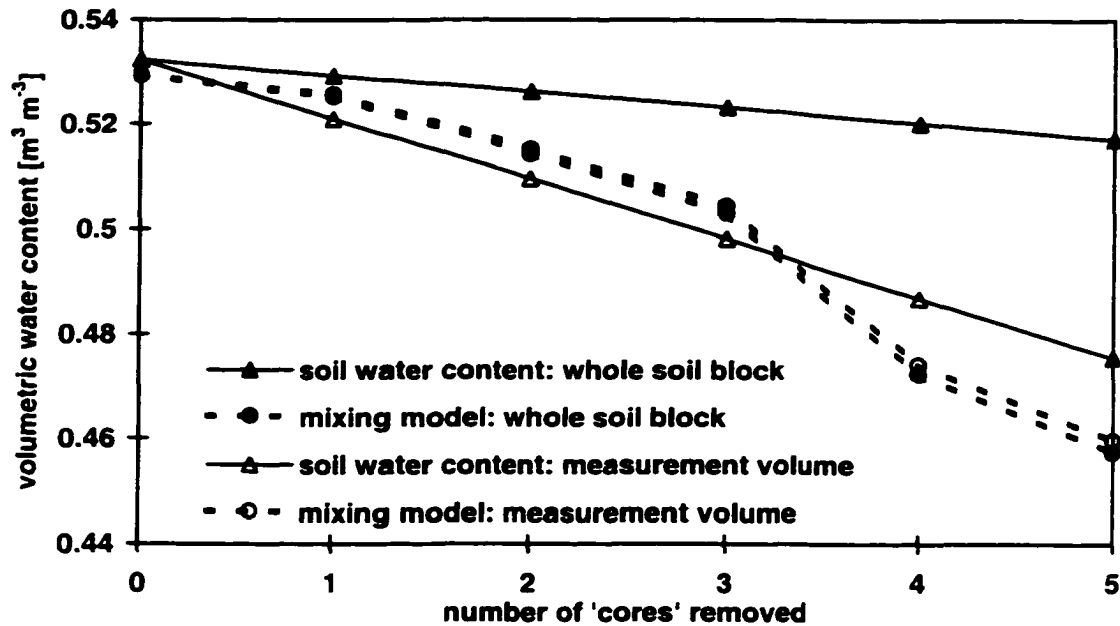


Figure 3.9: Effect of increasing number of artificial holes in a soil sample as used for calibration on estimated soil water content using a three-phase α mixing model with $\alpha = 0.47$ and gravimetrically determined water contents calculated for different soil volumes.

calculated for the measurement volume well, regardless of whether the reference volume used for recalculation of soil bulk density is the whole soil block or the TDR probe measurement volume only. This result confirms Heimovaara et al. (1994) who found that the three-phase- α mixing model shows relatively low sensitivity to small changes in bulk density. Thus using the three-phase- α mixing model for K_a values measured in situ will deliver acceptable estimates for soil water contents, also if some inhomogeneities in soil bulk density are present in the probe vicinity.

4. Discussion and Conclusion

We used undisturbed soil samples for our calibration experiment, assuming that these reflect site specific small scale variation in the spatial structure of the soil matrix.

Because most calibration studies sample bulk soil material, air dry, homogenize, sieve, repack and compact it to a desired bulk density before installing a TDR probe, the site inherent variability in soil composition and variation among replicated soil samples is minimized prior to the calibration experiment. Consequently the variation in replicated measurements of K_a and soil water content derived by gravimetric methods is reduced, resulting in a better RMSE compared to results of studies that use undisturbed soil samples. Jacobsen and Schjønning (1995) present RMSE values for a list of published models to show the performance of these functions on their data set derived from repacked soil samples. In general the calibration models tested performed better on their data (RMSE range 0.012 to 0.178) than on our data (RMSE range 0.021 to 0.525). In our study, the loamy *Hapludand* showed less variation in replicated measurements than the clayey *Humitropept*. This probably reflects the difference in soil structure between the soil types. The *Hapludand* is less severe aggregated than the *Humitropept*. The variation we find in our data is comparable to the variation Roth et al. (1990) presented for their calibration using undisturbed samples from various temperate zone soils. Furthermore, higher RMSE values result when using empirical calibration functions on our data because of errors implicit in extrapolation of models into high ranges of K_a . Empirical models derived for mineral soils of temperate zones poorly fit our data (RMSE range 0.031 to 0.525), because they generally are not validated for high volumetric water contents found in humid tropical soils of low bulk density.

Repacking homogenized soil material provides replicates with low variations, but it is likely that for most soils the original soil physical properties can not be re-established in the laboratory. This is especially true for the soils of andic origin and soils in which

very high biological activity causes well developed structure. Studies that homogenize soil may introduce a bias into the calibration results towards homogeneous soil conditions, which often are not reflected in the field. Application of calibration results on field installed TDR probes then transfers this bias into final estimates of field soil water content. From available studies a quantification of errors in calibrations introduced by homogenizing samples is not possible. However, a comparison of calibrations performed on undisturbed soils with calibrations done on homogenized samples from structured temperate zone soils would be a valuable study for evaluation of calibrations and their application to field measurements.

The validity of empirical models is restricted to the range of soil water contents of the source data, and to soils with soil properties comparable to those of the soils empirical functions were originally derived from (e.g. Roth et al., 1990; Dasberg and Hopmans, 1992; Roth et al., 1992; Dirksen and Hilhorst, 1994). Our study showed that extrapolation of empirical models to ranges of higher water contents is inadequate. The soils we studied have lower bulk density and higher organic matter content than most temperate zone soils. Published empirical models suggest that both lower bulk density and higher organic matter content result in higher water contents for given K_a values than estimated by the Topp-calibration function (for substances rich in organic matter: Herkelrath et al, 1991; Roth et al., 1992; Gray and Spies, 1995). The data published by Dirksen and Hilhorst (1994) for soils of low bulk density and for soils with high organic matter content confirm this observation. Extremely high bulk densities tend to show a negative effect on the relation between K_a and actual soil water content compared to Topp's-calibration (Vielhaber, 1996; Dirksen and Hilhorst, 1994). Published data reveal an

influence of soil organic matter content and bulk density, but the contribution of a particular variable has not been distinguished or partitioned yet.

Mixing models account for soil specific properties by including porosity for volumetric partitioning between soil components. Four-phase-mixing models also include soil specific surface area to account for water binding properties. Soil organic matter also has an effect on soil water binding, but organic matter is not specifically incorporated into mixing models. Mixing models appear to be robust approaches that are applicable to a broad range of soils of different physical and chemical composition. Jacobsen and Schjønning (1995) calculated a RMSE of 0.0421, when using the three-phase- α model (with α 0.5) for their data that originate from 10 mineral soils of the temperate zone. This is comparable to what we find for the clayey *Humitropept* (RMSE 0.043 for topsoil and 0.046 for subsoil); the RMSE we derived for the loamy *Hapludand* (0.021 for topsoil and 0.035 for subsoil) is even smaller. Using undisturbed soil samples, Roth et al. (1990) determined the geometry parameter α as 0.46, a value that fitted calibration data well for both of our soils, even though the major humidity range for our soils is covered by few measurements in the calibration performed by Roth et al. (1990).

Heimovaara et al. (1994) used a sensitivity analyses to show the impact of the different parameters in the four-phase- α mixing model. They showed that the model is sensitive to changes in thickness of bound water layer and soil bulk electrical conductivity. Because we did not measure any of these properties nor did we measure the soil specific surface area, we did not consider models that use bound water for the final selection of feasible calibration models. For our data the three-phase- α mixing models delivered best results. Because different experiments show that three-phase- α mixing

models are robust calibration approaches, we regard their application preferable to the use of empirical functions. In practice, three-phase- α mixing models are as easy to use as empirical calibration functions once the soil specific parameters are determined. Our experiment of artificially introducing air-filled cavities showed that the three-phase- α mixing model showed acceptable water content estimations with slightly varying bulk densities calculated. This indicates that valid reference bulk densities can be used in mixing models to estimate soil water content at long-term measurement plots. Measuring the parameter necessary in mixing models is a labor-intensive and site disturbing process. However, to ensure proper estimation of water content from TDR measurements, some calibration measurements (preferably using undisturbed soil samples) should accompany each TDR application, to verify a chosen calibration approach.

Our calibration study forms part of an ongoing research project that studies short-time-scale effects of soil water content on trace gas emissions from agricultural soils. For our project an accurate determination of soil water content is essential to evaluate biogeochemical processes and soil gas diffusion. Comparing the soil water content estimated using the Topp-calibration function, to that estimated using the three-phase- α mixing model with $\alpha = 0.47$ (Figure 3.10), clearly shows the importance of a proper calibration of the TDR technique. Using gravimetric methods in long term field studies we measured an average annual soil water content of $0.58 \text{ m}^3 \text{ m}^{-3}$, which is comparable to estimates from TDR measurements using the three-phase- α mixing model with $\alpha = 0.47$. Gas diffusion strongly depends on soil water content and soil structure. Because we use water filled pore space as a deterministic variable for soil trace gas emissions, a correct estimate of the field soil water dynamics is essential for estimations of nitrogen oxides

emissions. The three-phase- α mixing model is a robust and valuable tool in calibration of TDR technique. It should be considered for a broad range of soils.

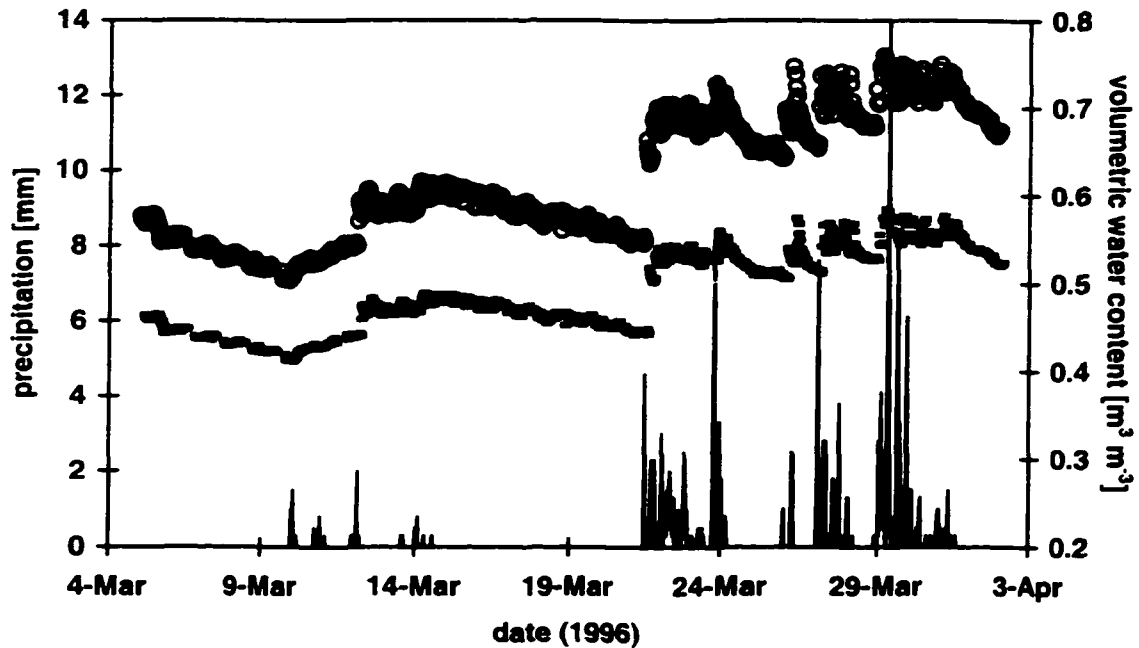


Figure 3.10: Comparison of soil water contents estimated using Topp's calibration function (dots) to those using a three-phase mixing model with $\alpha = 0.47$ (open circles) on field measured K_a values. Soil water content and precipitation (spines) are shown as half hourly measurements for the period March 4 to April 3, 1996. Measurements at 5 cm depth are shown for a wet and a dry period.

CHAPTER 4

EFFECTS OF SOIL MOISTURE DYNAMICS ON N₂O EMISSIONS FROM HUMID TROPICAL AGRICULTURAL SOILS

Abstract

We studied soil moisture dynamics and nitrous oxide (N₂O) fluxes from agricultural soils in the humid tropics of Costa Rica. Using a split-plot design on two soils (clay, loam) we compared two crop types (annual vs. perennial), each unfertilized and fertilized. N₂O emissions were measured at 4.6 hour interval, meteorological variables, soil moisture and temperature at 0.5 hour interval. Both soils feature relatively low bulk density, strong aggregation of the surface soil (0-0.03 m), and high organic matter content, water retention capacity, and hydraulic conductivity. Mean daily soil moisture content at 0.05 m depth range from 46% water filled pore space (WFPS) on clay in April 1995 to about saturation on loam in February 1996, though the aggregated surface layer prevailed unsaturated. Soils emitted N₂O throughout the year, temporal variation of fluxes was determined by agricultural management. Fertilization caused short-term peaks of N₂O fluxes, emissions were increased over a period of about 6 weeks. Weeding may affect N₂O fluxes for a period of about 4 weeks. After fading of management effects emissions continued at lower level. This was considered to be 'background flux'. Average N₂O fluxes from unfertilized loam under annual crop were 1.04 ± 0.72 ng N₂O-N cm⁻²h⁻¹ (mean \pm standard deviation) compared to 3.54 ± 4.31 ng N₂O-N cm⁻²h⁻¹ from fertilized loam (351 days measurement period); post-fertilization fluxes were 6.3 ± 6.5 ng N₂O-N cm⁻²h⁻¹ while background flux level were 2.2 ± 1.8 ng

$\text{N}_2\text{O-N cm}^{-2}\text{h}^{-1}$. Soil moisture dynamics modified fertilization effects. Post fertilization fluxes were highest from wet soils. Fluxes from a recently fertilized relatively dry soil increased only after rain re-wet the soil. Emissions were independent of soil moisture during phases of low nutrient availability. Statistical modeling using a multiple regression technique identified nutrient availability and soil moisture as major complementary controls on N_2O flux. First simulations with the process model DNDC (DeNitrification-DeComposition) suggested that moisture differences within the upper 0.03 m of soils could be important for N_2O fluxes, though prior to testing this hypothesis the current modeling of soil hydraulic behavior and the physiological parameterization for perennial crop require further modifications to improve the performance of the process model for humid tropical agricultural soils.

1. Introduction

Nitrous oxide (N_2O) is an important atmospheric trace gas (Rhode, 1990). It is involved in many essential environmental processes in atmospheric (Crutzen, 1981), (IPCC, 1996) and in biological systems (Galloway et al., 1995). Globally, soils are the major source of atmospheric N_2O . Forest soils in humid tropical regions are estimated to account for about 21% of the total global N_2O production on annual basis (Matson and Vitousek, 1990). For estimation of present and predictions of future N_2O emissions, it is critical to identify the sources and to understand the processes involved.

Soil microbes produce and consume N_2O during the natural processes of nitrification and denitrification (Williams et al., 1992). The conceptual model presented by Firestone and Davidson (Firestone and Davidson, 1989) provides a simple approach to the complex processes of nitrogen oxide (NO and N_2O) production and consumption. In

essence, the amount of nitrogen cycling in soils and the soil environmental conditions (e.g. soil temperature, moisture, pH, oxygen and carbon concentration) are the dominant controls on microbial processes that determine gaseous nitrogen loss. In humid tropical soils temperature and moisture content are in the optimal range for biological processes for most of the year resulting in generally large gaseous N-loss.

Soil moisture has multiple effects on nitrogen trace gas emissions. Water is essential for microbial survival and activity. Soil moisture dynamics determine the biogeochemical environment for microorganisms, affecting the dilution of the microbial populations and the availability of dissolved nutrients, such as organic carbon, ammonium and nitrate. Soil water content affects the oxidation-reduction conditions in soils as well as gas diffusion. Aerobic conditions in dry soils favor microbial nitrification from which the major gaseous product is NO. In moist soils under more reducing conditions denitrification dominates, resulting in the production and consumption of reduced nitrogen forms (N₂O and N₂). Denitrifiers are everywhere (Vermoesen et al., 1993) and denitrification depends on substrate availability and oxygen deficiency. Micro-scale variability in soil moisture and nutrient distribution cause nitrification and denitrification to occur simultaneously in soils (e.g. Robertson, 1989; Davidson, 1993) and results in generally high spatial variability of nitrogen oxide emissions.

Fertilization significantly increased the soil-atmosphere flux of N₂O on tropical soils (Matson et al., 1996; Veldkamp et al., 1998; Crill et al., in press). Expansion and intensification of tropical agriculture is expected to be a major contributor to increasing atmospheric N₂O concentrations (Rosenzweig, 1994). We performed a 2 years field experiment in the humid tropical lowland of Costa Rica to identify, quantify and evaluate

the major influencing factors on N₂O emissions from agricultural soils (Crill et al., in press). This paper studies the effects of soil moisture dynamics on N₂O fluxes using statistical and process based modeling approaches.

2. Study Area

We performed our field experiment at the La Selva biological station of the Organization for Tropical Studies in the Atlantic lowland of Costa Rica (10°3' N x 84° 0' W). The climate is humid tropical with an average annual air temperature of 25.8 °C (± 0.69 °C standard deviation) and total annual rainfall of 3961.8 mm (± 723.2 mm) (Sanford et al., 1994). Precipitation is well distributed throughout the year, with a slightly drier period from January through April. Mean monthly precipitation was lowest in March (152 mm) and largest in July (481 mm) over a 29 years period.

We studied two soil types, a loam (*fluventic Eutropept*) and a clay (*andic Dystropept*) (Table 4.1). Both Inceptisols are of andic origin. The pH is slightly more acidic in the clay compared to the loam. Both soils feature high organic matter content

Table 4.1: Soil characteristics of the loam (*fluventic Eutropept*) and clay (*andic Dystropept*) measured at 0-0.1 m depth. Data are mean values, standard deviation is given in brackets, n.a. means 'not available'. Field capacity (FC) is estimated from laboratory retention curves as soil moisture content at -6 kPa (upper FC value) and -30 kPa (lower FC value).

	Loam		Clay	
	Unfertilized	Fertilized	Unfertilized	Fertilized
C/N	9.5 (0.61)	9.3 (0.52)	10.1 (0.66)	10.3 (0.77)
N [%]	0.53 (0.11)	0.54 (0.08)	0.41 (0.10)	0.45 (0.05)
PH _{H2O}	7.07 (0.06)	6.64 (0.20)	5.13 (0.21)	5.02 (0.75)
Bulk dens. [g cm ⁻³]	0.70 (0.04)	0.69 (0.06)	0.79 (0.05)	0.79 (0.04)
FC _(6kPa) [WFPS]	0.82 (0.03)	0.83 (0.03)	0.66 (0.02)	0.68 (0.11)
FC _(30kPa) [WFPS]	0.76 (0.03)	0.78 (0.04)	0.56 (0.06)	0.52 (n.a.)
K _(sat) [cm d ⁻¹]	641 (105)	502 (103)	624 (172)	656 (136)

(about 7.5 % in the upper soil, and about 1-3 % in deeper layers), low bulk density (about 0.7 kg m^{-3} in the upper soil, to about 0.8 kg m^{-3} in deeper soil layers), and high saturated hydraulic conductivity (about $5\text{-}6 \text{ m day}^{-1}$ in upper soil layers, to about $6\text{-}9 \text{ m day}^{-1}$ in deeper layers).

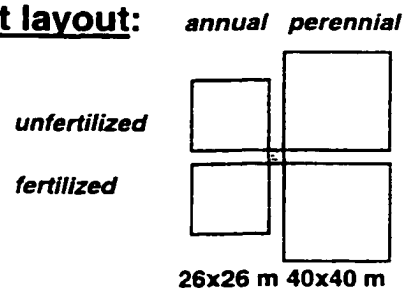
3. Experimental Design

We cleared about 1 ha from secondary forest on clay (February 1994) and loam (March 1994) and burned slash in March and in April 1994, respectively (Weitz et al., 1998). We established a split-plot experiment comparing the two soil types, each under two crop types (annual versus perennial), and two agricultural treatments (unfertilized versus fertilized; Figure 4.1). We installed four experimental plots on each cleared patch.

Split-plot design:

- * clay vs. loam
- * annual & perennial
- * unfertilized & fertilized

Plot layout:



 Air conditioned field laboratory

Field instrumentation:

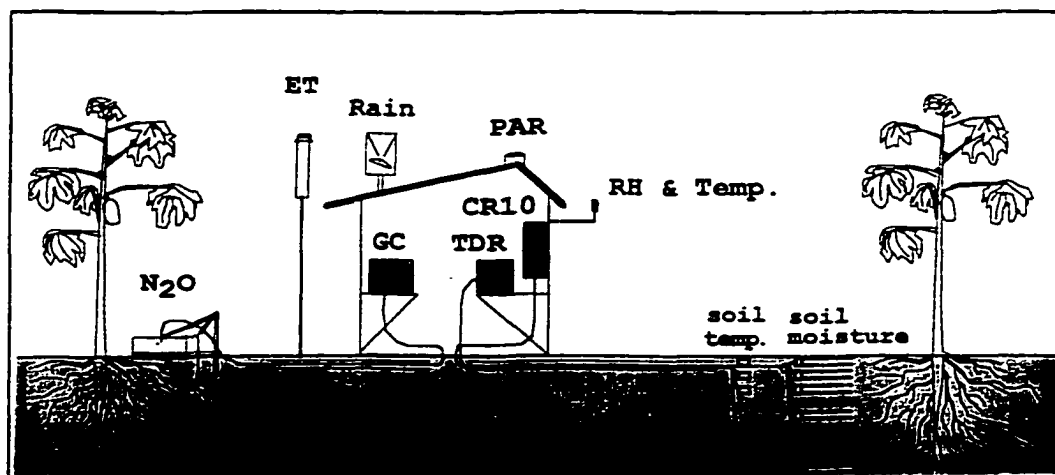


Figure 4.1: Plot design and instrumentation of field sites

Subplots were 25x25 m for annual crop, and 40x40 m for perennial crop. An air-conditioned field laboratory (3x3 m) was constructed in the center between subplots to house instruments. Buried PVC conduits guided electrical cables and nylon gas sampling tubes from each subplot into the laboratory. Only one automated system was available, therefore we switched the mobile above ground equipment between soil types after an individual cropping cycle for the annual crop was completed. Automated measurements were performed on the loam from November 10, 1994, through March 15, 1995, on the clay from March 16, 1995, through January 8, 1996, and again on the loam from January 9, 1996, through August 23, 1996.

4. Methods

Measurement techniques for automated sampling and analysis of N₂O fluxes are described in detail by Crill et al. (in press). In short, we installed two pneumatically operated chambers on each subplot. A total of 8 automated chambers were available, each of them was sampled for N₂O fluxes at a 4.6 hours interval. For measurements, one chamber at a time was closed for 23 minutes to sample fluxes from a soil surface area of 0.187 m². During sampling the chamber headspace was connected in a closed loop to the instruments inside the field laboratory. A pump maintained continuous air circulation. We used a gas chromatograph with electron capture detection (GC-ECD, *Shimadzu Mini-2*) for N₂O analysis. Automated valves alternated gas flow from the chamber headspace and from standard gases to the GC. We used commercially available calibrated standard gases (*Scott-Marin*, Sunnyvale, CA) for measurement calibration. Data was acquired and stored using a desktop computer. Fluxes were calculated from the linear increase of N₂O concentration in the chamber headspace during the time of chamber closure.

We used an automated time domain reflectometry (TDR) technique (e.g. Dobson et al., 1985; Topp et al., 1988; Roth et al., 1990) to identify soil moisture dynamics. A cable tester (*Tektronix 1502 B/C; Tektronix Inc., Redmond, Oregon*) was connected to 0.3 m long 2-rod TDR probes (Spaans and Baker, 1993) to measure the dielectric properties of soil. Probes were equipped with Belden 8219 RG-58 A/U coaxial cable and a 1:1 balun, which was reported to be preferable for measurements in wet soils (Spaans and Baker, 1993). We inserted TDR probes horizontally into the soil to avoid introduction of artificial water pathway along the probes and to confine measurements to a relatively short depth interval (about 0.06 to 0.07 m width; (Ferré et al., 1998)). On each subplot a total of nine TDR probes were installed at five depths (Figure 4.1), this report refers to the replicated measurements at 0.05 m depth only. We used five multiplexers for 50 Ohm coaxial cable (SDMX50; *Campbell Scientific Inc., Logan, UT*) in a two-level hierarchical design, to allow the measurement of multiple TDR probes by one cable tester. A 6590 transient suppressor (*Campbell Scientific Inc.*) protected the system from power surges and lightning damage. Communication between the cable tester and a CR10 data logger was permitted by a SDM1502 interface (both *Campbell Scientific Inc.*). We programmed the data logger for automated acquisition of the reflected TDR signal. A laptop computer accommodated data collection from the CR10 at 0.5 hours interval.

We used a modification of the TRACE.41 program developed by Spaans and Baker (personal communication, 1994) for automated interpretation of K_a from the TDR signal. K_a values were corrected for length of coaxial cable used for field measurements (Weitz, unpub. data), and then, together with bulk density and soil temperature data, employed in a 3-phase mixing model ($\alpha = 0.47$) to derive volumetric soil water content

values (Weitz et al., 1997; Table 3.1). Soil moisture was expressed as the ratio of the water filled pore space (WFPS) in soils (Linn and Doran, 1984). WFPS allowed to evaluate the soil moisture conditions for microbial activity (Davidson, 1993) and accommodated simulations with the DNDC model. We did not test for effects of increased electrical conductivity from fertilization on TDR measurement.

A tipping bucket (Model 6011, *Qualimetrics Inc.*, Sacramento, CA) and a combined temperature and relative humidity probe (HMP35C; *Campbell Scientific Inc.*) were installed in the vicinity of the field laboratory (Figure 4.1). The temperature probe had a thermistor (*Fenwal Electronics* UUT51J1) housed in a 12 plate Gill radiation shield. Soil temperature ($^{\circ}\text{C}$) was measured using thermocouple sensors (T-type wire) connected to a CR10 data logger through a AM416 low level analog signal multiplexer (*Campbell Scientific Inc.*). This report presents soil temperature data measured at 0.05 m depth only. The pulse output from the tipping bucket was recorded and stored half hour rainfall totals, the data logger read all other sensors at 2 minute intervals and stored data as 0.5 hour averages.

Soil pH was measured within a few hours after sampling of soil from 0 to 0.1 m depth using an auger. We mixed 20 g field moist soil with 50 ml deionized water and measured after the solution was allowed to equilibrate for about 30 minutes. We used a laboratory Corning 245 pH meter (*Corning Labware & Equipment*, Corning, NY) calibrated for pH 4 to 7. A LECO CNS-2000 C/N analyzer (*LECO Corp.*, St. Joseph, MI) was used for measurement of total soil nitrogen by thermal conductivity and total carbon by an infrared technique (LECO, 1994). Air-dried soil (0.2 g) was combusted at 1300 $^{\circ}\text{C}$. Analysis were performed by the laboratory of the International Institute for Tropical

Forestry (IITF), USDA Forest Service, in Rio Piedras, Puerto Rico.

Infrequently throughout the experimental period we determined soil moisture gravimetrically (Keller et al., unpublished data). Using an auger (0.02 m diameter) we sampled soil from 0-0.1 m depth at 8 different locations per sub-plot, combining samples from 4 locations. Gravimetric moisture content was determined after weighting and oven drying at 105 °C (Gardener, 1986) and converted into WFPS using bulk density and porosity data measured at 0.05 m depth on each sub-plot. Soil bulk density (Mg m^{-3}) was determined from undisturbed soil samples taken in metal cores of 300 cm^3 volume (0.07 m height) after drying at 105 °C for 24 hour (Blake and Hartge, 1986). We evaluated soil structure studying bulk density changes within 0 to 0.07 m depth on 48 core samples from the clay subplots. The soil core was pushed carefully out of the metal ring and subdivided into three layers (0-0.02, 0.02-0.04, and 0.04-0.07 m). Each subdivision was analyzed for bulk density and soil moisture content. This experiment could not be repeated on the loam because during sampling in August 1996 the soil was too wet to allow sub-sampling. Friction of soil material at the metal ring when pushing the soil out resulted in disturbance of the relatively plastic loam.

Soil water retention characteristics for the low suction range (0 to 30 kPa suction) were determined at the La Selva laboratory using undisturbed soil cores (300 cm^3) in a hanging water column device (Klute, 1986). Moisture retention for the high suction range (300 and 1500 kPa) was determined by the laboratory of the Soil Science Institute, Free University of Hamburg, Germany, using bulk soil samples in pressure chambers (Klute, 1986). Field capacity was estimated as WFPS at 6 kPa, wilting point as WFPS at 1500 kPa. Saturated and unsaturated hydraulic conductivity (cm d^{-1}) was measured in the field

using undisturbed soil columns of about 0.03 m³ volume (0.1 m² flow area) in the modified crust test (Booltink et al., 1991).

Statistical analysis was performed using the JMPIN software (Sall and Lehman, 1996). We applied a paired t-test to identify significant differences between replicated sensors and between treatments. We used linear regression analysis to correlate mean daily N₂O fluxes with soil moisture content and multiple regression analysis for correlation of the daily fluxes with soil moisture and temperature. Separate regression models were developed for background, weeding and post-fertilization phases of the crop-treatment combinations. Weeding effects were modeled through 28 days post weeding and fertilization effects through 42 days post fertilization, respectively. N₂O fluxes were simulated for each time step from field measured moisture and temperature data using the appropriate regression model for management phase. Simulation results were evaluated by the root mean square error (RSME) criteria

$$RMSE = (\sum (X_{\text{measured}} - X_{\text{estimated}})^2 / n)^{0.5}$$

where X is the variable of interest and n is the number of observations. In regression analysis we used the natural logarithm (ln) of N₂O flux data.

We applied the 'DeNitrification-DeComposition' (DNDC) model to simulate soil-atmosphere N₂O fluxes from daily precipitation and temperature data, information on agricultural practice, and soil physical and chemical properties. DNDC is a modular structured process-based model originally developed for agricultural systems in the temperate zone (Li et al., 1992a; Li et al., 1992b). Soil moisture and temperature dynamics are simulated within a thermal-hydraulic sub-module. Soil hydraulic behavior is estimated based on texture-water retention relations developed for temperate zone

soils. Plant growth is simulated within a cropping sub-module. Interaction between both sub-modules accounts for transpiration effect on soil water dynamics. Simulated soil climate together with information about agricultural management serve as input for the decomposition and the denitrification sub-modules. The decomposition sub-module simulates microbial mineralization of soil organic matter and nitrification, the denitrification sub-module models N_2O fluxes from denitrification in wet soils and after precipitation. DNDC parameters and code were adapted to simulate water dynamics and N_2O fluxes from agricultural soils in the humid tropics. We used soil chemical and physical parameters estimated from field measurements and laboratory measured soil hydraulic characteristics. An option for rapid movement of water through largely unsaturated soil (by-pass flow) was introduced in the code. Concomitant reduction of the flow velocity for water movement through the soil matrix allowed high water retention in soils. Adjustments account for the bi-modal hydraulic behavior frequently reported for highly porous tropical soils, which may conduct water rapidly resembling properties of coarse textured soils, while showing water retention properties similar to fine textured soils (e.g. (Radulovich et al., 1992)).

5. Agricultural Management

Corn (*Zea mays* L.) was planted twice after land clearing (Table 4.2). Only corn cobs were harvested, about 90% of the above ground biomass remained as mulch on the subplots. Following corn we cropped two cycles of nampi (*Colocasia esculenta* (L.) Schott). After harvest of tubers in December 1995 all of the above ground biomass remained on the plots. When the field experiments ended in August 1996 the second nampi crop was still growing. Papaya (*Carica papaya* L.) seedlings were planted in June

Table 4.2: Cropping cycles for annual and perennial crop through the experiment.

Annual Crop		Perennial Crop	
1 st Corn crop	May '94 to October '94	Papaya	June '94 to November '95
2 nd Corn crop	November '94 to March '95		
1 st Nampi crop	May '95 to December '95	Balsa	December '95 to August '96
2 nd Nampi crop	January '96 to August '96		

1994. After senescence plants were cut in November 1995, all of the aboveground biomass remained as mulch on the subplots. Balsa (*Ochroma lagopus* Swartz) seedlings were planted in December 1995. Trees reached about 10 m height by the end of the field experiment.

Soils were never ploughed during our experiment. Harvest of nampi tuber caused the only recognizable disturbance of the top-soil layer. Weeding was performed manually using a machete and a weed whacker. We followed recommendations of the Costa Rican agricultural handbook (Lizano, 1991) for fertilizer type, amount and timing (Table 4.3). During the first fertilization after forest conversion we applied about half of the recommended fertilizer amount on both crop types. We used granular fertilizer only and it was broadcast manually.

6. Results

Repeated fertilization increased mean N₂O emissions, except for clay under annual crop (Table 4.4). Manually measured N₂O fluxes showed slightly increased emissions from fertilized clay (Keller and al., unpublished data). The automated system measured highest mean N₂O fluxes from loam under perennial crop (12.5 ± 15 ng N₂O-N cm⁻²h⁻¹; mean ± standard deviation). Mean and variation of fluxes as well as percentage of fertilizer-N lost as N₂O-N were positively related to the total amount of fertilizer

Table 4.3: Fertilization schedule, amount of fertilizer addition, percentage of fertilizer-N lost as N₂O gas during 42 days post fertilization, and soil type studied for each fertilization. Ammonium-nitrate (NH₄NO₃) was applied as 12-24-12 N-P-K fertilizer, except on June 10, 1994, when 10-30-10 N-P-K fertilizer was used. Urea (CO(NH₂)₂) was used on corn only. (n.a. = not available)

Annual Crop						Perennial Crop					
Crop	Fert. Date	Type	[kg-N ha ⁻¹]	%-N Lost	Soil	Crop	Fert. Date	Type	[kg-N ha ⁻¹]	%-N Lost	Soil
1 st Corn	6/8/94	NH ₄ NO ₃	11	n.a.	Clay	Papaya	7/18/94	NH ₄ NO ₃	33	1.43	Clay
	6/22/94	CO(NH ₂) ₂	46	n.a.	Clay		9/8/94	NH ₄ NO ₃	65	1.39	Clay
2 nd Corn	11/25/94	NH ₄ NO ₃	30	1.21	Loam	11/11/94	NH ₄ NO ₃	65	0.86	Loam	
	12/6/94	CO(NH ₂) ₂	92	0.98	Loam	1/13/95	NH ₄ NO ₃	65	0.77	Loam	
1 st Nampi	6/17/95	NH ₄ NO ₃	15	0.76	Clay	3/18/95	NH ₄ NO ₃	65	0.18	Clay	
	8/5/95	NH ₄ NO ₃	34	0.34	Clay	5/24/95	NH ₄ NO ₃	65	0.41	Clay	
	9/29/95	NH ₄ NO ₃	24	0.32	Clay	7/27/95	NH ₄ NO ₃	65	0.22	Clay	
2 nd Nampi	2/23/96	NH ₄ NO ₃	15	1.30	Loam	9/29/95	NH ₄ NO ₃	65	0.27	Clay	
	4/3/96	NH ₄ NO ₃	34	0.64	Loam	Balsa	2/2/96	NH ₄ NO ₃	65	2.31	Loam
	5/20/96	NH ₄ NO ₃	24	1.82	Loam	3/28/96	NH ₄ NO ₃	65	1.31	Loam	
						6/17/96	NH ₄ NO ₃	65	4.86	Loam	

Ammonium-nitrate (NH₄NO₃) was applied as 12-24-12 N-P-K fertilizer, except on June 10, 1994, when 10-30-10 N-P-K fertilizer was used. Urea (CO(NH₂)₂) was used on corn only. (n.a. = not available)

Table 4.4: Mean emissions of N₂O-N (ng N₂O-N cm⁻²h⁻¹), and N-loss (kg-N ha⁻¹) from unfertilized and fertilized annual and perennial crop. Standard deviation is given in brackets. We measured a total of 348 days on loam and 298 days on clay.

	Annual Crop				Perennial Crop			
	Clay		Loam		Clay		Loam	
	Unfert.	Fert.	Unfert.	Fert.	Unfert.	Fert.	Unfert.	Fert.
N ₂ O flux	1.43	0.81	1.04	3.54	1.22	1.89	1.28	12.5
	[0.89]	[0.79]	[0.72]	[4.31]	[0.92]	[1.58]	[2.34]	[15.0]
N-loss	1.02	0.58	0.87	2.96	0.87	1.35	1.07	10.4
Appl. Fert.		73		195		260		325
N-loss [%] ^{o)}		-0.6		1.07		0.16		2.88
Background	1.10	0.58	0.75	2.23	0.98	1.71	1.32	8.64
	[0.59]	[0.534]	[0.62]	[1.78]	[0.55]	[1.62]	[2.85]	[9.29]
Post-fertiliz.	1.97	1.39	1.33	6.31	1.50	2.18	1.21	17.6
	[1.02] ^{**)}	[1.02]	[0.70] ^{**)}	[6.54]	[1.16] ^{**)}	[1.49]	[1.21] ^{**)}	[19.2]
N-loss ^{***)}		-0.8		2.55		0.26		5.04

^{o)} N-loss as percent of applied fertilizer [kg-N ha⁻¹] is calculated from the difference between fertilized and unfertilized plots.

^{**)} Post-fertilization fluxes are measured on both plots during 42 days following a fertilization of one plot.

^{***)} N-loss during post fertilization periods only.

applied when comparing different fertilization rates within soil types. Loss was smaller from clay compared to loam. N-loss was calculated from the difference of average fluxes from fertilized unfertilized soils to estimate the emissions due to fertilization.

Daily mean soil temperature at 0.05 m depth showed small variation throughout the experimental phase (Table 4.5). Soil temperatures were different between crop types and between unfertilized and fertilized soils for perennial crop, but similar between treatments under annual crop. Diurnal temperature amplitudes may reach about 10 °C. Mean differences between night and daytime soil temperatures were < 2.2 °C on either soil type. Minimal temperature fluctuations between day and night probably explain the lack of diurnal dynamics of N₂O emissions (Crill et al., in press). In this study we used daily averages for all variables.

Table 4.5: Mean soil temperature and water filled pore space ratio (WFPS) at 0.05 m depth.

	Annual Crop				Perennial Crop			
	Clay		Loam		Clay		Loam	
	Unfert.	Fert.	Unfert.	Fert.	Unfert.	Fert.	Unfert.	Fert.
Soil temp.	27.9	27.8	27.1	27.2	28.2	28.0	26.0	25.4
	[1.0]	[1.2]	[1.3]	[1.3]	[1.0]	[1.0]	[1.0]	[0.8]
WFPS	0.79	0.70	0.86	0.86	0.84	0.77	0.84	0.90
	[0.09]	[0.08]	[0.10]	[0.09]	[0.07]	[0.07]	[0.10]	[0.09]

Standard deviation in brackets.

High biological activity and lack of soil tillage maintained aggregation of the surface soil throughout the agricultural period. Aggregates were more stable on clay than on loam, mainly because of texture and mineral composition, but partly this may also be a remnant of high temperature effects on clay aggregates from burning with forest conversion. On both soil types aggregation of the top 0.02 to 0.03 m and high hydraulic

conductivity data (Table 4.1) suggested prevalence of macro porosity in the surface layer. Mean bulk density of the top 0.02 m in clay was 0.68 Mg m^{-3} compared to 0.89 Mg m^{-3} at 0.04 to 0.07 m depth (Figure 4.2); mean porosity declined with depth from about 0.74 to 0.66. Probably most of this difference is due to a reduction of inter-aggregate pore volume (mainly very large and large macro-pores) from the strongly aggregated near surface soil to the more compact soil at 0.04-0.07 m depth. In aggregated clay soil we measured much smaller moisture content in the surface soil than at 0.04 to 0.07 m depth (0.4 versus 0.88 WFPS; Figure 4.2). Variation in soil moisture content within distinguished soil layers was due to spatial rather than temporal variability.

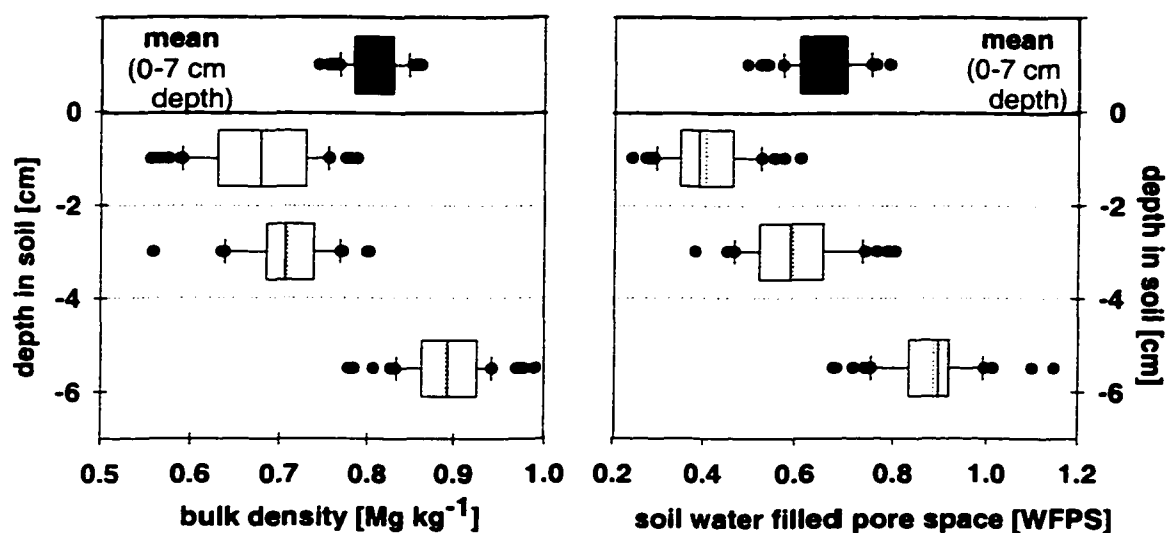


Figure 4.2: Mean bulk density and moisture content at 0-0.07 m depth and contribution of the sub-layers 0-0.02, 0.02-0.04, and 0.04-0.07 m to the mean. Bulk density sampling occurred at 3 different days.

Soil moisture dynamics measured at 0.05 m depth were similar between replicated TDR probes; measured moisture content differed between probes within a limited range (mean difference 0.15 WFPS), with one exception. From November 1994 to March 1995 we measured about 30% lower water content by one of the replicated TDR probes installed in loam under fertilized annual crop. Differences were possibly due to an air filled animal burrow within the measurement volume of that probe. Air filled gaps are a potential source for measurement error, affecting the reflection of the TDR signal (Ferré et al., 1996; Weitz et al., 1997). Data from this sensor were excluded from subsequent analysis.

In these highly porous soils, water content at 0.05 m depth was above 60% WFPS most of the year. Mean moisture content measured by TDR was higher in loam (0.86 ± 0.09 WFPS; mean \pm standard deviation) compared to clay (0.78 ± 0.08 WFPS). During rainy periods soils received precipitation almost daily. High precipitation amount and frequency together with high water retention capacity caused high soil water content over elongated periods (e.g. 0.95 ± 0.03 WFPS between November 15 and December 15, 1994 on loam; 0.82 ± 0.03 WFPS during July 1995 on clay). On days without rain soils drained pore water rapidly (mean about 0.02 WFPS per day during 5 dry days on either soil), drainage was fastest shortly after precipitation and slowed with elapsing time. Automated measurements recorded the driest conditions measured in all soils in clay towards the end of the dry phase in April 1995 (0.46 WFPS).

High moisture content was confirmed for both soils by infrequent gravimetric moisture measurements from the top 0.1 m of soils (0.81 ± 0.12 WFPS on loam; 0.74 ± 0.10 WFPS on clay) (Keller and al., unpublished data). Data from both TDR and

gravimetric measurement techniques were available on 15 days between January 1995 and May 1996 (Figure 4.3). The gravimetric moisture content reported for May 6, 1996, appears to be very low. The loam received only 27.5 mm rain throughout April 1 to April 26, but a total of 70.1 mm fell during the 10 days preceding the measurement on May 6. Small variability between gravimetric samples suggested that undetected problems in either sampling method rather than spatial variability could have caused the large deviation. We excluded the point from the analysis.

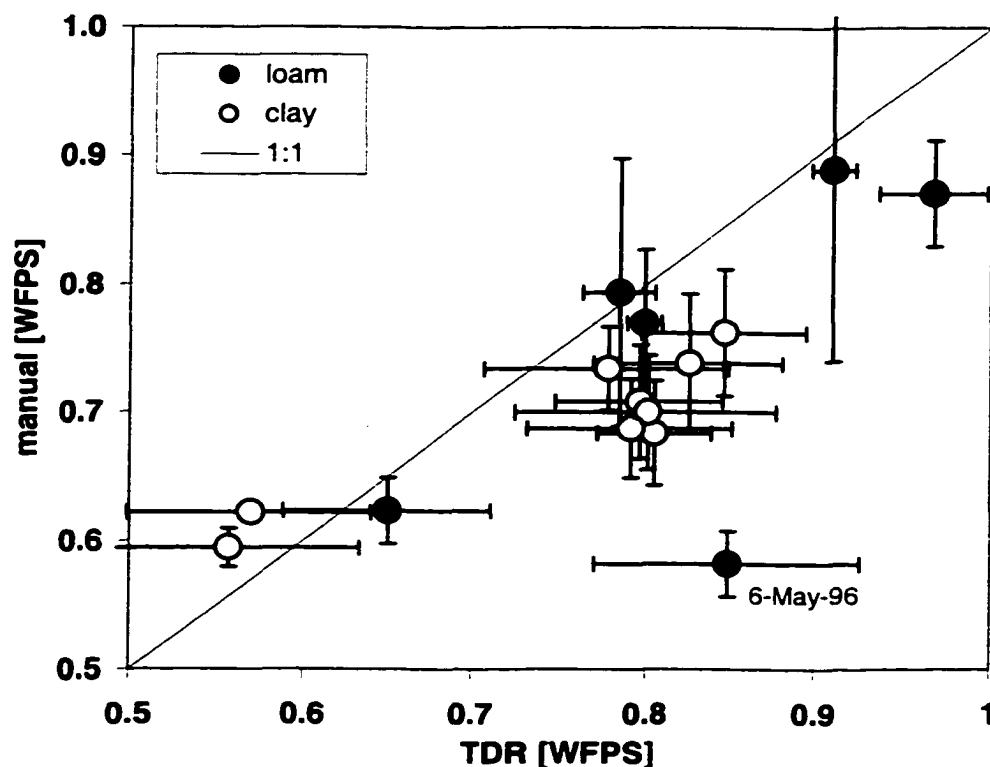


Figure 4.3: Comparison of automatically and manually measured soil moisture content at 0.05 m depth on loam and clay.

On daily basis, TDR technique yielded slightly higher soil moisture content in wet soils compared to manual measurements (between 0.01 and 0.1 WFPS), while results

were similar for relatively dry soils (Figure 4.3). We attributed this deviation to a combination of high spatial variability in soil moisture content (Weitz et al., in press) and differences in the sampling volume these two techniques refer to. TDR technique measured the dielectric properties of a cylindrical volume along the horizontally installed TDR probe, thus sampling from about 0.02 to 0.08 m depth. Consequently the TDR measurement volume largely involved soil depths with higher moisture content compared to relatively drier surface soil (Figure 4.2). Ideally soil augers provide an unbiased sample from 0 to 0.1 m depth. From field experience we expect that auger samples may contain proportionally more near surface material than soil from 0.1 m depth. Low stability of wet loam combined with relatively high friction of soil at the auger metal often compacted the loam during sampling by up to 20 %. In contrast, relatively high stability of clay at 0.1 m depth may have retained from sampling the entire 0.1 m column. Gravimetric sampling may overemphasize the near surface soil, which would yield lower soil moisture content than TDR technique. We scrutinized TDR data extensively without detecting a technical or methodological cause for higher measurement values.

Measured time series of N₂O dynamics and fluxes controlling variables are shown for the perennial crop on loam (Figure 4.4). Soil moisture content at 0.05 m depth was generally high, approaching 60% WFPS only during the relatively dry phase from February 15 through March 20, 1996 (total of 55.5 mm in 34 days). It rained almost every day between April 26 and August 8, 1996 (total of about 1591 mm within 105 days; max. 126 mm on May 14, 1996). Differences in soil water content between sub-plots were probably due to spatial variability resulting from water extraction by roots near the TDR probe. Rain increased moisture content of the topsoil rapidly, infiltrating

precipitation cooled the soil slightly. Soils drained fast during precipitation free days.

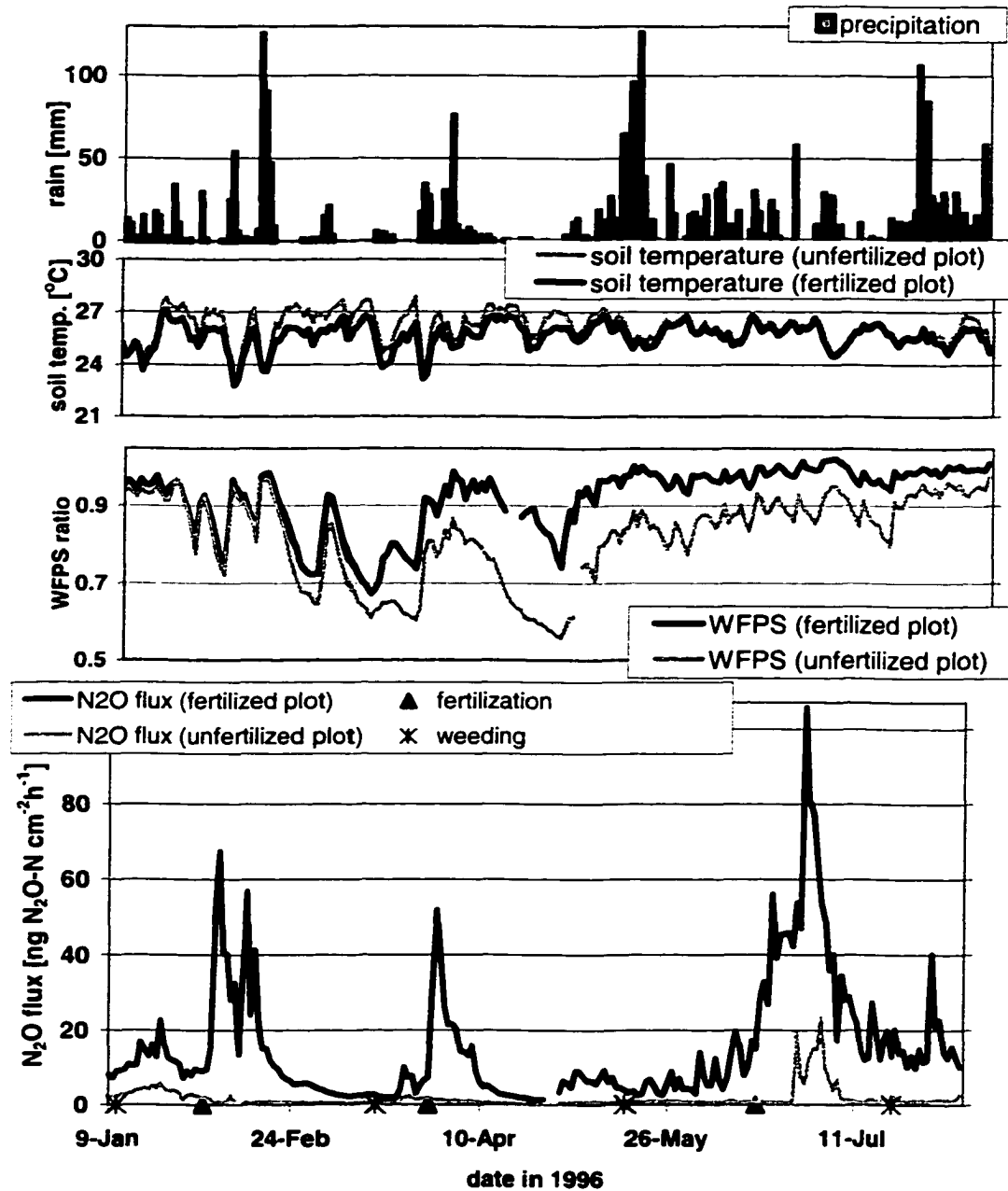


Figure 4.4: Daily precipitation (mm d^{-1}), daily means of soil temperature at 0.05 m depth, soil moisture content (WFPS) at 0.05 cm depth and soil-atmosphere N_2O fluxes measured on loam under unfertilized and fertilized perennial crop. Solid lines indicate time series measured from fertilized plots, dotted lines are measured from unfertilized plots. Dashed vertical lines indicate fertilization events, crosses mark weeding days.

Agricultural management was the major cause for temporal variability of N₂O fluxes from fertilized plots (Figure 4.4). Fertilization increased emissions for several weeks, soil moisture dynamics determined the pattern of post fertilization fluxes. N₂O emissions increased within a few hours when fertilizer was applied on wet soil and when precipitation transferred fertilizer nitrogen into the topsoil. When fertilization occurred during a dry phase (decreasing soil moisture content) emissions increased only after the first rain post fertilization. On February 2, 1996, fertilization occurred in the second half of 5 dry days. Fluxes increased by 72% compared to the previous day but only after 24.3 mm of rain on February 4. Post fertilization fluxes increased briefly whenever precipitation raised soil moisture content, though the magnitude of peaks commonly decreased over time after fertilization. Fluxes were 56.9 ng N₂O-N cm⁻²h⁻¹ on February 13, 11 days post fertilization, versus 27.5 ng N₂O-N cm⁻²h⁻¹ on July 16, 29 days after fertilizer application. Mean background fluxes on fertilized loam under perennial crop were 8.6 ng N₂O-N cm⁻²h⁻¹. High soil moisture content during the rainy period in June-July 1996 supported an elongated period of high fluxes from perennial crop. Slightly increased emissions from unfertilized perennial crop suggested that nutrient availability after clearing of papaya plants may have contributed to high fluxes.

Weeding and/or litter fall may increase N₂O emissions temporarily when increasing soil moisture content supports N₂O fluxes (e.g. March 22, 1996; Figure 4.4). On unfertilized plots weeding and litter fall were the only source for increased nutrient availability. The magnitudes of post weeding fluxes were comparable on both soil types and varied in the range of emissions from clay under annual crop. Repeated fertilization increased the mean level of background fluxes compared to fluxes from unfertilized soils.

Background fluxes were higher from loam than from clay (Table 4.4). Moisture dynamic had little control during background emissions.

Post fertilization fluxes varied in magnitude and temporal pattern (Figure 4.5a) due to the amount of applied fertilizer-N and prevailing soil moisture state and dynamics. Highest peaks were expected within the first week after fertilization, though later fluxes may exceeded initial peaks. Within soils, the magnitude of post fertilization fluxes differed with soil moisture content. Highest post-fertilization fluxes were measured from

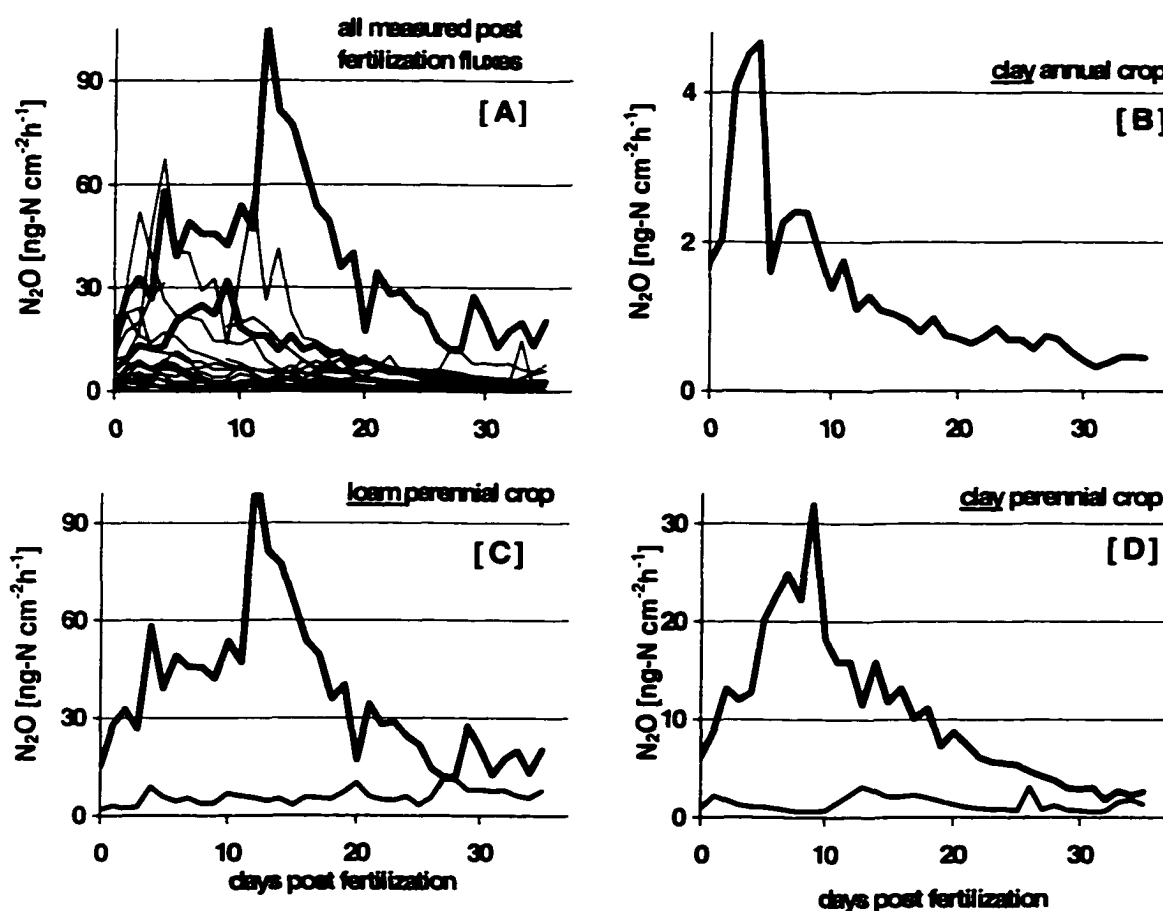


Figure 4.5: Post fertilization flux traces measured on clay and loam. Day of fertilization is zero. Figure 4.5a shows all measured traces to emphasize encountered variability. Figure 4.5b to d highlight the lowest (4.5b) and the highest flux measured (4.5c) and an example for an intermediate flux (4.5d). High fluxes in 4.5c and d were measured during wet phases, low traces indicate fluxes measured during drier phases; fertilization rate was the same between all 4 traces.

fertilized loam under perennial crop during a wet phase in June 1996 when 356 mm rain fell during 5 weeks. Mean moisture content at 0.05 m depth was 0.99 WFPS; 4.9 % of applied fertilizer-N lost as N_2O -N (Figure 4.5c). In January 1995 much lower fluxes were measured from the same site fertilized at the same rate. Mean moisture content at 0.05 m depth was 0.85 WFPS; 0.77 % of applied fertilizer-N lost as N_2O -N (Figure 4.5c). The lowest post fertilization fluxes were measured from clay under annual crop in June 1995 when 443 mm of rain resulted in a mean moisture content of 0.77 WFPS at 0.05 m depth. The fertilization rate was low, 0.32 % of applied fertilizer-N lost as N_2O -N (Figure 4.5b).

Time series clearly show the importance of soil moisture dynamics on N_2O fluxes. However, this variable was poorly correlated across individual sub-plots ($r^2 < 0.37$). Pooling post fertilization phase data from all plots produced the highest coefficient of determination ($r^2 = 0.64$; Figure 4.6). We derived separate multiple regression models for post fertilization, post weeding and background phases using soil moisture content and soil temperature as variables. Soil moisture was the dominant flux control for each regression model (Table 4.6). We applied the regression equations to estimate N_2O fluxes from measured soil moisture content and soil temperature. Simulation resulted a RMSE of 0.40 for unfertilized and 0.36 for fertilized annual crop, and 0.36 for unfertilized and 0.39 for fertilized perennial crop, respectively.

We simulated soil-atmosphere N_2O fluxes and soil moisture dynamics for the period November 1994 to August 1996 using the DNDC model (Figure 4.8a,b). Within this period the automated system was initially located on loam, moved to clay in March 1995, and switched back to loam in January 1996. We list employed soil parameters and the calculated root mean square error (RMSE) criteria in Table 4.7. Simulated moisture

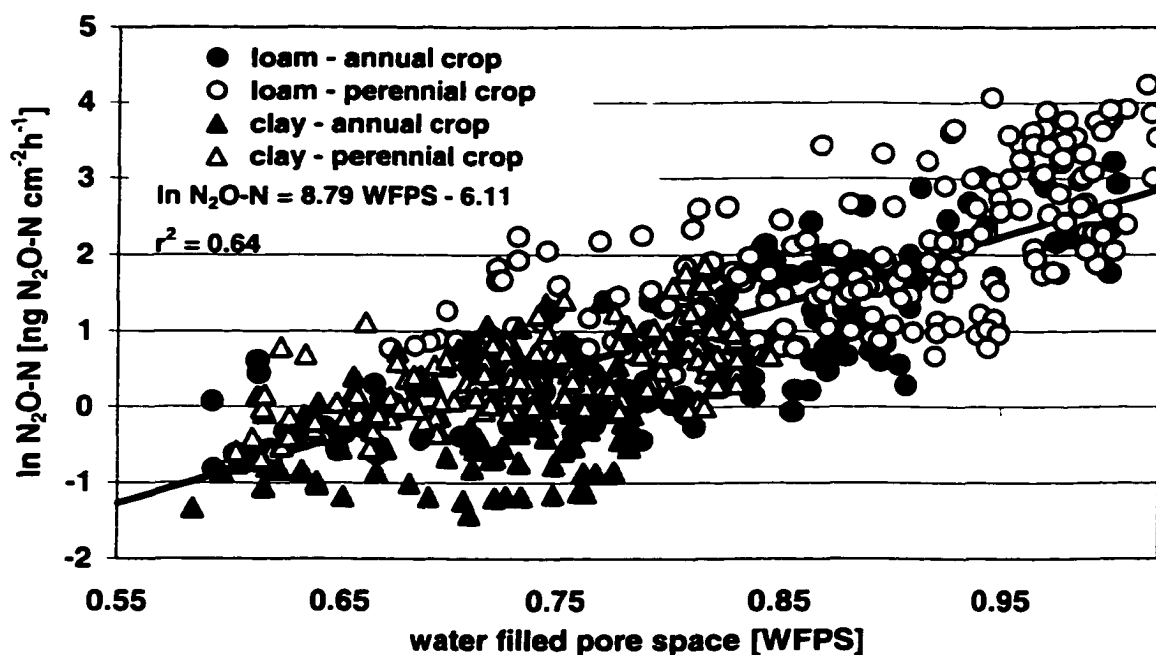


Figure 4.6: Linear regression between \ln -N₂O fluxes and soil moisture content for post-fertilization phases.

Table 4.6: Multiple regression models.

Annual crop, fertilized, post fertilization phase:	
$\ln\text{-N}_2\text{O} = 1.49 - 20.38 \text{ WFPS} + 18.51 \text{ WFPS}^2 + 0.13 \text{ T}$	($r^2 = 0.63$)
Annual crop, fertilized, post weeding phase:	
$\ln\text{-N}_2\text{O} = 63.84 - 73.43 \text{ WFPS} - 2.37 \text{ T} + 2.75 (\text{WFPS} \times \text{T})$	($r^2 = 0.36$)
Annual crop, fertilized, background phase:	
$\ln\text{-N}_2\text{O} = -3.24 - 8.36 \text{ WFPS} + 7.61 \text{ WFPS}^2 + 0.16 \text{ T}$	($r^2 = 0.36$)
Annual crop, unfertilized, post weeding phase:	
$\ln\text{-N}_2\text{O} = 48.68 - 57.05 \text{ WFPS} - 1.72 \text{ T} + 2.03 (\text{WFPS} \times \text{T})$	($r^2 = 0.21$)
Annual crop, unfertilized, background phase:	
$\ln\text{-N}_2\text{O} = -32.16 + 50.51 \text{ WFPS} - 16.79 \text{ WFPS}^2 + 0.85 \text{ T} - 0.96 (\text{WFPS} \times \text{T})$	($r^2 = 0.24$)
Perennial crop, fertilized, post fertilization phase:	
$\ln\text{-N}_2\text{O} = 8.8 - 17.55 \text{ WFPS} + 15.0 \text{ WFPS}^2 + 0.13 \text{ T}$	($r^2 = 0.70$)
Perennial crop, fertilized, post weeding phase:	
$\ln\text{-N}_2\text{O} = -0.4 + 5.67 \text{ WFPS} - 0.12 \text{ T}$	($r^2 = 0.45$)
Perennial crop, fertilized, background phase:	
$\ln\text{-N}_2\text{O} = 13.41 - 39.94 \text{ WFPS} + 28.94 \text{ WFPS}^2$	($r^2 = 0.82$)
Perennial crop, unfertilized, post weeding phase:	
$\ln\text{-N}_2\text{O} = 12.26 - 46.27 \text{ WFPS} - 32.34 \text{ WFPS}^2 + 0.13 \text{ T}$	($r^2 = 0.38$)
Perennial crop, unfertilized, background phase:	
$\ln\text{-N}_2\text{O} = -3.87 + 4.03 \text{ WFPS}$	($r^2 = 0.22$)

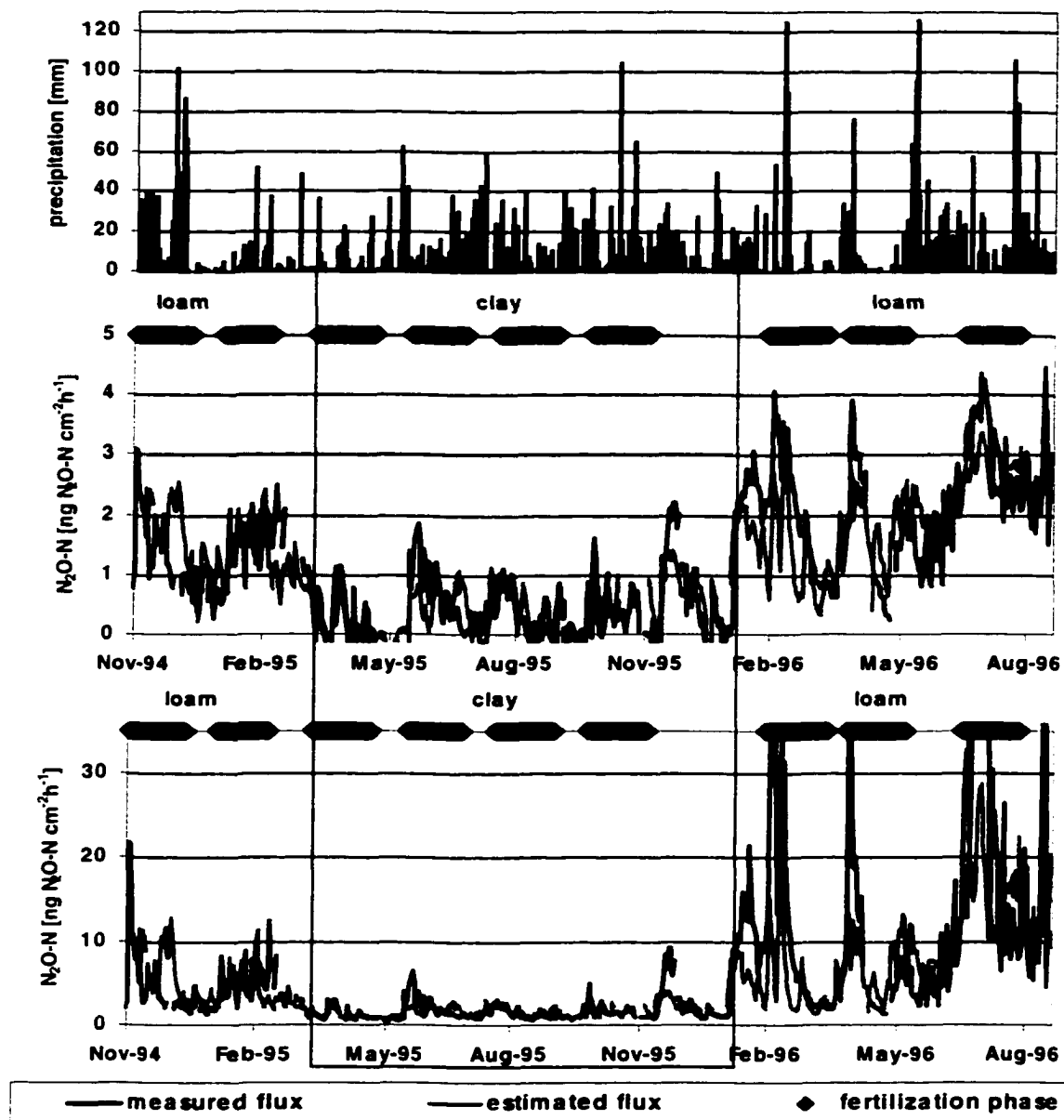


Figure 4.7: Daily mean N_2O fluxes from annual (middle panel) and perennial crop (bottom panel) simulated using the appropriate multiple regression equation for distinguished agricultural phases and compared simulated to measured flux traces.

contents were in the range of field data only when using higher than measured field capacity and wilting point values in DNDC. Simulated soil moisture dynamics matched measured data best for fertilized perennial crop (Figure 4.9). Under annual crop simulated

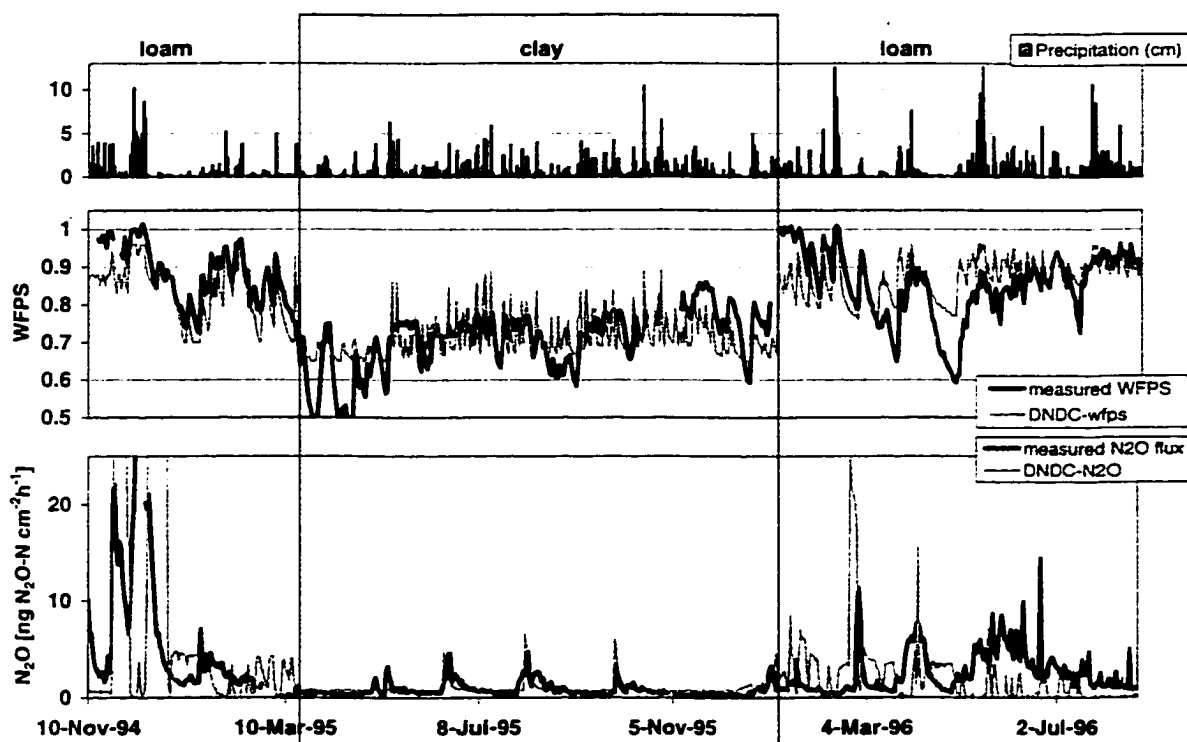


Figure 4.8a: Daily mean N_2O fluxes from annual crop and daily soil moisture content simulated using the process model DNDC and measured fluxes and moisture dynamics.

moisture content did not decrease as much as field measured water content; during drier periods less plant water uptake was simulated than occurred in the field. DNDC slightly overemphasized short-term moisture dynamics, overestimating soil water content after rain events and simulating faster and slightly deeper de-saturation of wet soil during days without precipitation.

For both soil types fertilization-induced temporal variation was simulated well (Figure 4.8 a,b). On clay the measured fluxes were matched well for annual crop, but were overestimated on plots with perennial crop. On loam, fertilizer-induced N_2O peaks matched well with simulations. Magnitudes of peaks and background fluxes diverged for both crops during the wet phase in June/July 1996. The mean level of simulated N_2O

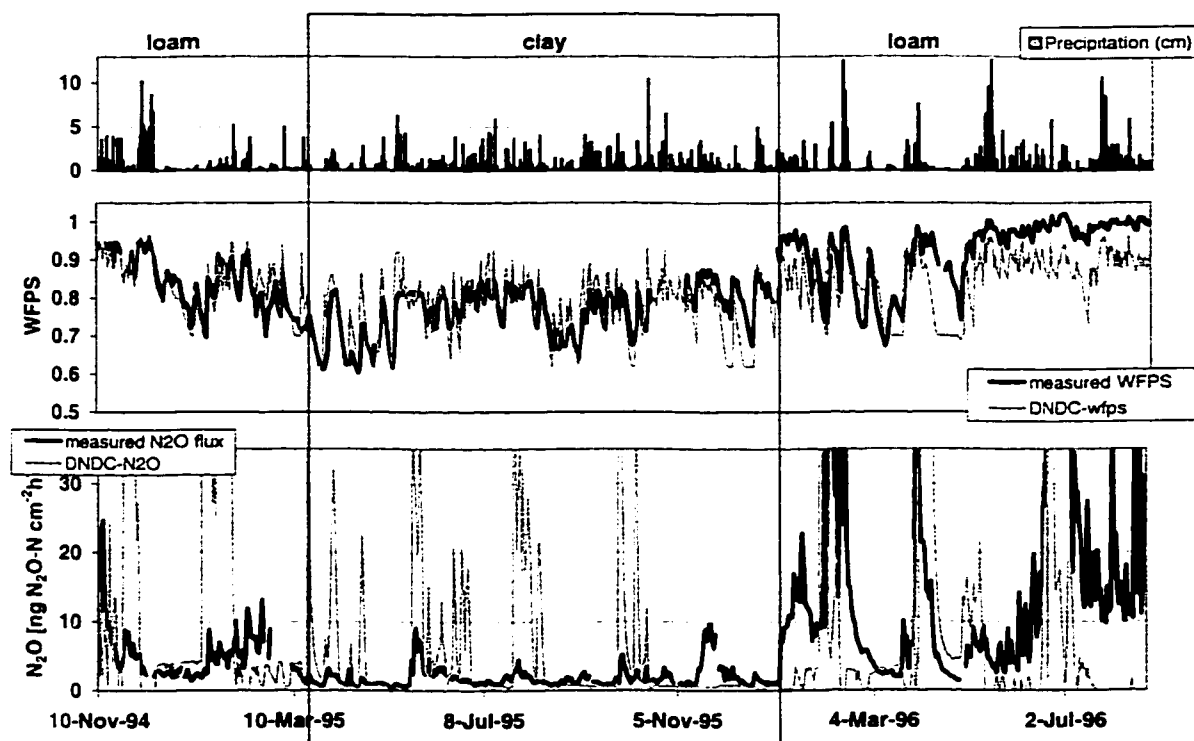


Figure 4.8b: Daily mean N_2O fluxes from perennial crop and daily soil moisture content simulated using the process model DNDC and measured fluxes and moisture dynamics.

emissions was slightly larger than measured on unfertilized loam. Simulated fluxes ceased after rain events and in very wet soils due to denitrification. In wet soils DNDC simulates increased N_2 fluxes at the cost of N_2O production. The model simulated little flux dynamic on unfertilized clay. In simulation scenarios, manipulating either the field capacity (FC) or the wilting point (WP) value, we found that mean N_2O fluxes decreased with soil moisture content increasing from 0.6 to 0.8 WFPS. Temporal dynamics of simulated N_2O fluxes were more strongly affected by fertilization than by water content.

7. Discussion

Soil moisture at 0.05 m depth was above 60% WFPS for most of the time during our field experiment. We assume that microbial denitrification, which increases with

Table 4.7: Soil characteristics of loam and clay used as input in DNDC.

	Loam: Annual Crop		Clay: Annual Crop	
	Unfertilized	Fertilized	Unfertilized	Fertilized
Field capacity	0.88 (0.83)	0.88 (0.85)	0.82 (0.73)	0.70 (0.66)
Wilting point	0.70 (0.56)	0.70 (0.45)	0.62 (0.62)	0.62 (0.62)
Clay fraction	0.40	0.40	0.67	0.67
Bulk density	0.72	0.68	0.81	0.79
pH	7.11	6.47	4.7	4.7
Initial WFPS	0.80	0.80	0.70	0.70
<i>RMSE</i> (WFPS)	0.078	0.077	0.078	0.077
<i>RMSE</i> (N ₂ O)	1.78	18.57	1.26	0.74

	Loam: Perennial Crop		Clay: Perennial Crop	
	Unfertilized	Fertilized	Unfertilized	Fertilized
Field capacity	0.86 (0.82)	0.88 (0.81)	0.85 (0.62)	0.80 (0.74)
Wilting point	0.65 (0.49)	0.70 (0.46)	0.58 (0.58)	0.62 (0.62)
Clay fraction	0.40	0.40	0.67	0.67
Bulk density	0.72	0.68	0.77	0.80
pH	7.11	6.47	4.7	4.7
Initial WFPS	0.80	0.80	0.70	0.70
<i>RMSE</i> (WFPS)	0.079	0.082	0.061	0.066
<i>RMSE</i> (N ₂ O)	3.16	26.58	1.31	11.47

Field capacity and wilting point are given as water filled pore space (WFPS). Values in brackets are laboratory data. All simulations used the retardation and the by-pass flow option; initial NO₃⁻ concentration at the surface was 3 mg-N kg⁻¹, initial NH₄⁺ concentration was 0.3 mg-N kg⁻¹; initial soil organic matter content was 0.05%. Root Mean Square Error (*RMSE*) values were calculated for each crop-treatment combination.

progressing saturation of the soil pore space (Firestone and Davidson, 1989), was the major source for measured N₂O fluxes on predominantly wet soils (Davidson, 1993). Small pores (< 0.1 μm) are continuously water filled, holding water below 1.5 MPa suction. Small pores account for about 60% of the total porosity in soils at La Selva, probably contributing to the high denitrification rates reported from La Selva soils (Radulovich et al., 1992).

Applied fertilizer increased nutrient availability for microbial processes. Automated N₂O measurements indicated that dissolution of granular fertilizer and

transfer of fertilizer-N into the soil by precipitation determines the appearance of initial post fertilization peaks. Generally, emissions were highest during the first 2-3 weeks after a fertilization event, and declined during subsequent weeks. Weeding increased N-availability for microbial processes after cut plant material decomposed. Measured N_2O fluxes were positively correlated with soil moisture content during post fertilization phases. Fluxes were weakly controlled by soil moisture during times of low nutrient availability (background phases; Table 4.6). Davidson predicts that N_2O production by denitrification is highest between 80-100% WFPS, but the net N_2O flux is affected by the increasing reduction of N_2O to N_2 above 80% WFPS (Davidson, 1993). Data from unfertilized plots suggest slightly less N_2O fluxes at very high soil moisture content. A decrease of emissions from very wet soils was reported earlier (Crill et al., in press). Similarly, highly saturated soils in Puerto Rico showed decreasing N_2O fluxes, suggesting reduction of N_2O to N_2 (Erickson and Keller, 1997). Arah et al. (1991) report significant N_2O consumption in the upper 0.05 m of poorly aerated soils. High post fertilization N_2O fluxes measured from very wet loam in June/July 1996 (>0.8 WFPS) suggest that increased nitrate (NO_3^-) concentration after fertilization possibly inhibited N_2O reduction to N_2 (Van Cleemput, 1994, Monaghan and Barraclough, 1993).

Our field observations generally conform with the conceptual model of microbial nitrogen oxide production and consumption during nitrification and denitrification (Firestone and Davidson, 1989). However, measured post fertilization N_2O fluxes varied largely between soil and crop types and even between individual post fertilization phases from a single site. Magnitudes and pattern of N_2O time series were mainly controlled by the interplay of fertilization rate and soil moisture dynamics.

Simulation by multiple-regression models showed that soil nutrient availability and moisture content together were the major flux controlling variables. However we found relatively low correlation coefficients even for post fertilization phases, probably due to high variability of N_2O emissions and soil moisture content (Parkin, 1993, Weitz et al., in press). Correlation was poor during periods of lower nutrient availability (weeding and background phases) when soil moisture was a less powerful flux control. Our empirical modeling approach was successful, though affected by variability, because the expected relation between N_2O fluxes, nutrient availability and moisture content was evident in the measured data. Extrapolation of the model to other than the experimental sites is problematic due to the high variability of the driving variables. If moisture and temperature dynamics could be provided for times other than the measurement period we expect reasonable prediction of fluxes by the regression model.

Appropriately parameterized and validated process based simulation models will allow estimation of N_2O fluxes for various locations. DNDC estimates N_2O fluxes by modeling the kinetics involved in the microbial processes of nitrification and denitrification (Li et al., 1992a). Nitrification is the dominant source for N_2O in prevailing aerobic soils. With increasing oxygen depletion and anoxic conditions in wet soils microbes reduce NO_3^- to N_2O and finally to N_2 (Davidson, 1991). N_2O consumption is supported by reduced gaseous diffusion in increasingly water filled porosity. Thus simulated soil water dynamics play a key role in the denitrification sub-module. DNDC simulated N_2O fluxes ceasing after rain and in very wet soils. In contrast, field measurements showed high post fertilization fluxes for both crops during the very wet phase from June to July 1996 (Figure 4.8).

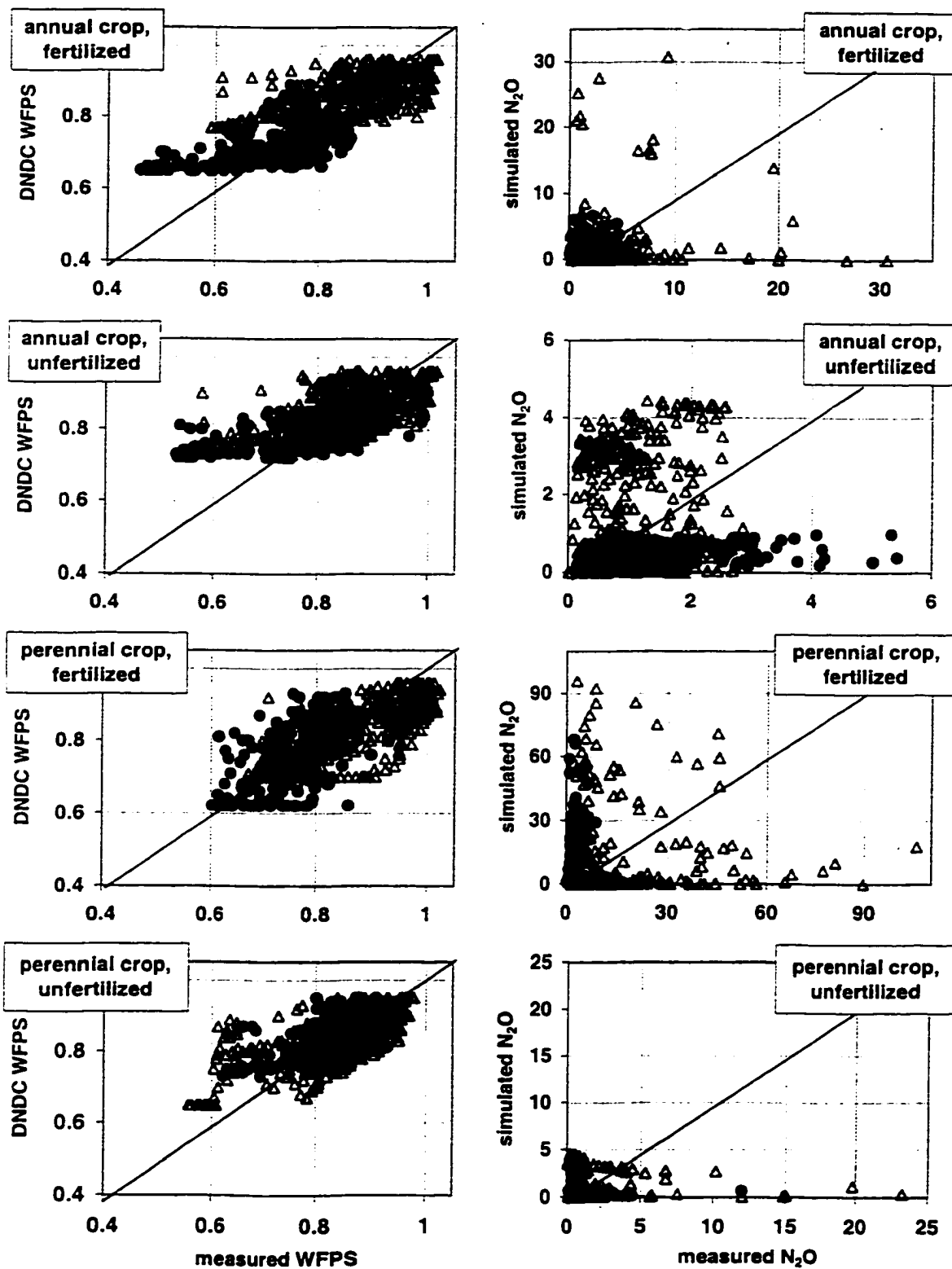


Figure 4.9: Comparison of simulated and measured fluxes and moisture content for all sub-plots

High post fertilization fluxes from loam under annual crop were affected by ants, which, starting in about February 1996, expanded their nest partly into the soil covered by chamber number 3 (Figure 4.10). Ants are not expected to produce N_2O . We did not account for soil chemical effects by the intrusion. However, ant activity disturbed the original soil structure in parts of the chamber flux area. Decreasing bulk density probably affected soil moisture locally. Ant activity probably exposed organic material, previously protected within aggregates, to roots, soil edaphon and microbial populations. Joint effects on N_2O emissions contribute to spatial and temporal variability of fluxes, and are beyond the processes covered by our modeling approach. Decomposition of cut papaya plants may have contributed to increased N_2O fluxes during the wet period from June to July, 1996. DNDC simulations included cutting of papaya plants.

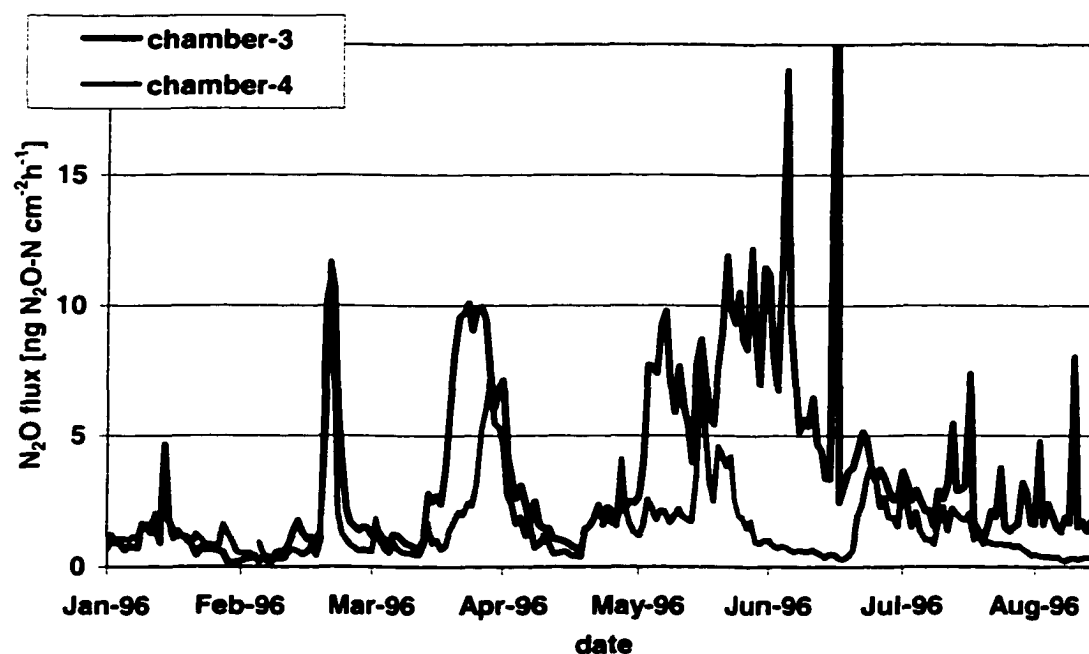


Figure 4.10: Effect of ants expanding their nest into the soil covered by chamber 3 compared to fluxes from replicated chamber 4.

From field observations, measured N_2O fluxes, soil moisture content data combined with our conceptual understanding of nitrogen trace gas production and consumption in soils we expect that for our experimental soils the aggregation of surface soil was the major contributor to high field measured N_2O fluxes, while soil at 0.05 m depth probably contributed less to net fluxes. Soil structure and texture determine pore size distribution, pore geometry and continuity, thus affecting soil hydraulic properties, soil aeration and diffusion. In well aggregated surface soil a large part of the inter-aggregate pore space most probably consisted of large macro-pores that drain rapidly after precipitation and are dominantly air filled at 0.2 kPa (Tomasella and Hodnett, 1996). Referring to our bulk density and moisture study on clay, we expect that most of the time the aggregated near surface soil is relatively drier than the soil at measurement depth of TDR probes. Results shown in Figure 4.2 suggest that on relatively dry clay the soil moisture content in the top layer is in the range favorable for nitrification. In contrast, the soil at 0.04 to 0.07 m depth is relatively more compact, resulting in higher water holding capacity. Pore sizes that are subject to capillarity prevail. Smaller macro-pores may temporarily hold water when soil is saturated above field capacity and drain within days, while meso- and fine pore space at 0.05 m depth remains largely saturated (Radulovich et al., 1992). Even though soils drain water relatively fast, during wet phases frequent rain refilled slow draining macro-pore space. Consequently we measured high soil moisture content at 0.05 m depth, favorable for denitrification processes (Davidson, 1993). Aggregation was more strongly developed on the clay soil than on the loam soil of this study, suggesting higher macroporosity and lower maximum water retention in the surface layer of the clay than the loam.

During predominantly wet phases N_2O production is probably high in aggregated near-surface soils, where anaerobic and aerobic micro-sites may develop adjacently. Inside large, mainly anoxic aggregates we expect predominantly denitrification (Smith, 1990). In more aerobic outer region of larger aggregates, inside small aggregates and in pore space between aggregates probably nitrification is the main N_2O source. High effective diffusivity in strongly aggregated soil supports rapid escape of produced nitrogen oxides. In laboratory experiments Bandidas et al. (1994) found that NO was mainly produced in drier near surface soil and N_2O in largely saturated pore space at 0.03 m depth and inside wet soil aggregates. Similarly, we measured high NO and N_2O fluxes during relatively dry periods on clay (Keller and al., unpublished data). These field observations are explained nicely by the hypothesized structure effect on fluxes and soil water content distribution in the topsoil.

We identified three potential sources for differences between modeled and measured N_2O fluxes. (1) Deviations partly may be an artifact of inappropriate resolution of soil moisture conditions near the soil surface by our automated measurement design. Small-scale changes in moisture content between near surface soil and at 0.05 m depth could not be resolved by TDR measurements, but probably affected field measured fluxes. From simulation scenarios we expect increasing N_2O fluxes with decreasing soil moisture content (0.8 to 0.6 WFPS). N_2O emissions were modeled assuming soil moisture conditions as measured at 0.05 m depth. (2) Differences may also result from inappropriate soil hydraulic parameterization by the process model. DNDC estimates soil hydraulic properties from soil texture information, employing relations derived from common temperate zone soils. Field data confirmed different hydraulic behavior of

highly porous soils in the humid tropics (Sanchez, 1976). (3) Deviations between simulated and measured fluxes may partly be due to yet un-validated plant physiological relations used by DNDC to describe the tropical agricultural crops other than corn. Nitrogen uptake by tropical agricultural crops is not appropriately parameterized yet. This work is in progress (Li et al., in prep.; Keller and al., unpublished data).

8. Conclusion

Automated sampling at high temporal resolution allowed us to identify fast response of N₂O fluxes from tropical agricultural soils to soil moisture dynamics. Agricultural management, via substrate availability for microbial processes, and soil moisture dominated the effects on the temporal variability of fluxes. Fertilization resulted in larger N₂O losses compared to unfertilized fields, generally increasing the mean level of N₂O emissions (background fluxes). Fertilization induced fast rising N₂O peaks shortly after fertilizer application, on wet soils emissions were increased for about 6 weeks post fertilization. Fertilization effects were strongest on wet soils, emissions were low from relatively dry soil. Fluxes increased after precipitation. Both variables, soil nutrient availability and moisture content, were important for a reliable simulation of N₂O fluxes from tropical agricultural soils using multiple regression models. Soil moisture was the major flux control within post-fertilization phases, control was less strong when nutrient availability was low. These results agree with the conceptual 'hole-in-the-pipe' model, where fluxes controlling hole sizes are less important when the flow through the pipe is low. Simulation using the process model DNDC (DeNitrification-DeComposition) confirmed the importance of fertilization for N₂O fluxes. However, currently employed soil hydraulic parameters, derived from temperate zone soils, and plant physiological

parameterization probably are not appropriate for conditions encountered on humid tropical agricultural sites. Field data suggest that soil moisture content may differ on centimeter scale between the strongly aggregated surface layer and soil at 0.05 m depth, the moisture gradient probably contributed to high measured N₂O emissions.

References

- ALPKEM Corporation, RFA 300 Operation Manual, Clackamas, Oregon, 1990.
- Ambus, P., and S. Christensen, Measurement of N₂O emissions from a fertilized grassland: An analysis of spatial variability, *J. Geophys. Res.*, 99, 16,549-16,555, 1994.
- Anderson, I.C., J.S. Levine, M.A. Poth, and P.J. Riggan, Enhanced biogenic emissions of nitric oxide and nitrous oxide following surface biomass burning, *J. Geophys. Res.*, 93(D4), 3893-3898, 1988.
- Arah, J.R.M., K.A. Smith, I.J. Crichton, and H.S. Li, Nitrous oxide production and denitrification in Scottish arable soils, *Journal of Soil Science*, 42, 351-367, 1991.
- Baker, J.M., and R.R. Allmairs, System for automating and multiplexing soil moisture measurement by time-domain reflectometry. *Soil Sci. Soc. Am. J.* 54, 1-6, 1990.
- Baker, J.M., and R.J. Lascano, The spatial sensitivity of time-domain reflectometry. *Soil Science* 147, 378-384, 1989.
- Bandidas, J., A. Vermoesen, C.J.d. Groot, and O.V. Cleemput, The effect of different moisture regimes and soil characteristics on nitrous oxide emission and consumption by different soils., *Soil Science*, 158 (2), 106-114, 1994.
- Blake, G.R., and K.H. Hartge, Bulk density, in *Methods of soil analysis, Part 1. Agronomy 9*, edited by A. Blake, pp. 363-375, 1986.
- Booltink, H.W.G., J. Bouma and D. Gimenez, A suction crust infiltrometer for measuring hydraulic conductivity of unsaturated soil near saturation. *Soil Sci. Soc. Am. J.* 55, 566-68, 1991.
- Born, M., H. Dorr, and I. Levin, Methane consumption in aerated soils of the temperate zone, *Tellus, Ser. A*, 42, 2-8, 1990.
- Bremner, J.M., and C.S. Mulvaney, Nitrogen - Total, in *Methods of Soil Analysis, part 2, Chemical and Microbiological Properties*, edited by A.L. Page, pp. 595-624, *Soil Sci. Soc. of Am., Madison, Wis.*, 1982.
- Brumme, R., and F. Beese, Effects of liming and nitrogen fertilization on emissions of CO₂ and N₂O from a temperate forest, *J. Geophys. Res.*, 97, 12,851-12,858, 1992.
- Cicerone, R.J., Changes in stratospheric ozone, *Science*, 237, 35-42, 1987.

- Clayton, H., J.R.M. Arah, and K.A. Smith, Measurement of nitrous oxide emissions from fertilized grassland using closed chambers, *J. Geophys. Res.*, 99, 16,599-16,607, 1994.
- Cleveland, W.S., and S.J. Devlin, Locally-weighted regression: An approach to regression analysis by local fitting, *J. Am. Stat. Assoc.*, 83, 596-610, 1988.
- Collin, M., and A. Rasmuson, A comparison of gas diffusivity models for unsaturated porous media, *Soil Sci. Soc. of Am. J.*, 52, 1559-1565, 1988.
- Crill, P.M., K.B. Bartlett, J.O. Wilson, D.I. Sebacher, R.C. Harris, J.M. Melack, S. MacIntyre, L. Lesack, and L. Smith-Morrill, Tropospheric methane from an Amazon floodplain lake, *J. Geophys. Res.*, 93, 1564-1570, 1988.
- Crill, P.M., Seasonal patterns of methane uptake and carbon dioxide release by a temperate woodland, *Global Biogeochem. Cycles*, 5, 319-334, 1991.
- Crill, P.M., P.J. Martikainen, H. Nykanen, and J. Silvola, Temperature and N fertilization effects on methane oxidation in a drained peatland soil, *Soil Biol. Biochem.*, 26, 1331-1339, 1994.
- Crill, P.M., M. Keller, A.M. Weitz, W.T. Grauel, and E. Veldkamp, Intensive field measurements of nitrous oxide emissions from tropical agricultural soils, *Global Biogeochem. Cycles*, in press, 1999.
- Crutzen, P.J., Atmospheric chemical processes of the oxides of nitrogen including nitous oxide, in *Denitrification, Nitrification and Atmospheric Nitrous Oxide*, edited by C.C. Delwiche, pp. 17-44, John Wiley & Sons, New York, 1981.
- Crutzen, P.J., and M.O. Andreae, Biomass burning in the tropics: Impact on atmospheric chemistry and biogeochemical cycles, *Science*, 250, 1669-1678, 1990.
- Dasberg, S., and J.W. Hopmans, Time domain reflectometry calibration for uniformly and nonuniformly wetted sandy and clayey loam soils. *Soil Sci. Soc. Am. J.* 56, 1341-1345, 1992.
- Davidson, E.A., Fluxes of nitrous oxide and nitric oxide from terrestrial ecosystems, in *Microbial Production and Consumption of Greenhouse Gases: Methane, Nitrogen Oxides, and Halomethanes*, edited by J.E. Rogers, and W.B. Whitman, pp. 219-235, American Society for Microbiology, Washington, 1991.
- Davidson, E.A., P.M. Vitousek, P.A. Matson, R. Riley, G. Garcia-Mendez, and J.M. Maass, Soil emissions of nitric oxide in a seasonally dry tropical forest of Mexico, *J. Geophys. Res.*, 96(D8), 15,439-15,445, 1991.

- Davidson, E.A., P.A. Matson, P.M. Vitousek, R. Riley, K. Dunkin, G. Garcia-Mendez, and J.M. Maass, Processes regulating soil emissions of NO and N₂O in a seasonally dry tropical forest, *Ecology*, 74, 130-139, 1993.
- Davidson, E.A., Soil water content and the ratio of nitrous oxide to nitric oxide emitted from soil, in *Biogeochemistry of Global Change: Radiatively Active Gases*, edited by R.S. Oremland, pp. 369-386, Chapman and Hall, New York, 1993.
- Davidson, E.A., and S.E. Trumbore, Gas diffusivity and production of CO₂ in deep soils of the eastern Amazon, *Tellus, Ser. B*, 47, 550-565, 1995.
- Davidson, E.A., and W. Kinglerlee, A global inventory of nitric oxide emissions from soils, *Nutrient Cycling Agro Ecosyst.*, 48, 37-50, 1997.
- De Clerck, P., Mesure de l'évolution de la teneur en eau des sols par voie électromagnétique, *Tech. Routière*, 3, 6-15, 1985.
- Dirksen, C., and S. Dasberg, Improved calibration of time domain reflectometry soil water content measurements. *Soil Sci. Soc. Am. J.* 57, 660-667, 1993.
- Dirksen, C., and M.A. Hilhorst, Calibration of a new frequency domain sensor for soil water content and bulk electrical conductivity, *Symposium on Time Domain Reflectometry in Environmental, Infrastructure and Mining Applications*, Northwestern University, Evanston, Illinois, Sept. 7-9, 1994.
- Dobson, M.C., F.T. Ulaby, M.T. Hallikainen, and M.A. El-Rayes, Microwave dielectric behavior of wet soil - Part II: Dielectric mixing models, *IEEE Transactions of Geoscience and Remote Sensing*, GE-23 (1), 35-46, 1985.
- Eichner, M.J., Nitrous oxide emissions from fertilized soils: Summary of available data, *J. Environ. Qual.*, 19, 272-280, 1990.
- Englund, E., and A. Sparks, GEO-EAS 1.2.1., *Geostatistical Environmental Assessment Software: User's Guide*, Environ. Monit. Syst. Lab., Off. of Res. and Dev., U.S. Environ. Prot. Agency, Las Vegas, Nev., 1991.
- Erickson, H.E., and M. Keller, Tropical land use change and soil emissions of nitrogen oxides, *Soil Use and Management*, 13, 278-287, 1997.
- Ewel, J., C. Berish, B. Brown, N. Price, and J. Raich, Slash and burn impacts on a Costa Rican wet forest site, *Ecology*, 62, 816-829, 1981.
- Ferre, P.A., J.H. Knight, D.L. Rudolph, and R.G. Kachanoski, The sample areas of conventional and alternative time domain reflectometry probes, *Water Resources Research*, 34, 2971-2979, 1998.

- Ferre, P.A., D.L. Rudolph, and R.G. Kachanoski, Spatial averaging of water content by time domain reflectometry: Implications for twin rod probes with and without dielectric coatings, *Water Resources Research*, 32 (2), 271-279, 1996.
- Firestone, M.K., and E.A. Davidson, Microbial basis of NO and N₂O production and consumption in soil, in *Exchange of Trace Gases Between Terrestrial Ecosystems and the Atmosphere*, edited by M.O. Andreae and D.S. Schimel, pp. 7-21, John Wiley, New York, 1989.
- Flessa, H., W. Pfau, P. Doersch, and F. Beese, The influence of nitrate and ammonium fertilization on N₂O release and CH₄ uptake of a well-drained topsoil demonstrated by a soil microcosm experiment, *Z. Pflanzenernaehr. Bodenkd.*, 159, 499-503, 1996.
- Folorunso, O.A., and D.E. Rolston, Spatial variability of field-measured denitrification gas fluxes, *Soil Sci. Soc. Am. J.*, 48, 1214-1219, 1984.
- Galbally, I.E., Factors controlling NO_x emissions from soils, in *Exchange of Trace Gases Between Terrestrial Ecosystems and the Atmosphere*, edited by M.O. Andreae and D.S. Schimel, pp. 23-37, John Wiley, New York, 1989.
- Galle, B., L. Klemetsson, and D.W.T. Griffith, Application of a Fourier transform IR system for measurements of N₂O fluxes using micrometeorological methods, and ultralarge chamber system, and conventional field chambers, *J. Geophys. Res.*, 99, 16,575-16,583, 1994.
- Galloway, J.N., W.H. Schlesinger, H. Levy II, A. Michaels, and J.L. Schnoor, Nitrogen fixation: Anthropogenic enhancement-environmental response, *Global Biogeochemical Cycles*, 9, 235-252, 1995.
- Gardener, W.H., Water content, in *Methods of Soil Analysis Part 1, Physical and Mineralogical Methods*, edited by A. Klute, pp. 493-544, Soil Sci. Soc. of Am., Madison, Wisconsin, 1986.
- Graedel, T.E., and P.J. Crutzen, *Atmospheric Change: An Earth System Perspective*, 446 pp., W.H. Freeman, New York, 1993.
- Gray, A.N., and T.A. Spies, Water content measurement in forest soils and decayed wood using time domain reflectometry. *Can. J. For. Res.* 25, 376-385, 1995.
- Groffman, P.M., and J.M. Tiedje, Denitrification in north temperate forest soils: Spatial and temporal patterns at the landscape and seasonal scales, *Soil Biol. Biochem.*, 21, 613-620, 1989.
- Grundmann, G.L., D.E. Rolston, and R.G. Kachanoski, Field soil properties influencing the variability of denitrification gas fluxes, *Soil Sci. Soc. Am. J.*, 52, 1351-1355, 1987.

- Hartshorn, G.S., Plants, in *Costa Rican Natural History*, edited by D.H. Janzen, pp. 118-157, Univ. of Chicago Press, Chicago, Ill., 1983.
- Hartshorn, G.S., and B.E. Hammel, Vegetation types and floristic patterns, in *La Selva: Ecology and Natural History of a Tropical Rain Forest*, edited by L.A. McDade et al., pp. 73-89, University of Chicago Press, Chicago, 1994.
- Heimovaara, T.J., and W. Bouten, A computer-controlled 36-channel time domain reflectometry system for monitoring soil water contents. *Water Res. Res.* 26, 2311-2316, 1990.
- Heimovaara, T.J., W. Bouten, and J.M Verstraaten, Frequency domain analysis of time domain reflectometry waveforms. 2. A four-components complex dielectric mixing model for soils. *Water Res. Res.* 30, 201-209, 1994.
- Herkelrath, W.N., S.P. Hamburg, and F. Murphy, Automatic, real-time monitoring of soil moisture in a remote field area with time-domain reflectometry. *Water Res. Res.* 27, 857-864, 1991.
- Hutchinson, G.L., and A.R. Mosier, Improved soil cover method for field measurement of nitrous oxide fluxes, *Soil Sci. Soc. of Am. J.*, 45, 311-316, 1981.
- Hutchinson, G.L., G.P. Livingston, and E.A. Brams, Nitric and nitrous oxide evolution from managed subtropical grassland, in *Biogeochemistry of Global Change: Radiatively Active Gases*, edited by R.S. Oremland, pp. 290-316, Chapman and Hall, New York, 1993.
- Intergovernmental Panel on Climate Change (IPCC), *Climate Change 1995*, 572 pp., Cambridge Univ. Press, New York, 1996.
- Isaaks, E.H., and R.M. Srivastava, *Applied Geostatistics*, Oxford Univ. Press, New York, 1989.
- Jacobsen, O.H., and P. Schjønning, Comparison of TDR calibration functions for soil water determination, in *Proceedings of the Symposium: Time-domain reflectometry. Applications in soil science*, edited by L.W. Petersen and O.H. Jacobsen, Research Center Foulum 16, 1994. SP Report No. 11, 25-33.
- Keeney, D.R., and D.W. Nelson, Nitrogen ó Inorganic forms, in *Methods of Soil Analysis, part 2, Chemical and Microbiological Properties*, edited by A.L. Page, pp. 643-709, Soil Sci. Soc. of Am., Madison, Wis., 1982.
- Keller, M., W.A. Kaplan, S.C. Wofsy, and J.M.D. Costa, Emissions of N₂O from tropical forest soils: Response to fertilization with NH₄, NO₃ and PO₄, *J. Geophys. Res.*, 93(D2), 1600-1604, 1988.

- Keller, M., M.E. Mitre, and R.F. Stallard, Consumption of atmospheric methane in soils of central Panama effects of agricultural development, *Global Biogeochem. Cycles*, 4, 21-27, 1990.
- Keller, M., E. Veldkamp, A.M. Weitz, and W.A. Reiners, Effect of pasture age on soil trace-gas emissions from a deforested area of Costa Rica, *Nature*, 365, 244-246, 1993.
- Keller, M., and W.A. Reiners, Soil-atmosphere exchange of nitrous oxide, nitric oxide, and methane under secondary succession of pasture to forest in the Atlantic lowlands of Costa Rica, *Global Biogeochem. Cycles*, 8, 399-409, 1994.
- King, G.M., and S. Schnell, Effect of increasing atmospheric methane concentration on ammonium inhibition of soil methane consumption, *Nature*, 370, 282-284, 1994.
- Klute, A., Water Retention: Laboratory Methods, in *Methods of Soil Analysis. Part 1: Physical and Mineralogical Methods*, edited by A. Klute, pp. 635-662, American Society of Agronomy, Inc., Soil Science of America, Inc., Madison, 1986.
- Knight, J.H., I. White, and S.J. Zegelin, Sampling volume of TDR probes used for water content monitoring, *Symposium on Time Domain Reflectometry in Environmental, Infrastructure and Mining Applications*, Northwestern University, Evanston, Illinois, Sept. 7-9, 1994.
- Koschorreck, M., and R. Conrad, Oxidation of atmospheric methane in soil: Measurements in the field, in soil cores and in soil samples, *Global Biogeochem. Cycles*, 7, 109-121, 1993.
- LECO, LECO CNS-2000 Elementar Analyzer. Instruction manual, St. Joseph, MI, 1994.
- Ledieu, J., P. De Ridder, P. De Clerck, and S. Dautrebande, A method of measuring soil moisture by time-domain reflectometry. *J. Hydrol.* 88, 319-328, 1986.
- Levine, J.S., E.L. Winstead, D.A.B. Parsons, M.C. Schols, R.J. Scholes, W.R. Cofer III, D.R. Cahoon Jr., and D.I. Sebacher, Biogenic soil emissions of nitric oxide (NO) and nitrous oxide (N₂O) from savannas in South Africa: The impact of wetting and burning, *J. Geophys. Res.*, 101(D19), 23,689-23,697, 1996.
- Li, C., S. Frohking, and T.A. Frohking, A model of nitrous oxide evolution from soil driven by rainfall events. 1. Model structure and sensitivity., *J. of Geophys. Res.*, 97 (D9), 9759-9776, 1992a.
- Li, C., S. Frohking, and T.A. Frohking, A model of nitrous oxide evolution from soil driven by rainfall events: 2. Model application., *Journal of Geophysical Research*, 97 (D9), 9777-9783, 1992b.

- Li, C., M. Keller, P.M. Crill, A.M. Weitz, W.T. Grauel, and E. Veldkamp, Intensive field measurements of nitrous oxide emissions from tropical agricultural soils: model evaluation, , in prep.
- Lide, D.R. (Ed.), Handbook of Chemistry and Physics 1997-1998, 78th ed., CRC Press, Boca Raton, Fla., 1997.
- Linn, D.M., and J.W. Doran, Effect of water-filled pore space on carbon dioxide and nitrous oxide production in tilled and nontilled soils, *Soil Sci. Soc. Am. J.*, 48, 1267-1272, 1984.
- Livingston, G.P., P.M. Vitousek, and P.A. Matson, Nitrous oxide flux and nitrogen transformations across a landscape gradient in Amazonia, *J. Geophys. Res.*, 93(D2), 1593-1599, 1988.
- Lizano, J.R., Aspectos tecnicos sobre cuarenta y cinco cultivos agricolas de Costa Rica, 560 pp., Ministerio de Agricultura y Ganaderia, Direccion General de Investigacion y Extension Agricolas, San Jose, Costa Rica, 1991.
- Luizao, F., P. Matson, G. Livingston, R. Luizao, and P. Vitousek, Nitrous oxide flux following tropical land clearing, *Global Biogeochem. Cycles*, 3, 281-285, 1989.
- Malicki, M.A., and W.M. Skierucha, A manually controlled TDR soil moisture meter operating with 300 ps rise-time needle pulse. *Irrig. Sci.* 10, 153-163, 1989.
- Matson, P.A., P.M. Vitousek, J.J. Ewel, M.J. Mazzarino, and G.P. Robertson, Nitrogen transformations following tropical forest felling and burning on a volcanic soil, *Ecology*, 68, 491-502, 1987.
- Matson, P.A., and P.M. Vitousek, Ecosystem approach for the development of a global nitrous oxide budget. Processes that regulate gas emissions vary in predictable ways, *Bioscience*, 40, 667-672, 1990.
- Matson, P.A., P.M. Vitousek, G.P. Livingston, and N.A. Swanberg, Sources of variation in nitrous oxide flux from Amazonian ecosystems, *J. Geophys. Res.*, 95, 16,789-16,798, 1990.
- Matson, P.A., C. Billow, and S. Hall, Fertilization practices and soil variations control nitrogen oxide emissions from tropical sugar cane, *J. Geophys. Res.*, 101, 18,533-18,545, 1996.
- Matson, P.A., R. Naylor, and I. Ortiz-Monasterio, Integration of environmental, agronomic, and economic aspects of fertilizer management, *Science*, 280, 112-115, 1998.

- Millington, R.J., and R.C. Shearer, Diffusion in aggregated porous media, *Soil Sci.*, 111, 372-378, 1971.
- Monaghan, R.M., and D. Barraclough, Nitrous oxide and dinitrogen emissions from urine-affected soil under controlled conditions, *Plant and Soil*, 151, 127-138, 1993.
- Mosier, A.R., and G.L. Hutchinson, Nitrous oxide emissions from cropped fields, *J. Environ. Qual.*, 10, 169-173, 1981.
- Mosier, A.R., Chamber and isotope techniques, in *Exchange of Trace Gases Between Terrestrial Ecosystems and the Atmosphere*, edited by M.O. Andreae and D.S. Schimel, pp. 175-187, John Wiley, New York, 1989.
- Mosier, A.R., D.S. Schimel, D.W. Valentine, K. Bronson, and W.J. Parton, Methane and nitrous oxide fluxes in native, fertilized and cultivated grasslands, *Nature*, 350, 330-332, 1991.
- Mosier, A.R., and J.A. Delgado, Methane and nitrous oxide flux in grasslands in western Puerto Rico, *Chemosphere*, 35, 2059-2082, 1997.
- Mosier, A.R., J.A. Delgado, and M. Keller, Methane and nitrous oxide fluxes in an acid oxisol in western Puerto Rico: Effects of tillage, liming and fertilization, *Soil Biol. Biochem.*, 30, 2087-2098, 1998.
- Neff, J.C., M. Keller, E.A. Holland, A.M. Weitz, and E. Veldkamp, Fluxes of nitric oxide from soils following the clearing and burning of a secondary tropical rain forest, *J. Geophys. Res.*, 100(D12), 25,913-25,922, 1995.
- Nelson, D.W., and L.E. Sommers, Total carbon, organic carbon, and organic matter, in *Methods of Soil Analysis, part 2, Chemical and Microbiological Properties*, edited by A.L. Page, pp. 570-571, Soil Sci. Soc. of Am., Madison, Wis., 1982.
- Parkin, T.B., Spatial variability of microbial processes in soil: A review, *J. Environ. Qual.*, 22, 409-417, 1993.
- Petersen, L.W., A. Thomsen, P. Moldrup, O.H. Jacobsen, and D.E. Rolston, High-Resolution time domain reflectometry: Sensitivity dependency on probe design. *Soil Science* 159, 149-154, 1995.
- Radulovich, R., P. Sollins, P. Baveye, and E. Solorzano, Bypass water flow through unsaturated microaggregated tropical soils, *Soil Sci. Soc. Am. J.*, 56, 721-726, 1992.
- Ramanathan, V., L. Callis, R. Cees, J. Hansen, I. Isaksen, W. Kuhn, A. Lacis, F. Luther, J. Mahlman, R. Reck, and M. Schlesinger, Climate-chemical interactions and effects of changing atmospheric trace gases, *Rev. Geophys.*, 25, 1441-1482, 1987.

- Reiners, W.A., A.F. Bouwman, W.F. Parson, and M. Keller, Tropical rain forest conversion to pasture: Changes in vegetation and soil properties, *Ecol. Appl.*, 4, 363-377, 1994.
- Rhode, H., A comparison of the contribution of various gases to the greenhouse effect, *Science*, 248, 1217-1219, 1990.
- Robertson, G.P., Nitrification and denitrification in humid tropical ecosystem: Potential controls on nitrogen retention, in *Mineral Nutrients in Tropical Forest and Savanna Ecosystems*, edited by J. Proctor, Blackwell Scientific Publ., Boston, Mass., 1989.
- Robertson, G.P., and P. Sollins, Biological control of soil charge chemistry in a humid tropical ecosystem in Costa Rica, Central America, *Ecol. Soc. of Am. Bull.*, 68, 46, 1987.
- Robertson, G.P., and J.M. Tiedje, Deforestation alters denitrification in a lowland tropical rain forest, *Nature*, 336, 756-759, 1988.
- Rolston, D.E., Gas diffusivity, in *Methods of Soil Analysis, part 1, Physical and Mineralogical Methods*, edited by A. Klute, pp. 1089-1102, Soil Sci. Soc. of Am., Madison, Wis., 1986.
- Rosenzweig, C., Agriculture in a changing global environment, *Soil Sci. Soc. Am. J.*, 41, 59-71, 1994.
- Roth, K., R. Schulin, H. Fluehler, and W. Attinger, Calibration of time domain reflectometry for water content measurements using a composite dielectric approach. *Water Res. Res.* 26, 267-2273, 1990.
- Roth, C.H., M.A. Malicki, and R. Plagge, Empirical evaluation of the relationship between soil dielectric constant and volumetric water content as the basis for calibrating soil moisture measurements by TDR. *J. Soil Sci.* 43, 1-3, 1992.
- Sall, J., and A. Lehman, *JMP Start Statistics. A Guide to Statistics and Data Analysis Using JMP and JMP IN Software.*, Duxbury Press, Boston, Mass., 1996.
- Sanchez, P.A., *Properties and management of soils in the tropics*, John Wiley & Sons, New York, 1976.
- Sanford, R.L., Jr., P. Paaby, J.C. Luvall, and E. Phillips, The La Selva ecosystem: Climate, geomorphology, and aquatic systems, in *La Selva: Ecology and Natural History of a Tropical Rain Forest*, edited by L.A. McDade et al., pp. 19-33, Univ. of Chicago Press, Chicago, Ill., 1994.

- Schimel, D., Alves, D., Enting, I., Heimann, M., Joos, F., Raynaud, D., Wigley, T., Prather, M., Derwent, R., Ehhalt, D., Fraser, P., Sanhueza, E., Zhou, X., Jonas, P., Charlson, R., Rohde, H., Sadasivan, S., Shine, K.P., Fouquart, Y., Ramaswamy, V., Solomon, S., Srinivasan, J., Albritton, D., Derwent, R., Isaksen, I., Lal, M., Wuebbels, D., Radiative forcing of climate change, in *Climate Change 1995: The Science of Climate Change*, edited by J. T. Houghton, pp. 65-131, Cambridge Univ. Press, New York, 1996.
- Shepherd, M.F., S. Barzetti, and D.R. Hastie, The production of atmospheric NO_x and N₂O from a fertilized agricultural soil, *Atmos. Environ.*, 25A, 1961-1969, 1991
- Silver, W.L., and K.A. Vogt, Fine root dynamics following single and multiple disturbances in a subtropical wet forest ecosystem, *J. Ecol.*, 81, 729-738, 1993.
- Smith, K.A., Clayton, H., Arah, J.R.M., Christensen, S., Ambus, P., Fowler, D., Hargreaves, K.J., Skiba, U., Harris, G.W., Wienhold, F.G., Klemetson, L., Galle, B., Micrometeorological and chamber methods for measurement of nitrous oxide fluxes between soils and the atmosphere: Overview and conclusions, *J. Geophys. Res.*, 99, 16,541-16,548, 1994.
- Smith, K., Anaerobic zones and denitrification in soil: Modeling and measurement, in *Denitrification in soil and sediment*, edited by N.P. Revsbech, and J. Sørensen, pp. 229-244, Plenum Press, New York, 1990.
- Sollins, P., F. Sancho, R. Mata, and R.L. Sanford, Soils and soil process research, in *La Selva: Ecology and Natural History of a Tropical Rain Forest*, edited by L.A. McDade, K.S. Bawa, H.A. Hespenheide, and G.S. Hartshorn, pp. 34-53, Univ. of Chicago Press, Chicago, Ill., 1994.
- Spaans, E.J.A., and J.M. Baker, Simple baluns in parallel probes for time domain reflectometry. *Soil Sci. Soc. Am. J.* 57, 668-673, 1993.
- Stuedler, P.A., R.D. Bowden, J.M. Melillo, and J.D. Aber, Influence of nitrogen fertilization on methane uptake in temperate forest soils, *Nature*, 341, 314-315, 1989.
- Striegl, R.G., Diffusional limits to the consumption of atmospheric methane by soils, *Chemosphere*, 26, 715-720, 1993.
- Tomasella, J., and M.G. Hodnett, Soil hydraulic properties and van Genuchten parameters for an oxisol under pasture in central Amazonia., in *Amazonian Deforestation and Climate*, edited by J.H.C. Gash, C.A. Nobre, J.M. Roberts, and R.L. Victoria, pp. 101-124, J. Wiley & Sons, New York, 1996.
- Topp, G.C., J.L. Davis, and A.P. Annan, Electromagnetic determination of soil water content: measurements in coaxial transmission lines. *Water Res. Res.* 16, 574-582, 1980.

- Topp, G.C., M. Yanuka, W.D. Zebchuk, and S. Zegelin, Determination of electrical conductivity using time domain reflectometry: Soil and water experiments in coaxial lines, *Water Resources Research*, 24 (7), 945-952, 1988.
- Van Cleemput, O., Biogeochemistry of nitrous oxide in wetlands, *Current topics in wetland biogeochemistry*, 1, 3-14, 1994.
- van Cleemput, O., and A.H. Samater, Nitrite in soils: Accumulation and role in the formation of gaseous N compounds, *Fertilizer Res.*, 45, 81-89, 1996.
- Van den Pol-van Dasselaar, A., W.J. Corre, A. Prime, A.K. Klemmedtsson, P. Weslien, A. Stein, L. Klemmedtsson, and O. Oenema, Spatial variability of methane, nitrous oxide, and carbon dioxide emissions from drained grassland, *Soil Sci. Soc. Am. J.*, 62, 810-817, 1998.
- Veldkamp, E., and M. Keller, Nitrogen oxide emissions from a banana plantation in the humid tropics, *J. Geophys. Res.*, 102(D13), 15,889-15,898, 1997.
- Veldkamp, E., M. Keller, and M. Nunez, Effects of management on N₂O and NO emissions from pasture soils in the humid tropics of Costa Rica, *Global Biogeochemical Cycles*, 1998.
- Velthof, G.L., and O. Oenema, Nitrous oxide fluxes from grassland in the Netherlands, II, Effects of soil type, nitrogen fertilizer application and grazing, *Eur. J. Soil Sci.*, 46, 541-549, 1995.
- Vermoesen, A., O.v. Cleemput, and G. Hofman, Nitrogen loss processes: mechanisms and importance, *Pedologie*, XLIII (3), 417-433, 1993.
- Vielhaber, B., Temperatur abhängiger Wassertransport in Deponieoberflächenabdichtungen - Feldversuche in bindigen mineralischen Dichtungen unter Kunststoffabdichtungsbahn. PhD thesis University of Hamburg, *Hamburger Bodenkundliche Arbeiten* 29, Germany, 1995.
- Wagner-Riddle, C., and G.W. Thurtell, Nitrous oxide emissions from agricultural fields during winter and spring thaw as affected by management practices, *Nutrient Cycling in Agroecosystems*, 52, 151-163, 1998.
- Weitz, A.M., W.T. Grauel, M. Keller, and E. Veldkamp, Calibration of time domain reflectometry technique using undisturbed soil samples from humid tropical soils of volcanic origin, *Water Resources Research*, 33 (6), 1241-1249, 1997.
- Weitz, A.M., E. Veldkamp, M. Keller, J. Neff, and P.M. Crill, Nitrous oxide, nitric oxide, and methane fluxes from soils following clearing and burning of tropical secondary forest, *J. Geophys. Res.*, 103, 28,047-28,058, 1998.

Weitz, A.M., P.M. Crill, M. Keller, and E. Linder, Spatial and temporal variability of nitrogen oxides and methane fluxes from a fertilized tree plantation in Costa Rica, *Journal of Geophysical Research*, *in press*.

Williams, E.J., G.L. Hutchinson, and F.C. Fehsenfeld, NO_x and N_2O emissions from soil, *Global Biogeochem. Cycles*, 6, 351-388, 1992.

Appendix

Millington and Shearer's [1971] model of gaseous diffusion in aggregated soils divides the total porosity of a soil into intra-aggregate porosity and interaggregate porosity. Gas may flow through dry aggregated soils using two different pathways: the continuous (effective) pore spaces in the interaggregate porosity only, and the effective intra-aggregate and connecting interaggregate pore spaces. Estimation of the effective diffusivity in a dry aggregated medium accounts for both possible gas flow pathways. Intra-aggregate and interaggregate porosity of soils may be partly or completely water filled. Water in soil pores interrupts the described gas flow path through continuous air-filled pore spaces, restricting the total effective area for flow in moist aggregated soils compared to flow through dry aggregated soil. The effective diffusivity is calculated as the diffusivity of a gas in the soil normalized to the molecular diffusivity of that gas in air and equals the total effective flow area in the aggregated and moist soil. The Millington and Shearer model for gas diffusion in unsaturated, aggregated soil reads,

$$\frac{D_s}{D_o} = \frac{(1 - S_{WA})^2 \left(\frac{A - \theta_A}{A + S}\right)^{2n} (1 - P^{2x}) [(P - \theta_P) - (P - \theta_P)^{2y}]}{(1 - S_{WA})^2 \left(\frac{A - \theta_A}{A + S}\right)^{2n} (1 - P^{2x}) + (P - \theta_P) - (P - \theta_P)^{2y}} + (1 - S_{WP})^2 (P - \theta_P)^{2y}$$

where D_s is gas diffusivity in soils ($\text{cm}^2 \text{s}^{-1}$); D_o is molecular diffusivity of that gas in air ($\text{cm}^2 \text{s}^{-1}$); A is intra-aggregate porosity ($\text{cm}^3 \text{cm}^{-3}$); P is inter-aggregate porosity ($\text{cm}^3 \text{cm}^{-3}$); S is solid phase ($\text{cm}^3 \text{cm}^{-3}$); θ_A is volumetric water content of the intra-aggregate porosity; θ_P is volumetric water content of the interaggregate porosity; S_{WA} is fractional water saturation of the intra-aggregate porosity; S_{WP} is fractional water

saturation of the interaggregate porosity; and x, y , and n are related to the effective pore area of the different pore spaces; and x is related to the effective interaggregate pore area and is derived from

$$1 = P^{2x} + (1 - P)^x$$

y is related to the effective, unsaturated interaggregate pore area by

$$1 = (P - \theta_p)^{2y} + (1 - (P - \theta_p))^y$$

and n is related to the effective intra-aggregate pore area and is derived from

$$1 = \left(\frac{A - \theta_A}{A + S}\right)^{2n} + \left(1 - \left(\frac{A - \theta_A}{A + S}\right)\right)^n$$

These three equations can be written in a generalized form as

$$1 = M^{2b} + (1 - M)^b$$

Using the relation given by Collin and Rasmusson [1988, Figure 1], we approximated b linear as

$$b = 0.25M + 0.58$$

This line diverts from the original only for very small or large porosity values. In our spread sheet calculations we used this linear approximation of each parameter x, y , and n with the appropriate terms given in the three equations.

To estimate effective CH_4 diffusivity in aggregated soils based on the Millington and Shearer model we used the molecular diffusion coefficient of CH_4 in air (D_0) of $0.219 \text{ cm}^2 \text{ s}^{-1}$ at standard pressure of $101,325 \text{ Pa}$ and 298 K as calculated from data given in the *Handbook of Chemistry and Physics* [Lide, 1997]. We applied the formula given by Rolston [1986] to calculate the D_0 at 298 K from any other diffusion coefficient of CH_4 in air measured at a known temperature. We followed the approach of Davidson and

Trumbore [1995] and used field capacity θ_{fc} as threshold value to distinguish macropore volume from mesopore and fine-pore volume. Assuming the total porosity of an aggregated soil is P_T , then the interaggregate porosity P (macropore porosity) calculates as $(\varepsilon - \theta_{fc})$, and the interaggregate porosity A (mesopore and fine-pore porosity) equals field capacity θ_{fc} . We used daily averages of field measured soil water content values in the Millington and Shearer model and estimated effective diffusivity for CH_4 for each measurement day. For soil water contents above field capacity the Millington and Shearer model simulates an exponential decrease of D_{eff} with increasing water content, while below field capacity, decreasing soil moisture increases high D_{eff} only slightly.